

Dissertation

Testbed-based Evaluation of Mobile Communication Systems

ausgeführt zum Zwecke der Erlangung des akademischen Grades
eines Doktors der technischen Wissenschaften

eingereicht an der Technischen Universität Wien
Fakultät für Elektrotechnik und Informationstechnik

von

Sebastian Caban

Zanaschkagasse 12/31/30, 1120 Wien

<http://www.caban.at>

geboren am 13. März 1980 in Wien

Matrikelnummer: 0025464

Wien, im September 2009

Begutachter:

Univ. Prof. Dr.-Ing. Markus Rupp

Institut für Nachrichtentechnik und Hochfrequenztechnik
Technische Universität Wien
Österreich

Prof. Luis Castedo Ribas

Electronics and Systems Department
University of A Coruña
Spain

I hereby certify that the work reported in this thesis is my own,
and the work done by other authors is appropriately cited.

Caban Sebastian

Sebastian Caban

Vienna, September 1, 2009

Abstract

The ever increasing demand for mobility calls for new mobile communication systems that deal more efficiently with the very limited bandwidth available. While such systems do exist and work well in computer simulations, little is known about their performance under real world conditions. Little is also known about how to best determine and compare the throughput performance of such wireless communication schemes in specific, realistic outdoor scenarios. The range of effective answers spans from performing numerical simulations to building prototypes.

In recent years we have determined that a cost, time, and manpower efficient—as well as effective—method is that of carrying out quasi-realtime testbed measurements. In this approach, all possible transmit data is generated off-line in MATLAB, but only the required data is then transmitted over a wireless channel which is altered by moving the receive antennas. The for closed-loop transmissions required feedback is instantly carried out in approximately 40 milliseconds in MATLAB. The received data itself is not evaluated in real-time but off-line using a cluster of PCs. Results for the scenario measured are automatically obtained using the same script that has already controlled the complete measurement procedure and documentation.

The potential of this efficient approach is demonstrated exemplarily on MIMO single carrier, MIMO HSDPA, and MIMO WiMAX measurements in indoor, urban outdoor, and Alpine outdoor scenarios. We present the results obtained in terms of physical layer throughput over transmit power as well as over transmit antenna element spacing.

Kurzfassung

Der ständig steigende Bedarf nach Mobilität erfordert die Entwicklung immer neuerer Telekommunikationssysteme, die in der Lage sind, die verfügbaren Frequenzbänder noch effizienter zu nützen. Während solche Systeme in Simulationen bereits existieren und gut funktionieren, ist deren exakte Leistungsfähigkeit unter realen Einsatzbedingungen noch weitestgehend unbekannt. Überdies ist ebenso unklar wie der Durchsatz eines solchen neuartigen Kommunikationssystems am effizientesten unter realen Umgebungsbedingungen ermittelt werden kann. Die Bandbreite der dafür in Frage kommenden Methoden reicht von rein numerischen Simulationen bis hin zur Entwicklung von Prototypen.

Im Laufe der letzten Jahre stellten wir fest, dass quasi Echtzeit Testbedmessungen einen kosten-, zeit- und arbeitskrafteffizienten sowie auch effektiven Ansatz zur Lösung dieses Problems darstellen: Dazu werden alle denkbaren Sendedaten zuerst offline in Matlab generiert. Diese werden dann je nach Bedarf über einen echten Funkkanal übertragen. Das für die Übertragung benötigte Feedback wird instantan in Matlab berechnet. Die Empfangsdaten selber werden nicht während der Messung, sondern erst danach in einem Rechnerverbund ausgewertet. Die gesamte Messung sowie die detaillierten Messdokumentation werden voll automatisiert durch ein einziges Skript gesteuert.

Die folgende Arbeit demonstriert das Potenzial dieser effizienten Messmethode am Beispiel von mehrantennen Einzelträger, HSDPA und WiMAX Messungen innerhalb sowie außerhalb von Gebäuden. Wir präsentieren die dabei erzielten Resultate als Durchsatz über Sendeleistung bzw. Durchsatz über Abstand der Sendeantennen.

Contents

Acknowledgements	viii
1 Motivation	1
2 Measurement Methodology	4
2.1 Basic Idea	4
2.2 Problem Formulation	6
2.3 Employing the Basic Idea	8
2.4 Data Collection	11
2.4.1 More Sophisticated Sampling Techniques	12
Sampling Homogenous Subpopulations	12
Sampling Spatially Autocorrelated Populations	13
2.4.2 Variance Reduction Techniques	15
2.4.3 Bias	17
2.4.4 Outliers	18
2.4.5 Parameter Estimation	19
2.5 Evaluating and Summarizing the Data	20
2.6 Statistical Inference	23
2.6.1 Inferring the Population Mean	23
2.6.2 Precision and Sample Size	24
2.6.3 Reproducibility and Repeatability	27
2.7 Measurement Automatization	29
2.8 Dealing with Feedback and Retransmissions	30
2.9 Summary and Criticism	32

3	Testbed Design	33
3.1	Basic Idea	34
3.2	Transmitter	36
3.3	Receiver	38
3.4	Synchronization	41
3.5	Possible Pitfalls	43
3.5.1	Digital Baseband Hardware	43
3.5.2	Tool and Component Selection	44
3.5.3	Analog RF Front-Ends	45
3.5.4	Cost	46
3.5.5	Matlab Code and Testbeds	47
3.6	Summary, Issues, and Criticism	49
4	On the Influence of Antenna Spacing	51
4.1	Indoor – Un-coded Single Carrier	52
4.1.1	Existing Research	52
4.1.2	Experiment I, 2×1 Indoor	54
	Results	55
4.1.3	Experiment II, 2×2 Indoor	57
	Results	59
4.2	Outdoor – HSDPA	63
4.2.1	Existing Research	63
4.2.2	Experiment III, 190 m Urban	64
	TX Antennas – Flat Panel 2X-Pol Antennas	64
	RX Antennas – Printed Monopole Antennas	66
	Performance Metric – HSDPA Throughput	67
	Measurement Procedure	69
	Plotting the Results	70
	Correcting for the Average Path Loss	71
	Results for Equal Polarization	73
	Results for X Polarization	76
4.2.3	Experiment IV, 460 m Urban	78
	TX Antennas – Flat Panel X-Pol Antennas	78
	RX Antennas – Printed Monopole Antennas	79
	Results	80

4.2.4	Experiment V, 5.7 km Alpine Valley	80
	RX Antennas – Rod Antennas	81
	TX Antennas – Flat Panel 2X-Pol Antennas	82
	Results	83
4.3	Summary and Criticism	84
5	On Antenna Switching	85
5.1	Motivation	85
5.2	Existing Research	86
5.3	Receive Antenna Selection	87
	5.3.1 Antenna Selection Based on System Throughput	88
	5.3.2 Hardware Aspects of Antenna Selection	89
5.4	Experiment VI - Urban 460m	90
	Results for $1 \times N_r$ HSDPA	91
	Results for $2 \times N_r$ HSDPA	93
5.5	Summary and Criticism	93
6	Conclusion and Outlook	95
	LTE - The Next Challenge	98
A	Bibliography	100
A.1	Self References	100
	A.1.1 Authored Book Chapters	100
	A.1.2 Authored Journals	100
	A.1.3 Authored Papers	100
	A.1.4 Authored Talks	102
A.2	Theses by Researchers Involved	103
A.3	Recommended Books by Other Authors	103
A.4	Journals and Papers by Other Authors	104
A.5	Existing MIMO Testbeds	109
A.6	Hardware Suitable for MIMO Testbeds	112
B	Statistical Inference – A Numerical Example	113
C	Kathrein Antennas	117

Acknowledgements

Developing a measurement system that barely fits in two rooms is never meant to be the work of a single person. That is why I have decided to write the following thesis in the first person plural—paying tribute to all the people that have helped me during the last few years:

First and foremost, I want to thank my very good friend Christian Mehlführer [29, 34] for the endless nights and weekends of coding. Regarding the measurements presented in Chapters 4 and 5, I owe much to José Antonio García Naya, Armin Disslbacher-Fink, and Michal Šimko for spending really freezing winter days mounting antennas and moving hardware from one building to another. On the radio frequency side I want to thank Lukas W. Mayer [32] and Robert Langwieser [33] for their endless support and the best working RF-modules I have ever used, and Constantine Kakoyiannis for providing me with printed monopole antennas [118, 119]. Regarding FPGA programming, I want to thank Christian Raschko, Klaus Doppelhammer, and Christoph Prieschl. Even if most of their work never got used, we have gained a lot of experience from it. I also want to thank my two professors, Arpad L. Scholtz and Markus Rupp for their support on a scientific, financial, and personal basis.

Unfortunately, developing a measurement system that barely fits in two rooms is also never meant to be a nine-to-five job. I therefore hereby want to thank my (girl)friend Martina for her understanding and support.

Finally, and most importantly, I want to thank my family, especially my mother and my father.

1. Motivation

Modern wireless communication systems rely on complex algorithms to extract the maximum performance from a radio link. They do so by exploiting the characteristics of a channel in an ingenious way. In the end —although it is sometimes a good benchmark— it is not the bit error ratio or the theoretically achievable capacity that counts, but the throughput actually achieved by the system under investigation.

Determining the throughput-performance of ingenious transmission schemes, on the other hand, is a different story. To do so, usually, the communication system is simulated in MATLAB and the channel¹ is replaced with sounded coefficients and/or a channel model—that is, in essence, a simplified numerical replica of reality. But what effects should be considered in such a model? What about quantization effects, power amplifier non-linearities, mutual antenna coupling, and phase noise? And, more importantly, are there *yet unknown* and maybe critical influences on the performance?

The alternative extreme is to build the entire system, or at least a prototype, to determine its performance under real-world conditions. Unfortunately, this approach also has some severe drawbacks; namely, it requires a lot of time, money, and manpower, in addition to offering little flexibility. For example, how to

¹ The wireless communication channel was originally presented by Claude Shannon in [55, p.5]. Including all antenna and communication effects, a channel suffers from imperfections of the hardware used as well as additive (thermal noise) and multiplicative distortions (characteristics of antennas, absorption, diffraction, reflection, and scattering), usually referred to as fading (path loss + shadowing + multipath fading).

test a new channel coding scheme in a short space of time? Hence, the usability of prototypes in “university-style” research is very limited.

Between those two extremes lies “testbedding”. The essence of testbedding is to make no assumptions on the channel at all (including DA/AD converters, mixers, amplifiers, antennas, etc.) but simplifying the wireless communication system at some other point, for example, real-time capability or equipment-size/mobility.

During the past five years we have tried many different measurement approaches, including channel sounding and real-time implementation, to determine the average throughput of communication systems under real-world conditions. We have found that —especially for our case of academic research which has limited financial resources— the testbedding approach presented in this thesis is very attractive due to its excellent trade-off between effectiveness and efficiency.

Our goal is to scientifically obtain throughput curves that show/compare the average performance of wireless communication systems in a specific, realistic scenario (like the .SVG² file shown in Figure 1.1) with one, fully automatized script.

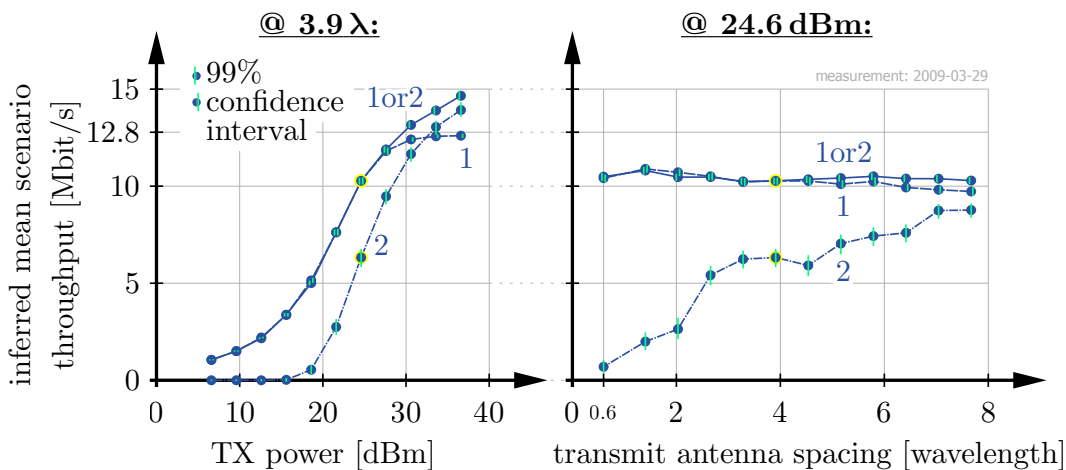


Figure 1.1: Measured throughput of different 2×2 HSDPA transmission modes (1, 2, and 1or2 streams) over transmit power and transmit antenna distance. See Section 4.2.2, page 64, for further details.

² SVG ... Scalable Vector Graphics is a standard to describe two dimensional vector graphics in XML-Syntax. We programmed our own plot functions for creating SVG files using MATLAB, which itself currently does not support *high quality* plot outputs.

Chapter Overview

This thesis is structured as follows:

In Chapter 2, the **measurement methodology** used to obtain the throughput of a mobile communication system is explained. Particular emphasis is placed on how to efficiently increase and gauge the precision of a measurement carried out. The Monte Carlo [54], sampling [48], experimental design [42, 43, 47], variance reduction [41], statistical inference [51], and bootstrapping techniques [38] thus required should have been well known for several decades. However, we could not easily find recently published paper in the area of communication engineering that, for example, presents confidence intervals for the results obtained therein.

The **testbed design** presented in Chapter 3 perhaps is —besides many others [147–189]— just another approach to building a piece of “publishable” MIMO measurement hardware. The engineering part of Chapter 3 was therefore kept short, yet describes all the parts of our testbed before listing possible issues regarding testbed design in general. What actually differentiates our approach from others is the quantity of efficiently produced measurement results [1–3, 6–9, 11–16, 18, 19, 22–25] showing more than scatter plots, estimated transfer functions, or estimated mutual information:

Exemplarily, Chapter 4 reports **on the influence of antenna distance** on the bit error ratio of a single carrier 4QAM MIMO, as well as on the physical layer throughput of a MIMO HSDPA transmission. Measurement results were obtained in realistic indoor, urban outdoor, and Alpine outdoor scenarios using realistic transmit and receive antennas.

Chapter 5 reports **on antenna switching**, presenting a new antenna selection criterion applicable to HSDPA and other mobile communication systems. The criterion takes into account the entire system design and is based on the SINR expressions describing the behavior of the whole link including the receiver, instead of using only channel state information.

A **Conclusion and Outlook** finally summarizes all the results that have currently been obtained and are planned to be obtained with the testbed presented in this thesis [1–9, 11–35].

For readers not familiar with statistical inference [48], bootstrapping [38], and (stratified) random sampling [48], an easy to follow numerical example is presented in **Appendix A**.

2. Measurement Methodology

When it comes to evaluating the performance of mobile radio communication systems, the most common method by far is computer simulations. Fortunately, much of the backbreaking work has been eliminated by the incredible amount of computing power and pre-defined toolboxes available nowadays. Although certainly convenient, such simplicity is bewitching.

As we will show in this chapter, measuring the performance of the physical layer of a mobile communication system can be *remarkably similar* to simulating it. The main difference is that a measurement has to obey the laws of nature. For example, one cannot just assume perfect channel knowledge, perfect frequency and timing synchronization, known noise variance, double-precision feedback, and so on. One also cannot measure a million independent channel realizations within a small scale fading scenario. Compared to simulations, all this may seem troublesome; on the other hand, reality is like this.

In other words, simulations reflect the simulation environment (and may reflect reality) while measurements do reflect reality.

2.1. Basic Idea

“Simulation is always a form of sampling experiment whenever the model contains one or more stochastic variables (although it is a very special type of sampling experiment since simulations are performed on abstract models instead of real-life objects)” [53, p.xi]. Figure 2.1 shows such an abstract model

which will henceforth be used to obtain the average throughput performance of a radio transmission:

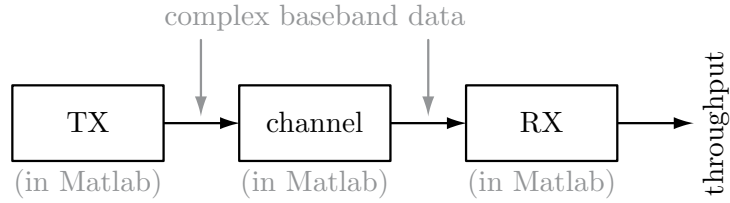


Figure 2.1: Simulating a sample for a throughput simulation.

The Monte Carlo simulation now works as follows:

1. *Random* complex-valued baseband data is created in the block named “TX”. Next, this data is sent through a *random* channel realization disrupted by *random*, usually Gaussian, noise. Finally, the resulting baseband data is decoded in the block named “RX” to calculate the throughput of one transmitted block.
2. The above transmission is repeated to receive an average throughput.
3. The above procedure is repeated to receive a set of average throughputs over the factor of interest (e.g. different TX power levels):

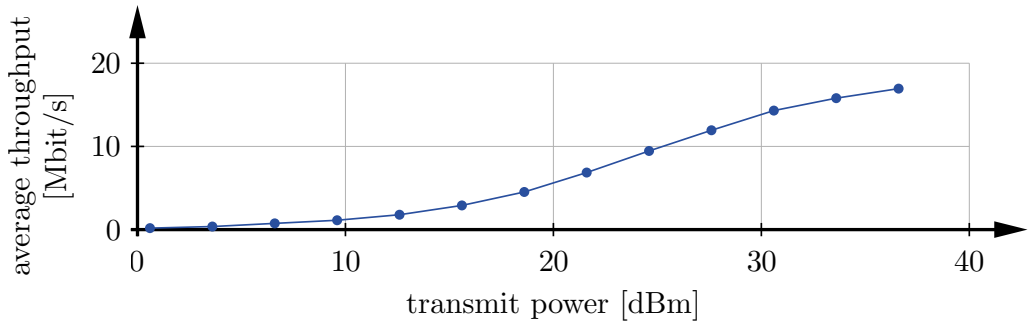


Figure 2.2: Average throughput versus transmit power.

Measuring the performance of a mobile communication system can be carried out in a very similar way by “simply” replacing the channel with some real hardware (in our case, a testbed); that is, transmitting the data in a realistic scenario over a wireless channel (see Figure 2.3):

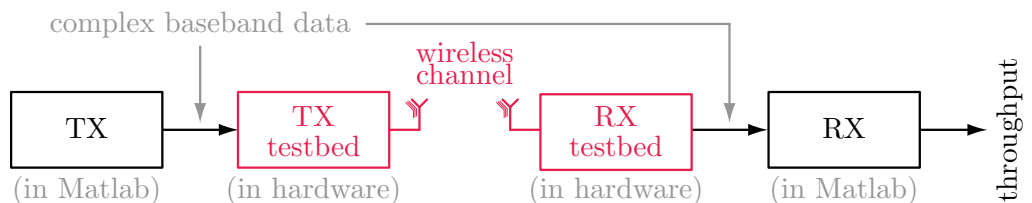


Figure 2.3: Measuring a sample for a throughput measurement.

However, the following differences to simulation arise:

- The different channel realizations created by moving the RX antennas of the testbed may not be independent and subject to drift.
See Section 2.4.1, page 12, on sampling and Section 2.4.3, page 17, on bias.
- The channel can be disturbed by undesired interference.
See Section 2.4.4, page 18, on outliers.
- The receiver cannot have genie driven knowledge of the channel and the timing.
See Section 2.4.5, page 19, on parameter estimation.
- The channel cannot be controlled as it can be in simulations. Especially, it is impossible to hold the channel constant over a given period of time or even to switch it back to a previous state.
See Section 2.6.3, page 27, on reproducibility and repeatability, as well as Section 2.8, page 30, on feedback and retransmissions.
- Measurement speed is limited due to the fact that a measurement cannot be parallelized on lots of computers. Neither is it possible to transmit faster than the actual transmission. Furthermore, changing the TX power (by using a programmable attenuator) or changing the RX antenna positions (by using a linear guide) takes a considerable amount of time. As a result, a thorough statistical design and analysis, especially regarding the required sample size, is needed.
See Section 2.6, page 23, on statistical inference.
- The quasi-realtime testbed design employed by us requires the transmitted data blocks to be pre-generated in MATLAB, stored on flash hard-disks for fast access, and then transferred to small but real-time capable FIFOs. Therefore, to speed up and simplify things, the TX blocks used may not be random but constant during one complete experiment.
See Chapter 3, page 33, for more details on our testbed.
- Starting a new experiment, the testbed may simply refuse to work as expected because, for example, a cable is loose.
See Section 2.3, page 8 on pretesting.

2.2. Problem Formulation

Compared to pure simulations, measurements usually require a frequently underestimated amount of money, manpower, and time. Unfortunately, this

amount can never be reduced to the level required for simulation, as the simulation itself is still required as “part” of the measurement to validate the measurement. Nevertheless, we still try to minimize our research expenses by simplifying our measurements compared to “commercial systems” in the following way:

- We only analyze the physical layer of radio communication systems, namely we do not investigate multi user scheduling and other higher layer issues.
- We only employ one TX and one RX unit with a maximum of four antennas each (16 each by employing switches in the radio frequency frontend). Therefore, we can only consider the up-/downlink scenario from a single base station to a single user. By measuring in an unused band we can later choose between having no interference at all (noise is only thermal) or adding interference from other previously made measurements with different TX locations in the digital domain (assuming that the receiver is linear).
- We only consider such scenarios on a block-by-block basis in real-time, that is, the time between blocks is short (some milliseconds) but typically longer than in most real systems.
- We do not put constraints on the size of our TX and the RX unit. Currently, they are as big as a small table.
- We use more sophisticated radio frequency hardware than a low-cost commercial product would. We do so for three reasons. Firstly, to carry out the very precise measurements required by some experiments. Secondly, to be prepared to meet the specifications of future communication systems. Thirdly, to easily evaluate the throughput-impact of a commercial component by comparing it to our “reference” (for example, the impact of a low-cost, noisy oscillator).
- We (optionally) employ external synchronization in frequency and time (see Section 3.4, page 41). This gives us the choice to measure with no, a constant, or a randomly selected frequency offset.
- We implement all necessary algorithms in MATLAB/C in floating point. In addition to being “feasible”, this gives us all the flexibility needed to quickly change the code if new ideas arise that need to be tried out (for example, LDPC instead of Turbo channel coding).
- We measure systems employing feedback only in sufficiently static sce-

narios in order to have enough time for calculating the feedback and, as a result, the required new transmit signal (see Section 2.8, page 30).

Given the above-mentioned simplifications, our goal is to **scientifically** compare the **performance** of given **wireless communication schemes** in specific, **realistic scenarios**.

In the aforementioned goal

- **scientifically** “suggests a process of objective¹ investigation that ensures that valid conclusions can be drawn from the experimental study” [43, p.3]. Furthermore we want this process to not only be effective, but also efficient².
- **performance** may be, for example, expressed in terms of average throughput or median bit error ratio.
- **wireless communication schemes** can be, for example, simple single carrier uncoded transmissions or more complex systems such as WiMAX or HSDPA. Their actual implementation, however, is not of importance for our measurements as long as a MATLAB code for the transmitter and receiver exists.
- **compare** means that we have to be able to measure different communication systems using the same hardware over channels that are as similar as possible, that is, to transmit the block with scheme two immediately after the one with scheme one.
- **realistic scenarios** are, for example, indoor-to-indoor, outdoor-to-indoor, and outdoor-to-outdoor urban/sub-urban/Alpine scenarios. For us, a realistic scenario also includes the usage of realistic antennas, as for example, 60° flat panel X-polarized antennas at the base-station. Monopole antennas at the base-station are not realistic in our opinion.

2.3. Employing the Basic Idea

To reach the above stated goal and produce, for example, Figure 2.6, we perform five basic steps:

¹ “independent of individual thought and perceptible by all observers” [56]

² The difference between effectiveness and efficiency is easily visualized by the following example: Killing a fly with a sledgehammer is effective, but not efficient.

1. We design a testbed that enables us to transmit baseband data pre-generated in MATLAB over realistic channels (see Chapter 3, page 33).

In the case of Figures 2.4, 2.5, and 2.6, the testbed has to transmit blocks of 2×2 HSDPA and 2×2 WiMAX that are already stored in its memory. (Details of the 2×2 HSDPA [9] and 2×2 WiMAX [2] systems as well as the scenario in which we measured this curve (see Section 4.2.2, page 64) are not important to understand the following sections. The techniques presented from here onwards work with virtually any MATLAB code representing the transmitter and receiver of a communication system.)

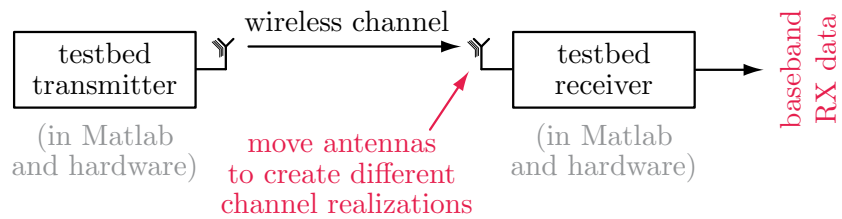


Figure 2.4: Measuring a sample of baseband data that in a subsequent step is automatically converted by a cluster of PCs (see Section 2.5, page 20) into the corresponding throughput values.

2. We carry out a pretest [48, p.7], that is, we collect a very few observations of the experiment outcome.

We do so to find and solve problems before spending a lot of time on a complete measurement, only to discover afterwards that, for example, a cable was not mounted correctly and the throughput is just zero all the time.

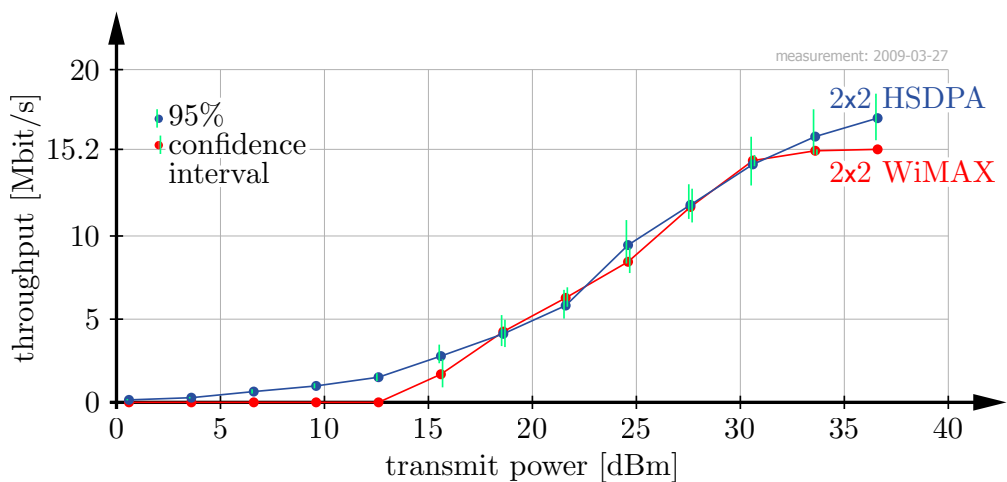


Figure 2.5: Inferred mean throughput performance of a scenario using only 20 throughput observations: By visual inspection we conclude that measurement works.

3. We continue collecting measurement data, that is, we collect a representative sample of the population of interest (see Section 2.4, page 11).

In the case of Figures 2.5 and 2.6, the target population is the aggregate of all possible throughputs in a specific urban scenario.

4. After evaluating the measured baseband data by a PC cluster, we summarize and analyze the data obtained, that is, we draw inferences from the collected sample to plot graphs or tables showing estimated parameters of the target population (see Section 2.5, page 20).

In the case of Figure 2.6, the average throughput of the scenario is inferred from the measured sample. Having no other information than the throughputs of our sample at hand, the “best” estimate for the population mean is the sample mean [80] (see Section 2.6, page 23). Figure 2.6 plots this estimated throughput versus transmit power.

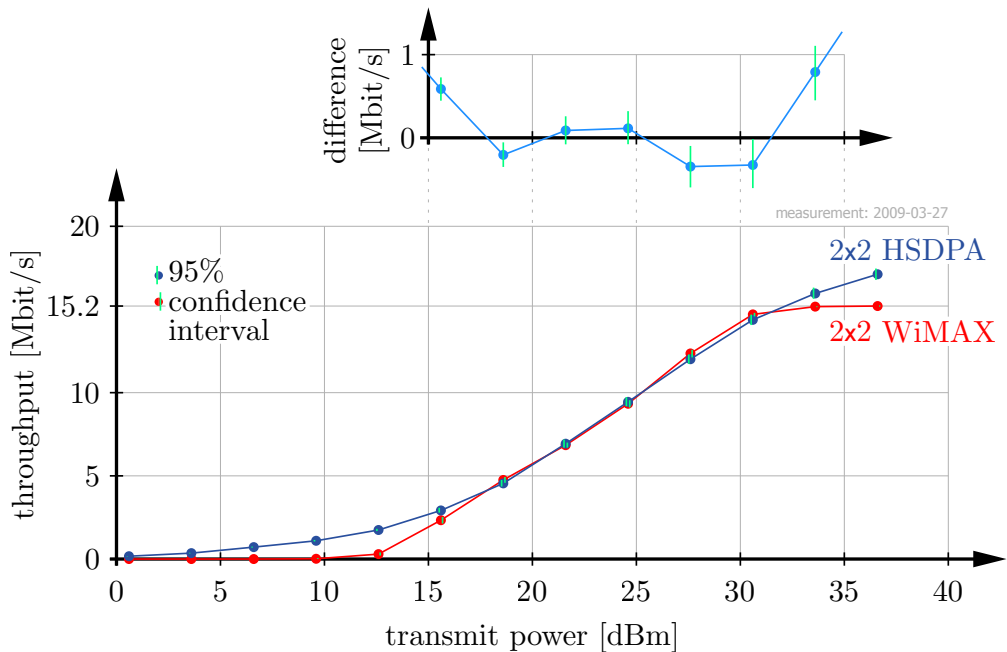


Figure 2.6: Inferred mean throughput performance (of the scenario pretested in Figure 2.6) using all 434 throughput observations. Note that the size of the confidence intervals is considerably smaller than in Figure 2.5.

5. We determine the precision of our results (see Section 2.6, page 23).

In the case of Figure 2.6, we draw the 95% BC_a confidence intervals for the mean, that is, 95% of the confidence intervals are supposed to cover the population mean of interest.

6. We compare our results to previously measured results and theoretical bounds (as, for example, the mutual information) to check for plausibility.
7. If possible, we use the results and experience gained to upgrade our testbed and measurement procedure. Then we continue with Step 2.

2.4. Data Collection

Having a testbed that can transmit a given block of data, we identify three sources of variation in our experiment set-up (see Figure 2.7):

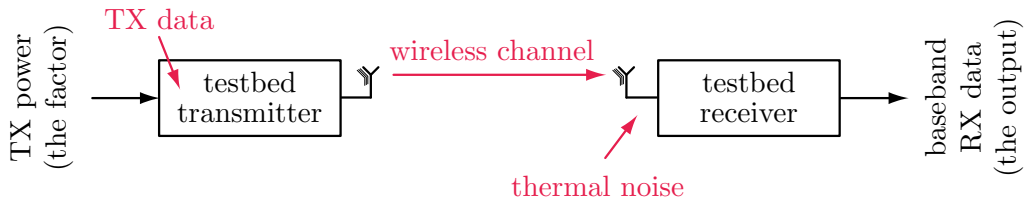


Figure 2.7: Measuring a sample.

1. the **TX data** to be transmitted that consists of many different bits: we are interested in the performance for all combinations.
2. the **wireless channel** that is determined by the measurement scenario as well as the TX and RX antenna positions: we are interested in the performance for a small area, lets say 3×3 wavelengths ($=36 \text{ cm} \times 36 \text{ cm}$)³.
3. **thermal noise** that disturbs the received signal: we measure in unused frequency bands to ensure no expected interference from other sources.

The output⁴ of a single transmission carried out by the testbed consists of baseband data samples that can be evaluated to obtain, for example, a throughput. The input⁵ to our experiment is, for example, the transmit power for which we want to infer the average throughput of a scenario.

³ By considering only such a small area, we exclude large scale fading effects in our investigations.

⁴ The literature knows many names for the output of an experiment, for example, dependent variable, the observed values, the explained variable, the response variable, or the outcome variable [38–54].

⁵ The literature also knows many names for the input of an experiment, for example, the independent variable, the controlled variable, the explanatory variable, or the manipulated variable [38–54].

In order to obtain parameters of the target population, one method would be to conduct a census, that is, measuring *all* possible combinations of input signals, channel realizations, and noise—or in other words, *all* items of the target population. Obviously, this is not possible.

Fortunately, collecting a *representative* sample for a given transmit power is easy: Fix the transmit power and observe the throughput for

1. a block of random transmit data (by using a pseudo-random generator),
2. a random channel realization (by moving the RX antennas to a pseudo-random position and rotation within the area of interest⁶), and
3. random noise (by ensuring that there is no interference).

When collecting such a “simple random sample”⁷, the precision can then be doubled by quadrupling the sample size⁸ (see Section 2.6, page 23).

For those not familiar with sampling and statistical inference, Appendix B, page 113, presents an easy to follow numerical example explaining most of the important terms and ideas used in the following sections.

2.4.1. More Sophisticated Sampling Techniques

“The art of sampling consists in making the most efficient use of available resources so as to afford the best possible estimate concerning the quality of a population under consideration as is consistent with the ever-present limitation in time and funds” [44, p.15]. “The purpose of sampling theory is to make sampling more efficient” [48, p.8].

Sampling Homogenous Subpopulations

The first goal is stratification, that is, dividing the heterogenous population of interest into subpopulations—so called strata—that by themselves experience a smaller variation than does the entire population as a whole⁹. Having such homogenous subpopulations at hand, their mean can be precisely estimated

⁶ Note that we define the scenario to be investigated by the area and orientations our receive antennas can cover. Otherwise we would not be able to sample the target population.

⁷ In simple random sampling, at each draw, every possible item of the population should have the same probability of being chosen [48, p.18].

⁸ “For a random sample of size n with variance σ from an infinite population, it is well known that the variance of the mean is $\frac{\sigma^2}{n}$ ” [48, p.24].

⁹ Stratification may be used for other reasons, variance reduction being just one of them.

by using only a few samples. A precise estimate for the whole population can then be obtained by combining the subpopulation means. “If intelligently used, stratification nearly always results in a smaller variance for the estimated mean or total than is given by comparable simple random sampling” [48, p.99]. See also page 115 for an easy-to-follow numerical example.

In our example the variation of the throughput introduced by different transmit bits is much lower than the variance introduced by the different channel realizations. In the case of un-coded single carrier 4 QAM transmissions, we can even conduct a census in our subpopulation, that is, measuring all four symbols of the 4 QAM. In the case of HSDPA, simulations and experience have shown that measuring many channel realizations at the cost of only transmitting one deterministic block¹⁰ of data does indeed reduce the variance of the sample collected. The same holds true for WiMAX.

Sampling Spatially Autocorrelated Populations

Regarding the wireless channel, simple random sampling is also not the best method. As shown in Figure 2.8 we have to deal with spatial data where the observations are correlated due to their positions in space. Simply speaking, sampling at distances below 0.2 wavelengths (2.4 cm) ceases to work efficiently because it just repeats the same values. For this case of autocorrelated populations experiencing negative exponential correlation functions (see the spatial correlograms¹¹ in Figure 2.8), the literature suggests the use of *systematic sampling*, that is, sampling a grid of fixed size, thus minimizing correlation [51, p.180]. However, systematic sampling is not only an efficient procedure but also a dangerous one, especially when periodic variations exist in the area to be sampled. In the end, the choice of sampling procedure is a tradeoff between the loss of precision due to correlation and possible errors introduced by the systematic sampling approach [48, p.221]. See [51, p.180 and follows] for a detailed analysis of this topic.

To measure, for example, 324 different throughputs in an area of 3×3 wavelengths (36×36 cm), we utilize a fully automated $XY\Phi$ positioning table that can move the receive antennas along its x and y-axis, as well as rotate them (see Figure 2.9).

¹⁰Measuring less than a complete block is not possible because of the coding that requires a complete block to be transmitted over a constant channel.

¹¹A correlogram plots the correlation of items some distance (x-axis) apart over this distance.

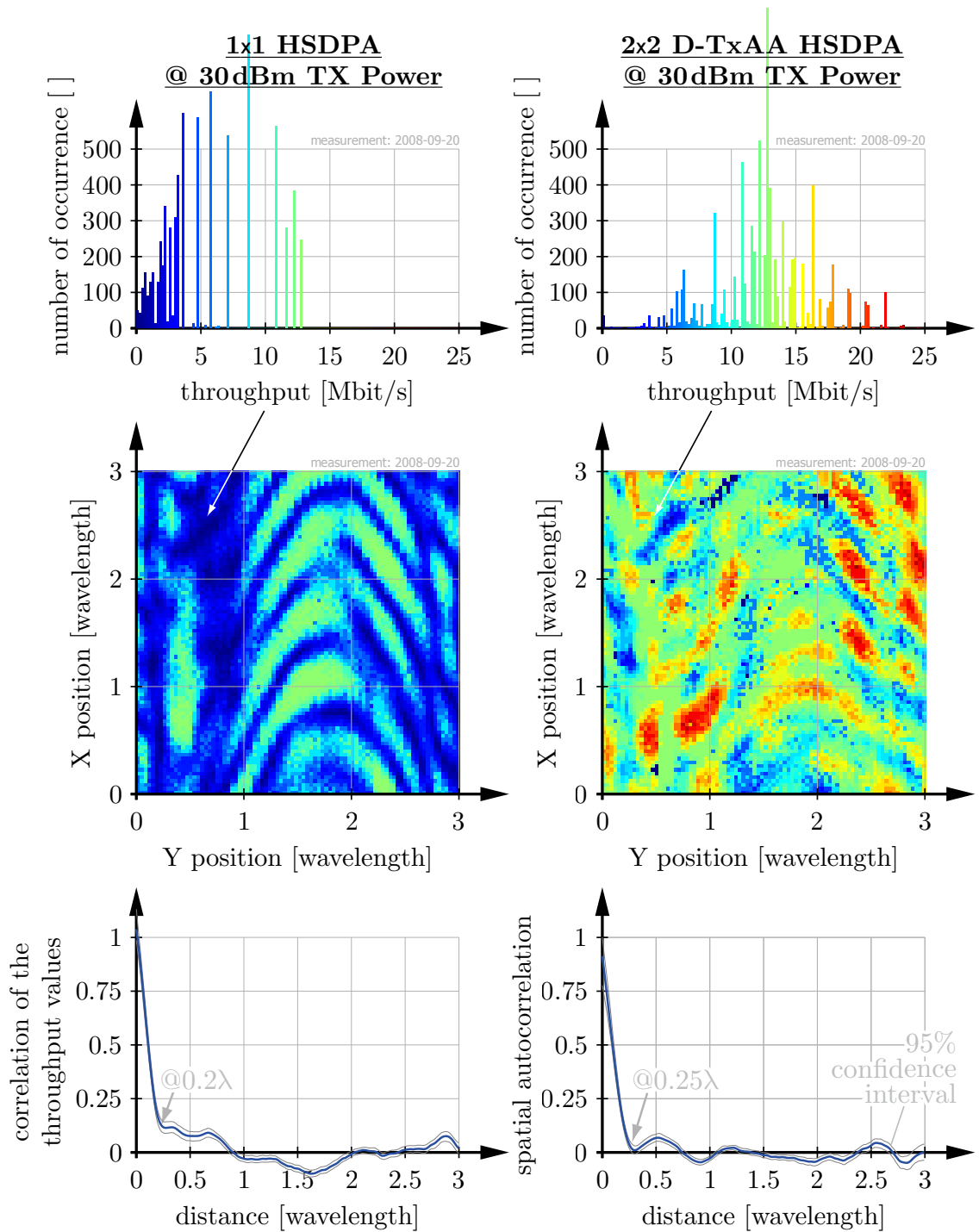


Figure 2.8: To visualize the spatial correlation observed in 1×1 and 2×2 HSDPA, we systematically sampled (see also Figure 2.9, page 15) an area of 3×3 wavelengths to obtain 7360 throughput observations.

The top of the figure shows two histograms, the middle two XY-plots, and the bottom spatial correlograms (see [79] on how they are constructed) for these measured throughput values. Note that for distances larger than a quarter of a wavelength, the throughputs turn out to be uncorrelated ($|\rho| < 0.2$).

- To reduce vibrations created by very fast moving/accelerating antennas, we employ a very heavy, low profile, “tank-proof” constructed positioning table.
- To minimize the effects of possible periodic variations, we make sure that the x and y position increments are some prime value, that is, 0.17 in our case ($\approx 3/\sqrt{324}$). Then we position the table such that its axes do not run parallel with the walls of the room. This helps us to determine later whether the metal of the table has influenced the measurement.

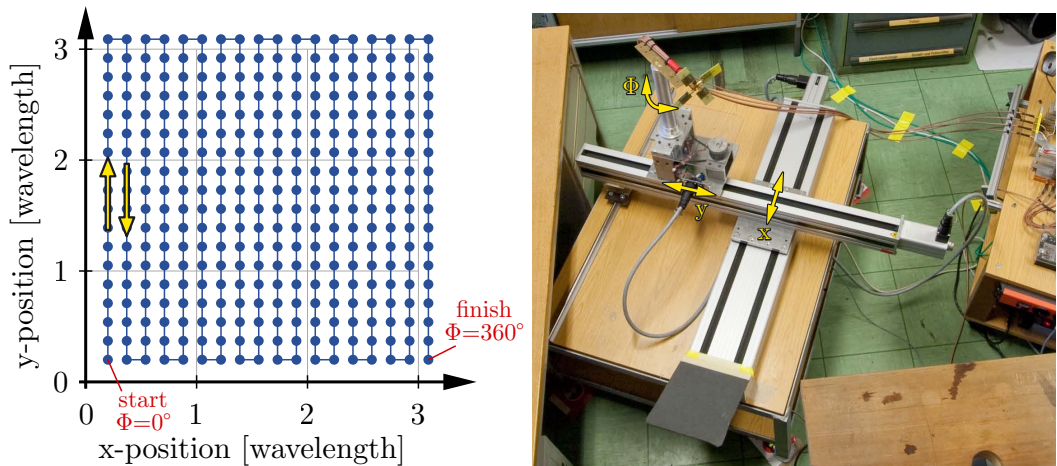


Figure 2.9: Systematically sampling an area of $3 \times 3 \lambda$.

We measure 324 positions as follows (see Figure 2.9):

- We move the antennas on the XY Φ positioning table to the reset position of $x=0\lambda$, $y=0\lambda$, and $\Phi=0^\circ$.
- Starting at an offset of $0,2\lambda$ (due to mechanical reasons specific to our linear guide), we first move the antennas in the direction of the linear guide on the top to reduce vibrations.
- During the measurement, we rotate the antennas increasingly from 0° to 360° . As the rotation unit employed by us is very slow compared to the linear guides, we are forced to only utilize such small rotation increments to keep the measurement time low.

2.4.2. Variance Reduction Techniques

When inferring, for example, the mean of a target population, increasing the sample size is by no means the only way of enhancing the estimate’s precision. As shown above, for example, employing more sophisticated sampling

techniques might be an easier alternative. More generally, D.C.Handscomb calls a technique variance reducing “if it reduces the variance proportionately more than it increases the work involved” [46]. Because such techniques have been well known in the literature for decades (see for example [41] from 1935), we only briefly mention here the most important ones used in our experiments:

- **Comparison:** As it is very hard to reproduce measurement results exactly (see Section 2.4.3, page 17, on bias), comparing different communication schemes is far more accurate [47, p.23].

For example, we compare 2×2 HSDPA with 2×2 WiMAX in Figure 2.6, page 10. Note that the confidence intervals shown in this figure only account for the precision of the estimates, not for their accuracy.

- **Local Control:** This includes transmitting the schemes to be compared (**grouping**) immediately after each other over the same channels (**blocking**), equally often (**balancing**) [43, p.316].

For comparing 2×2 HSDPA with 2×2 WiMAX in Figure 2.6 this means that we transmit WiMAX and HSDPA for different TX powers over the same different channels, and not in some other order (see also Section 4.1.2, page 54, on how we measured over antenna distance). The goal of local control is to keep the measurement conditions as similar as possible for the different schemes to be compared over time, since, for example, snow may fall during the measurement and change the channel (see Section 2.6.3, page 27, on reproduceability).

- **Randomization:** At first, randomizing the order of the transmitted blocks allows for “time trends to average out” [42, p.5]. In addition, randomization ensures that all transmitted blocks face —on average— the same measurement conditions (for example regarding training, antenna swing¹², and interference from adjacent blocks [47, p.19]). The third reason for randomization is to avoid the measurement fitting some pattern in the uncontrolled variation producing systematic errors [47, p.74].

For comparing 2×2 HSDPA with 2×2 WiMAX in Figure 2.6, page 10, this means that we randomly shuffle the order of the adjacent HS-

¹²When moving, for example, 25 kg base station antennas quickly from measurement to measurement position, they will never be absolutely static.

DPA and WiMAX blocks. For the comparison of different single carrier schemes in Figure 4.9, page 58, this means that we shuffle the blocks around the training sequence in a random way. In Figure 4.25, page 74, we also shuffled the different schemes measured. Nevertheless, even if in principle the best would be to shuffle everything, we did not always do so in order to keep things simple and avoid errors (which are really hard to detect).

- **Factorial Experiments:** When evaluating the influence of several factors on a transmission, the use of one-factor-at-a-time experiments¹³ is not advisable [43, p.316], as the factors may jointly influence the response.

See Chapter 4, page 51, on experiments carried out jointly investigating transmit-power, antenna-distance, and antenna-polarization.

- **Concomitant Observations:** A supplementary (concomitant) observation that is correlated with the observations of interest can be used to increase precision [47, p.48].

See, for example, Section 4.2.2, page 71, on how we corrected for the average path loss of MIMO transmissions by using the corresponding SIMO transmissions.

2.4.3. Bias

Systematic errors, or so called bias, “affect all measurements in the same way, pushing them in the same direction” [52, p.103]. This fundamental property is, on the one hand, a real godsend as it does not introduce any error when looking at the difference between two measured communication systems—and that is what we do¹⁴. On the other hand, a bias is hard to detect. The only way is to compare the measurement result to some external standard, such as a measured throughput curve to a mutual information curve, a simulation result, or a result obtained using different measurement equipment. In any case, detecting biases is a very demanding, (boring, in no way publishable) yet necessary Sisyphean

¹³for example, only investigating antenna distance while keeping the transmit power and polarization constant.

¹⁴The absolute position of the curves in the figures plotted is never really of interest for us. What we are interested in is their relative positions. A bias would shift all curves alike, thus not change their relative positions.

task¹⁵ best to be started by measuring uncoded single carrier SISO schemes over a coaxial cable instead of a channel.

2.4.4. Outliers

An outlier is “an observation which deviates so much from the other observations as to arouse suspicions that it was generated by a different mechanism” [49, p.1]. For example, the marked observation in Figure 2.10 is more than ten standard deviations away from the mean. Such an extreme off measurement result should, at least, attract our attention.

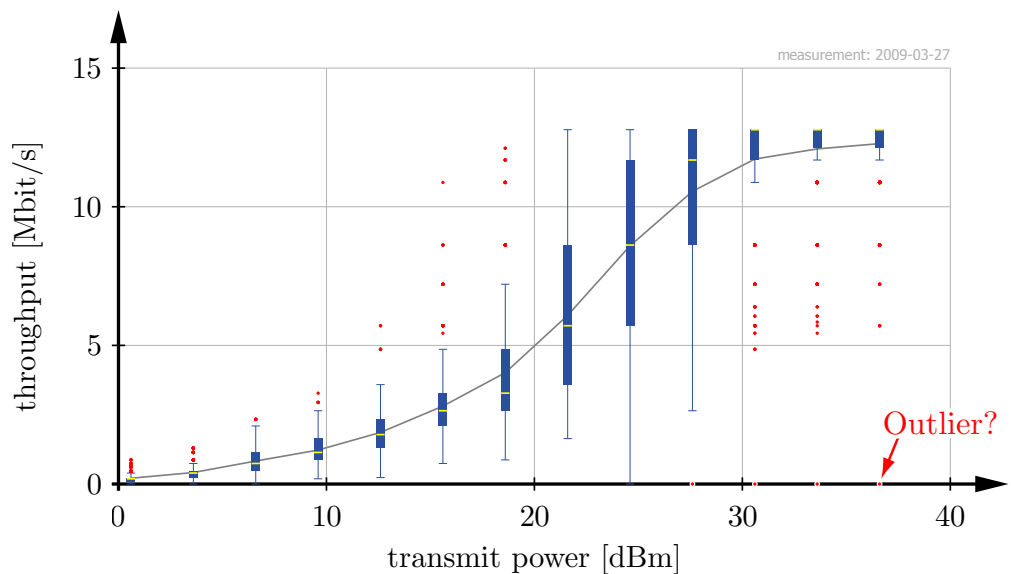


Figure 2.10: Boxplot of 434 samples taken at different TX power levels. Note the marked zero-throughput observation.

Outliers can arise due to errors in the measurement or its execution [50, p.28]. Possible causes may be:

- equipment malfunction
- unexpected, typically not repeating events such as door-slam, people moving through the room, or window washers climbing on the facade in front of the antennas.

Such errors can be detected by examining web-cam pictures, or prevented by blocking access to the measurement site.

¹⁵A personal piece of advise for those wishing to build a testbed by themselves: Do not underestimate the work needed to test and validate a testbed, it takes *at least* a year.

- interference from other transmitters in the same frequency band

The way we detect undesired interference is remarkably simple, yet effective and not dependent on the data transmitted. As shown in Figure 2.11, page 20, we do not transmit anything immediately adjacent to the data frames. These “noise gaps” can then be used in the evaluation to detect deviations from the known¹⁶ noise power, thus identifying interference that is usually not shorter than a transmitted block.

- errors in the MATLAB code

Since the received data samples are stored for off-line evaluation it is easy to step through the MATLAB code of the receiver in order to find possible errors¹⁷.

On the other hand, outliers may also arise due to inherent variability in the measurement result [50, p.27], that is, the population measured is simply not as homogenous as we might believe.

In the case of Figure 2.10, page 18, the marked outlier may at first glance look like a measurement error. We searched for its cause to find possible flaws in our measurement set-up but could not find one—therefore we did not reject the zero throughput observation, as it might be a legitimate part of the measurement result¹⁸.

2.4.5. Parameter Estimation

In order to obtain realistic estimates we need training that is separate from our data. Ideally this training would come in the form of some new data from the same population that produced the original samples. If the transmission scheme itself does not include a preamble (as, for example, WiMAX) we additionally transmit a known training sequence (see Figure 2.11). Using the data to be received in a genie driven procedure to estimate the channel, which is then used for maximum likelihood decoding, is a dangerous procedure (because the genie-driven knowledge can lead to unrealistic results).

¹⁶Since noise is thermal, its power is expected to remain constant during the course of a measurement.

¹⁷Some errors do not affect pure simulations, especially those arising from unanticipated real world channel conditions.

¹⁸A possible explanation: In the scenario we measured 1×1 HSDPA. This communication system is designed to have a block error ratio of 10%. One block may be retransmitted twice, resulting in about 1‰ of blocks with zero throughput. At 434 blocks measured, the probability of observing an “outlier” is in the order of 50%.

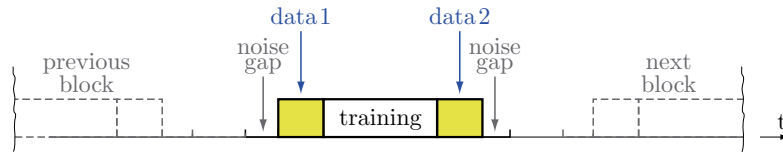


Figure 2.11: Obeying the principles outlined in Section 2.4.2, page 15, we use the data transmitted to compare the throughput of “data1” and “data2” (comparison) by transmitting them immediately next to each other (blocking), randomly shuffling their order (randomization).

In order to estimate the SNR at the receiver independently of the transmission scheme used (nonparametric) we obtain two intermediate estimates for each block received (index i):

- $P_{i,\text{signal+noise}}$, the average power of the signal received, that is, also including noise
- $P_{i,\text{noise}}$, the power of the noise estimated in the noise gaps before and after the signal (see Figure 2.11)

These intermediate estimates are then averaged over all blocks transmitted. Since noise and data are uncorrelated, the estimated average SNR can be easily calculated using the equation:

$$\overline{\hat{\text{SNR}}} = \frac{\hat{P}_{\text{signal}}}{\hat{P}_{\text{noise}}} = \frac{\text{average}(\hat{P}_{i,\text{signal+noise}}) - \text{average}(\hat{P}_{i,\text{noise}})}{\text{average}(\hat{P}_{i,\text{noise}})}$$

Note that the averaging has to be carried out before the nonlinear division (see J. L. W. V. Jensen from 1906 [81]).

2.5. Evaluating and Summarizing the Data

To evaluate our measurements, we employ a self written cluster software that is set up for the parallel processing of large data sets on standard Windows-PCs. The basic idea is simple:

- During the measurement, the complex-valued received data is collected at the receiver site in the form of one large file per RX antenna position (for example, 434 files requiring 1.5 GBytes each). In addition, a central server is informed each time data for a new receive position becomes available.
- Employees leaving their workplace at night start a simple client program for every processor core they want to make available for carrying out our

evaluations. This client program then contacts the server, checks for the availability of a new RX antenna position, copies the data required for the evaluation, evaluates it, and finally writes the results of the evaluation back to the server.

- The progress of the current evaluation can easily be checked at the central server. Furthermore, the results of the previously calculated RX antenna positions can be gathered at any time during the calculation, so the data can be easily pre-tested, pre-analyzed, and pre-summarized.

During the last three years, we have identified two critical bottlenecks in this procedure. Depending on the type of evaluation required their influence varies greatly (for example, many different channel estimators using the same received data, or very simple receivers each using different receive data):

1. **Time to copy the data:** For example, just copying 500×1.5 GBytes = 750 GBytes of data takes a theoretical minimum of about 16 hours on a 100 Mbit/s local area network. During the last three years, we actually reduced this time by a factor of more than ten by employing gigabit Ethernet connections¹⁹, dedicated high performance servers, and optimized server to client data transfer.
2. **Calculation time:** Here things are straightforward as the evaluation can be split over several computers on a position-by-position basis. Doubling the number of clients available halves the time required for evaluation. In typical numbers this means that 50 clients need one day for an evaluation that would otherwise require about 50 days on a single core.

The evaluation results stored on the server are then automatically combined to calculate the desired result. For example, gathering the calculated throughputs at each RX antenna position²⁰ and TX power produces, averaged over the 434 RX antenna positions measured, the graph shown in Figure 2.12.

¹⁹At first, we had to set up our own gigabit Ethernet connections. Recently, the infrastructure of our institute has been upgraded to gigabit Ethernet.

Note that employing gigabit Ethernet instead of 100 Mbit/s Ethernet only allows for an approximate threefold increase in speed in practice, due to excessively slow client computer components. This limitation was overcome by transferring data to several clients simultaneously.

²⁰RX antenna position or, in other words, channel realization

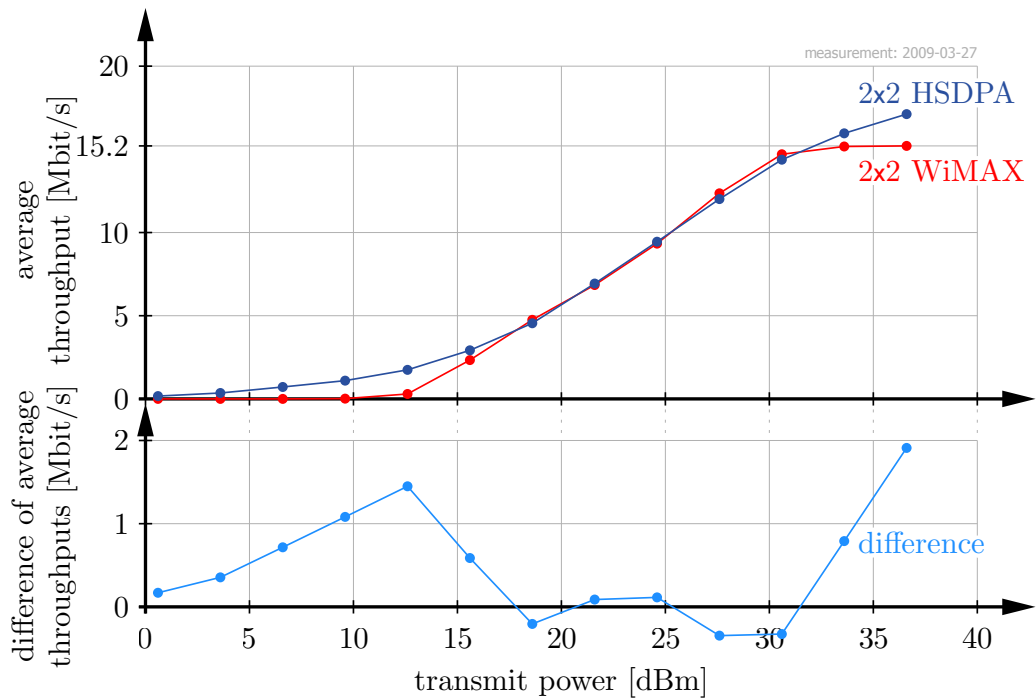


Figure 2.12: Average throughput of the measured HSDPA and WiMAX sample (and the corresponding difference) over TX power.

As average values tell us only little about the distribution of the sample, cumulative probability functions can be drawn to provide further insight:

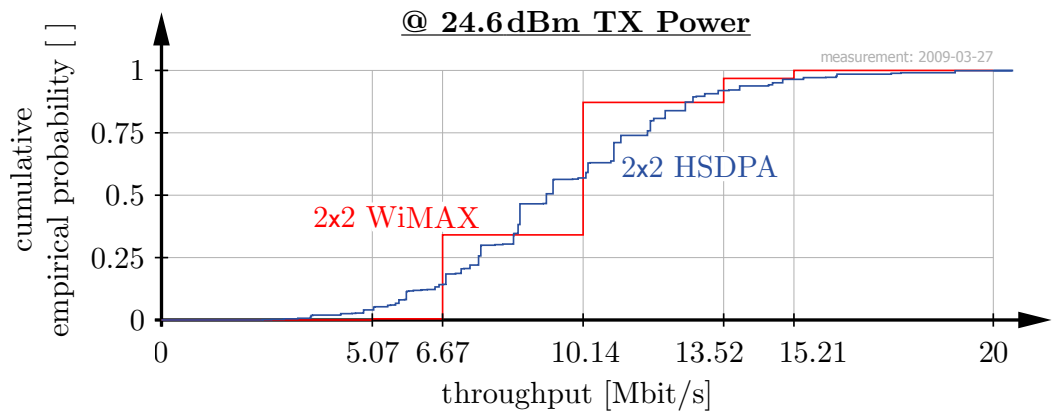


Figure 2.13: Cumulative empirical probability of the 434 HSDPA and WiMAX samples measured at a transmit power of 24.6 dBm.

Since HSDPA offers 256 [120, Table 7I, pp. 54] different modulation and coding schemes in contrast to seven [123, Section 8.3.3.2.3] in the case of WiMAX, the HSDPA curve shows a much finer granularity.

The corresponding boxplot is shown in Figure 2.14:

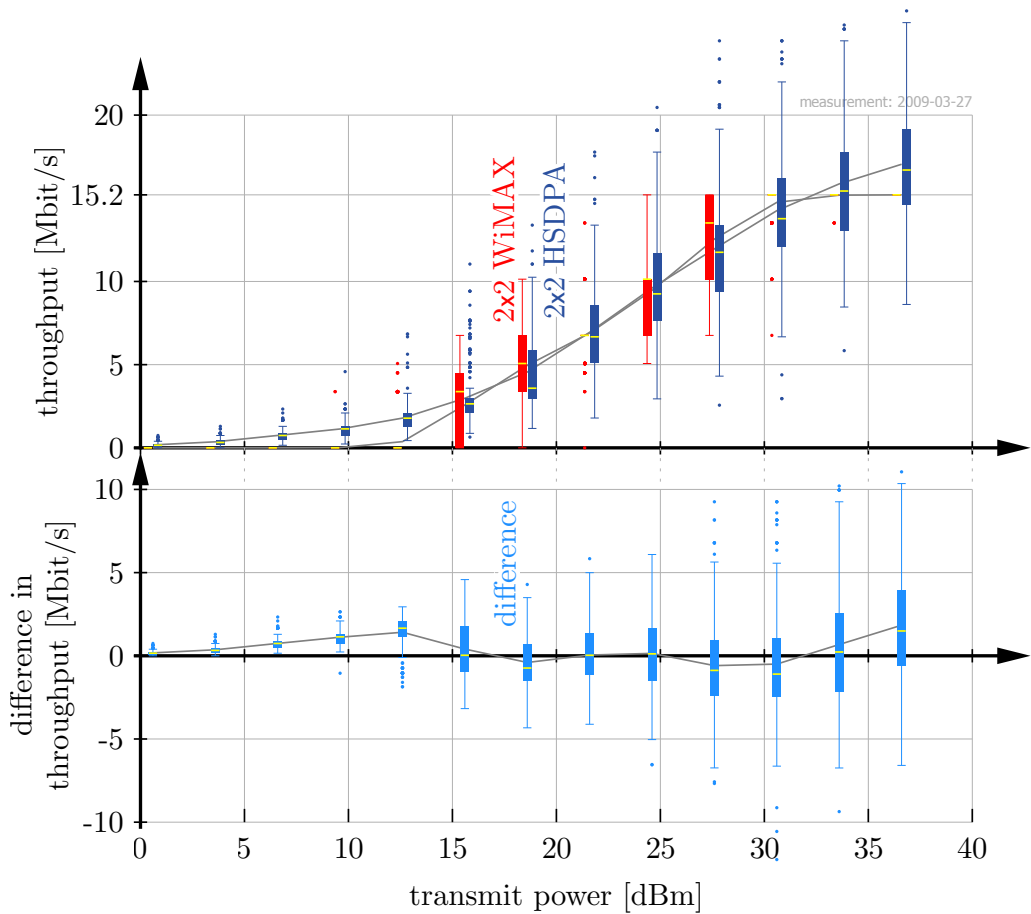


Figure 2.14: Boxplot of the HSDPA and WiMAX throughputs measured for the same TX powers (the boxplots have deliberately been shifted to avoid overlap).

2.6. Statistical Inference

Once a representative sample of the population of interest has been collected (see Section 2.4, page 11), we are not only interested in summarizing this sample but also in inferring population parameters. That is the goal of statistical inference—to say what we have learned about the population from the sample [38, p.18].

2.6.1. Inferring the Population Mean

The left-hand side of Figure 2.15 shows the average throughput of 434 samples obtained per transmit power. The calculated value is exact (which is why

no confidence intervals are drawn), as there is no doubt about the average throughput actually achieved *given* the collected sample because WiMAX and HSDPA receivers use deterministic algorithms.

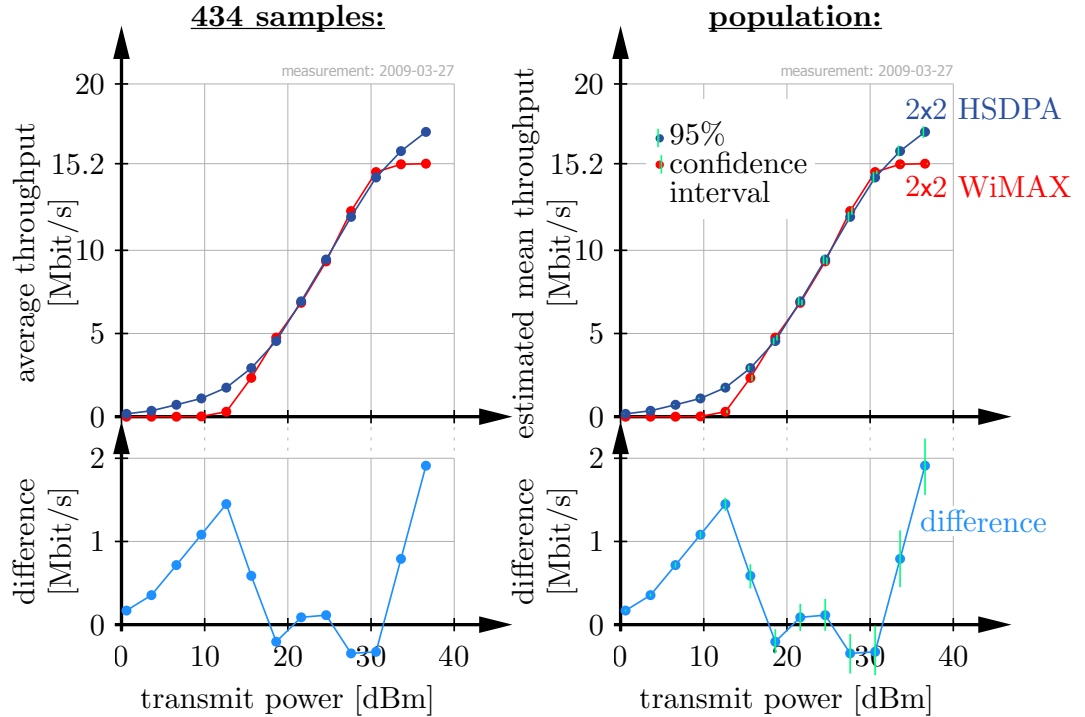


Figure 2.15: Sample average = estimated population mean.

If now all samples receive the same weight, the sample average is the *only* unbiased estimator for the population mean [80]. If there is no other information about the population than the sample obtained this estimated mean also “cannot be improved on” (see plug-in principle, [38, p.37]).

2.6.2. Precision and Sample Size

In complicated situations, gauging the uncertainty of an estimate based on an assumed probability model is “tedious and difficult”. In addition, inappropriate simplifications and assumptions may lead to potentially misleading results [40, p.1]. The Bootstrap is a recently developed technique for avoiding such calculations. It is “a computer-based method for assigning measures of accuracy to statistical estimates” thereby “aiming to carry out familiar statistical calculations like confidence intervals in an unfamiliar way: by purely computational means, rather than through the use of mathematical formu-

lae”. [38, p.10,p.392] “The nonparametric bootstrap²¹ is a fairly crude form of inference that can be used when the data analyst is either unable or unwilling to carry out extensive modeling. Nonparametric bootstrap inferences are asymptotically efficient - that is, for large samples they give accurate answers no matter what the underlying population.” [38, p.395]. Nevertheless, the real power of the bootstrap lies in the analysis of small data sets from an unknown population—and that is what we do here.

Simply speaking, the bootstrap does —through resampling of the few observations obtained— what we “would do in practice if it were possible: repeat the experiment” [39, p.4]. The new sets of observations thus created are then used in a subsequent step to calculate, for example, confidence intervals. The inferences of the thus used percentile-t, BC_a , or ABC algorithm [38] “are not perfect, but they are substantially better than most in the other traditional inference methods” [38, p. 393]. As programs such as MATLAB are already equipped with ready to use functions²² we will skip the details of the algorithms and refer the interested reader to Appendix B, page 113, for an easy-to-follow numerical example as well as [38] for additional theoretical background.

Being able to gauge the precision of the results is important in order to determine the number of measurements needed to reach the desired degree of precision. Looking back at the 434 observations measured in Figure 2.15, page 24, the right-hand side also shows next to the estimated population mean (that is, the sample average) the corresponding 95% bootstrap BC_a ²³ confidence intervals (that is, 95% of the confidence intervals are supposed to cover the true, for us unknown, population mean²⁴).

²¹Experience has shown that the use of a non-parametric bootstrap approach is more accurate than a parametric bootstrap approach with incorrect model assumptions [39, p.28].

²²The MATLAB function for the BC_a algorithm is `bootci()`, whilst for the accelerated ABC algorithm a built-in function does not exist but can be downloaded from the internet. The R function for the BC_a algorithm is `boot.ci{boot}`. For the accelerated ABC algorithm it is `abc.ci{boot}`.

²³bias corrected and accelerated [38, p.176]

²⁴Because “the chances are in the sampling procedure, not in the parameter”, it would be wrong to say that the true population mean is covered by a given confidence interval with a probability of 95% [52, p.384].

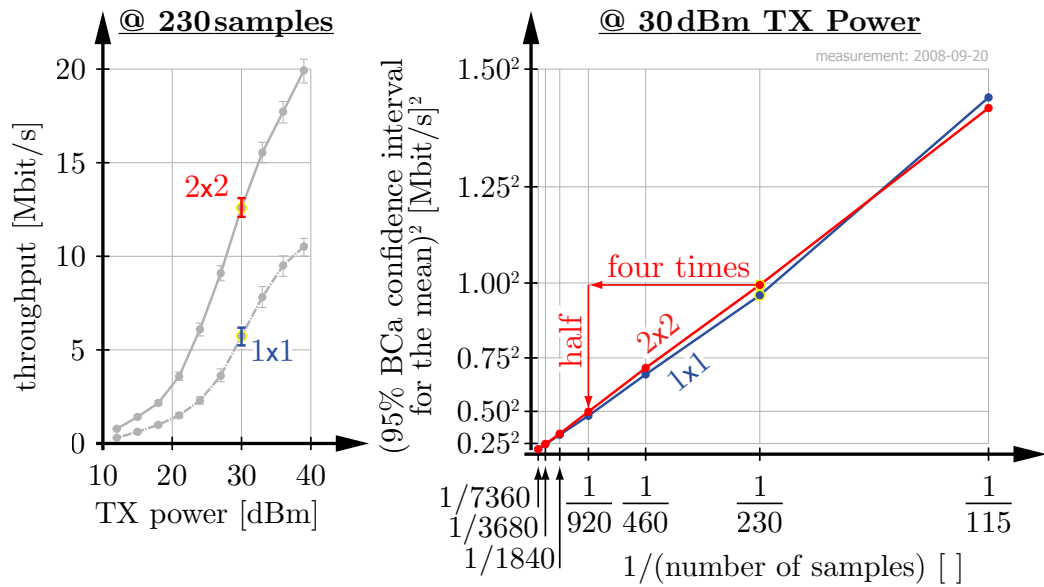


Figure 2.16: In a different scenario, we measured 7360 positions of 1×1 and 2×2 HSDPA to relate the size of the 95% confidence intervals to differently sized sub-samples.

As the variance of the mean decreases reciprocal to the number of samples, so does the square root of the confidence-interval-size²⁵ (see Figure 2.16). For the 230 samples measured, we obtain the precision shown in Figure 2.17:

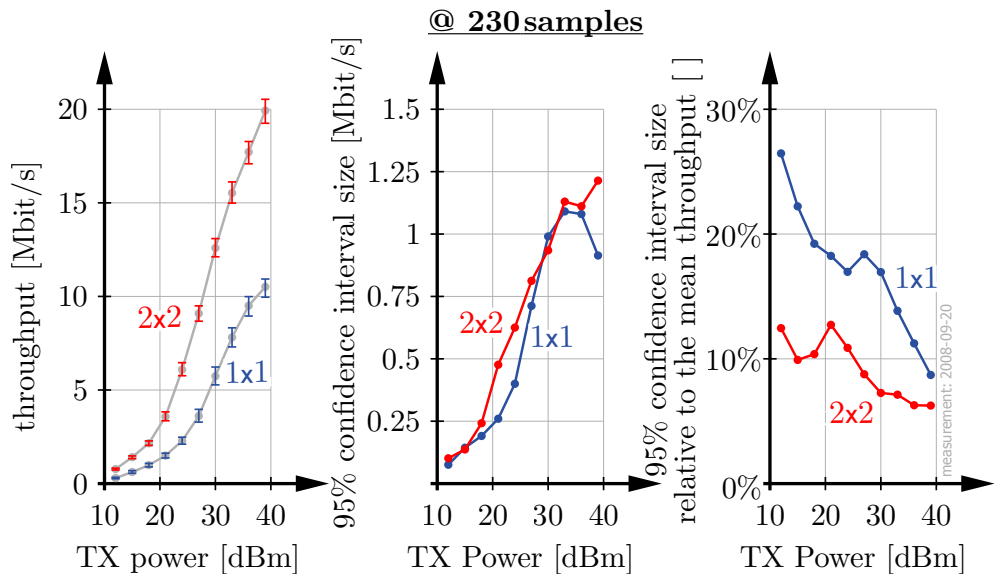


Figure 2.17: For the scenario shown in Figure 2.16, page 26, we plot the absolute and relative size of the 95% confidence intervals over TX power.

²⁵the size of the range the confidence interval covers

In the case of a narrow band single carrier 4QAM transmission, about 8610 RX antenna positions are needed to obtain the same relative precision of about 10% (see Figure 2.18). Further details on this measurement can be found in Section 4.1.2, page 54.

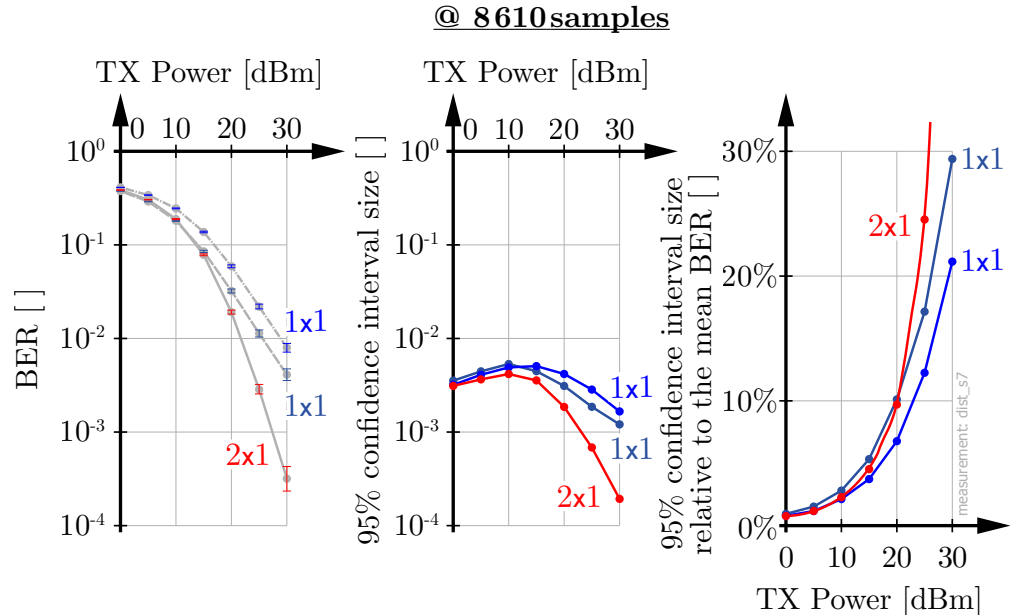


Figure 2.18: For the experiment presented in Section 4.1.2, page 54, (narrow band indoor single carrier 4QAM SISO on TX antenna 1 and 2 as well as 2×1 Alamouti) we evaluate the absolute and relative size of the 95% confidence intervals (for the mean bit error ratio) over TX power.

2.6.3. Reproducibility and Repeatability

To judge the reproducibility²⁶ of our measurements, consider the following outdoor-to-indoor experiment carried out in the inner city of Vienna, Austria (see Section 4.2.2, page 64, for further details on the measurement scenario):

- Three equal measurements, each lasting 12 hours, evaluating many different HSDPA schemes—we only look at a single result, namely the throughput of 2×2 D-TxAA HSDPA.

²⁶reproducibility. . . ”The closeness of agreement between independent results obtained with the same method on identical test material but under different conditions (different operators, different apparatus, different laboratories and/or after different intervals of time).” [57]

- **The first measurement** was commenced in good weather conditions. After about 10 hours, towards the end of the first measurement, a snowstorm covered the dry roofs and streets with a 3 cm thick layer of wet snow.
- **The second measurement** was carried out when the snowstorm had already ended, although the wet snow remained.
- **The third measurement** was carried out another 12 hours later, under similar weather conditions as measurement number two.

Figure 2.19 shows the resulting mean throughput of 2×2 D-TxAA HSDPA obtained from these three measurements. The lower two subplots show the absolute and relative difference between the two later measurements carried out under similar conditions.

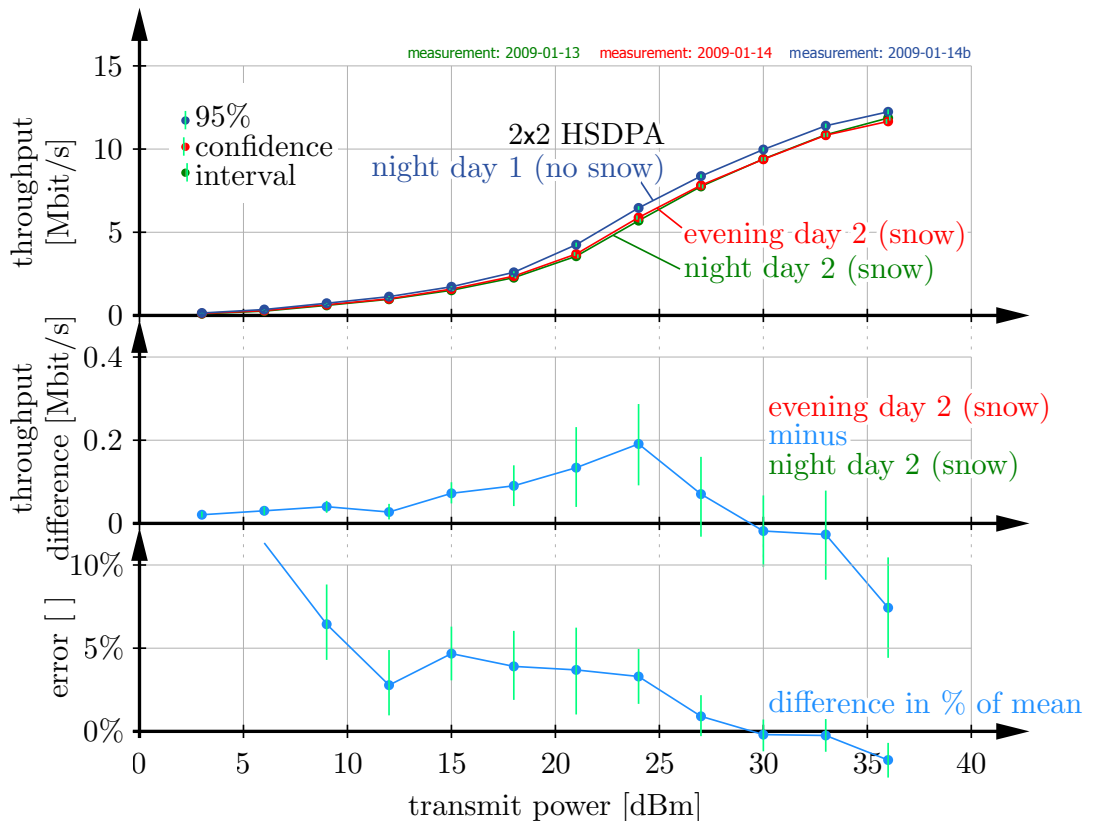


Figure 2.19: Reproducing the same measurements 12 and 24 hours later.

Variance reduction techniques, as explained in Section 2.4.2, page 15, are therefore necessary to combat undesired influences such as drifts and changes in the environment. Simply speaking, if repeated randomly shortly after each other, different transmission schemes can be more precisely compared.

Unfortunately, we did not measure two equal transmission schemes in any of the above-mentioned urban scenarios. To show how accurately measurements can be repeated²⁷ we have to refer to a measurement carried out in an Alpine scenario (see Section 4.2.4, page 80). In this measurement, which lasted approximately 12 hours, a radio frequency switch malfunctioned, and we therefore measured the same 2×2 D-TxAA HSDPA transmission twice (see Figure 2.20). Note that as the observations of the two measured curves are highly correlated, the confidence intervals for their difference are much smaller than suggested by the confidence intervals for the absolute values.

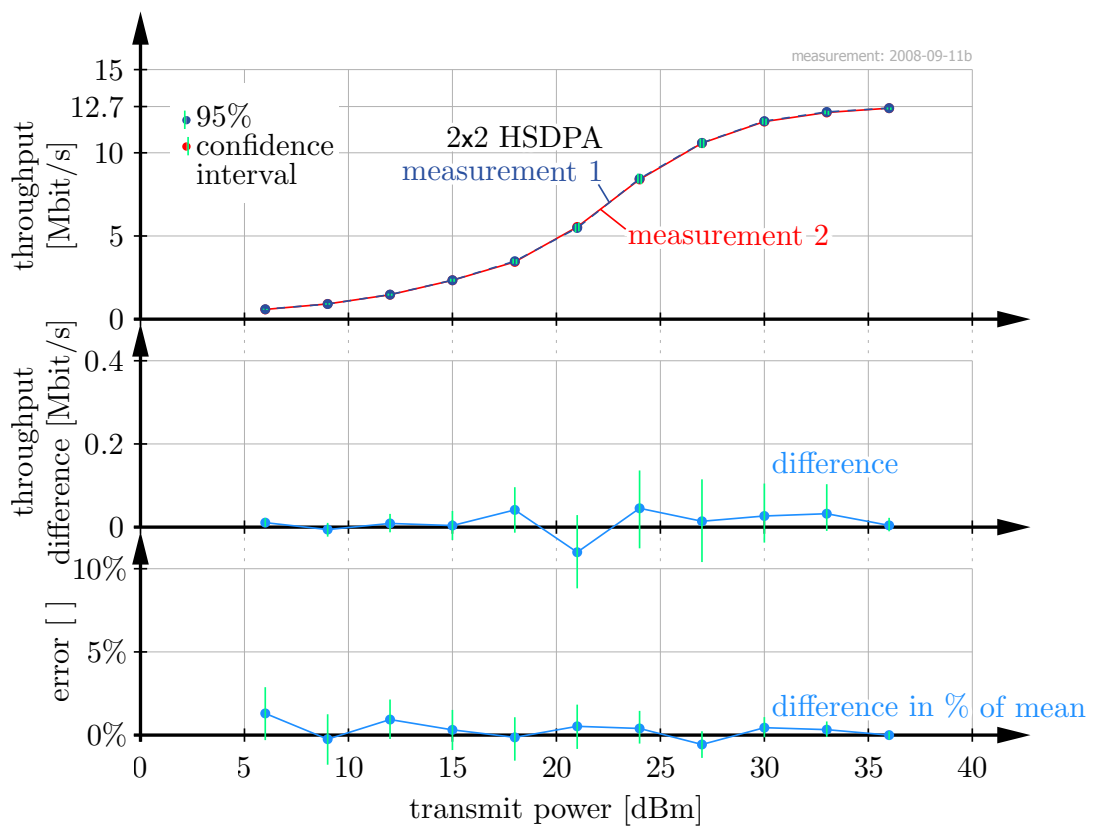


Figure 2.20: Repeating the same measurement at the same RX positions.

2.7. Measurement Automatization

As already noted, the whole measurement, evaluation, and graph-plotting procedure is carried out using a single, fully automatized, script. This also includes

²⁷repeatability... “The closeness of agreement between independent results obtained with the same method on identical test material, under the same conditions (same operator, same apparatus, same laboratory and after short intervals of time).” [57]

elements whose value is sometimes underestimated such as:

- taking webcam pictures at the beginning and during the measurement,
- constantly monitoring temperature and humidity at the TX and RX site,
- texting the operator in charge if there is an important issue like a linear guide getting stuck,
- and archiving the complete source codes used for this particular measurement and for every single evaluation carried out using the measurement data.

At first sight, automatized absolutely everything seems to be a waste of resources, particularly time. In addition, automatization by itself also offers no protection from errors in the measurement procedure and set-up. On the other hand, scripts execute the programmed steps with 100% certainty. Even if this does not imply that these steps are correct, the scripts can be gradually improved over time to cover every possible flaw in the measurement procedure.

Humans executing steps manually —at best from a checklist— behave differently. Especially, they tend to take shortcuts, either because they are lazy or try to be smart. For example, on one occasion we did not archive the source code of a measurement to save time because we thought that all the parameters were equal to the previous measurement anyway. Now, we find that there is no back-up of some important parameters.

To sum up, in our opinion, *complete* automatization is the only means of creating repeatable and consistently documented measurements.

2.8. Dealing with Feedback and Retransmissions

As radio channels stay constant over short periods of time, systems employing adaptive channel adjustment, such as WiMAX and HSDPA, can be efficiently measured using one of the two following approaches:

- If the feedback from the receiver is limited to only a few possible values (for example, seven in WiMAX), transmitting all possible transmit blocks immediately after each other is the method of choice.

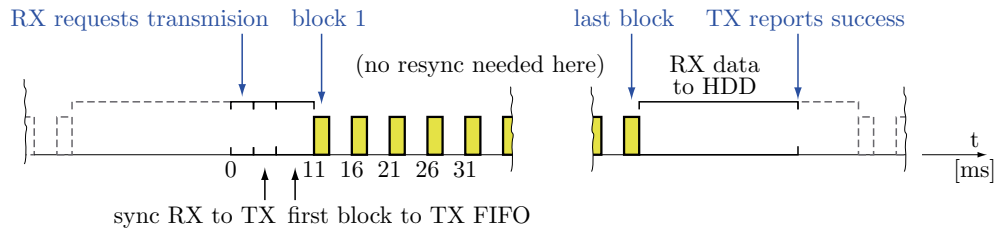


Figure 2.21: Measuring all possible transmit blocks.

As shown in Figure 2.21 for WiMAX, we transmit all possible blocks one after the other without calculating any feedback information. As an advantage of this method, we will later still be able to evaluate the throughput impact of different algorithms for calculating the feedback. Furthermore, we can also evaluate all possible combinations of one, two, three, and four receive antennas off-line from the same set of recorded data. The same holds true when, for example, trying different receiver types. The downside of this method is that the received data increases linearly with the number of possible transmit blocks.

- If the number of possible transmit blocks becomes too large (for example, a few thousand in MIMO HSDPA because of precoding and feedback), transmitting all of them may no longer be feasible. The method of choice is then to employ the feedback in a quasi-realtime fashion. Therefore, we first pre-generate all possible transmit blocks at the transmitter before the measurement is started. At every single transmission, a “previous block” is transmitted first. Next, the receiver calculates *just* the feedback bits in MATLAB, which requires considerably less computational effort than evaluating the complete received block. The resulting TX block number is then used to trigger the transmitter (see Figure 2.22). Note that the throughput-evaluation of the data blocks is still carried out later off-line.

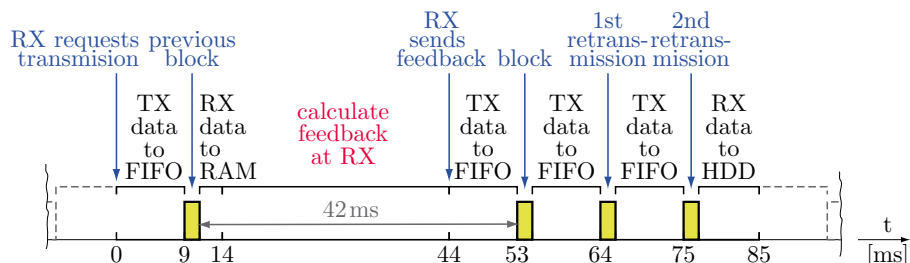


Figure 2.22: Calculating the feedback in MATLAB to transmit pre-generated transmit blocks and the possibly required feedback via a LAN connection. If the feedback is carried out via a wireless LAN bridge or similar, about 4 ms have to be added for the feedback time.

If a communication system requires the retransmission of data blocks in case of an erroneous detection at the receiver (as is also the case in HDSPA), we always transmit all possible retransmissions (see Figure 2.22). If required, we evaluate them later off-line.

2.9. Summary and Criticism

During the last four years, we figured out that one very efficient and effective way of dealing with testbed measurements is the **quasi real-time approach** presented in this chapter: In this approach, all possible transmit data is generated off-line in MATLAB, but only the required data is then transmitted over a wireless channel which is altered by moving the receive antennas. The feedback calculation that may be required for such a transmission is instantly carried out in some 40 milliseconds in MATLAB. The received data itself is not evaluated in real-time but off-line using a cluster of PCs. Results for the scenario measured are automatically obtained using the same script that has already controlled the complete measurement procedure and documentation. If more general results are of interest, measuring a representative sample of scenarios—using the procedure described above—would allow for such inferences. The measurement effort thus required should not be underestimated.

However, determining the real-world throughput performance of a communication system in a specific scenario *itself* is not really research—it is only a tool for further research, as for example, investigating and improving the algorithms used.

Consequently, the next research step should be to use the data obtained “to help in the art of modeling and simulation of such systems (e.g., indicate where specific assumptions made in present simulation methodologies are not supported by the measurements they obtained). It would be good to investigate the sorts of models that have been proposed in the literature to simulate the given scenarios, fit these models to the channel measurements, and then see how well they predict the throughputs that you actually measured.”²⁸. Unfortunately, the measured data do not allow for extracting channel data of sufficiently high quality—if it did, we would have built the cheapest channel sounder ever by far.

²⁸Quote from an anonymous journal-review.

3. Testbed Design

Setting up a testbed for wireless multiantenna measurements can be considered a straightforward task [147–189]. Several companies promise off-the-shelf working baseband hardware and software, whilst other companies offer the high frequency hardware also required [190–210]. To put the elements together, “nothing more” than a skilled engineer is required.

An error-free testbed that is able to *reliably* carry out novel *outdoor* wireless measurements 24 hours a day, seven days a week, is another story. It is a story of ongoing redesign, spending five times as much on accessories than on the actual testbed hardware, always searching for bugs and faulty hardware, and never having enough computing, let alone manpower.

This chapter will first introduce our testbed design before reporting on possible pitfalls regarding testbed design in general.

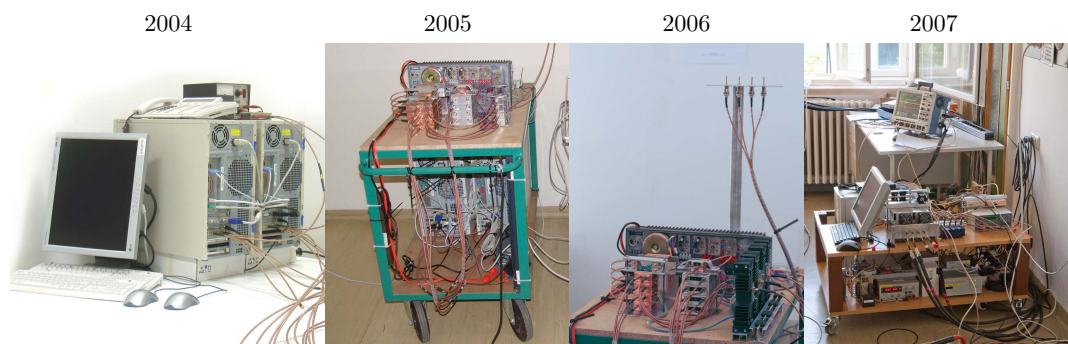


Figure 3.1: Development of our testbed. It took about four years from the first publication in 2004 to actually carry out realistic real-world outdoor-to-indoor throughput measurements at the end of 2007.

3.1. Basic Idea

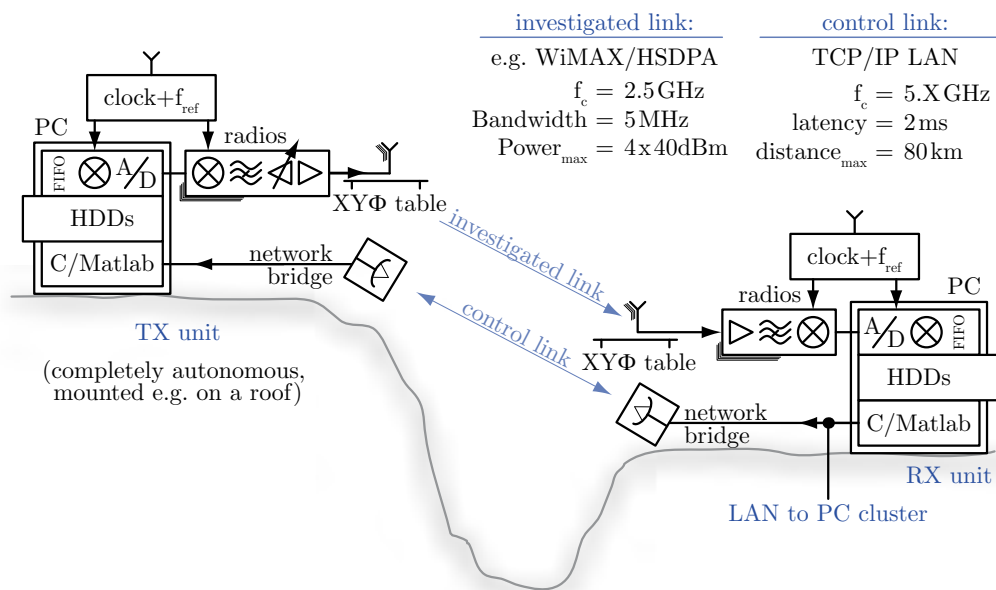


Figure 3.2: The Vienna MIMO Testbed.

To carry out measurements as described in all the following chapters we designed a 4×4 MIMO testbed that consists of the following key parts:

- **a TX unit**

that is capable of transmitting pre-generated, complex-valued base band data samples on four antennas at a center frequency of 2.5 GHz, a bandwidth of 5 MHz, and a maximum transmit power of 4×40 dBm (which still allows for linear operation).

- **moveable- and rotatable antennas**

at the transmitter as well as the receiver site (see Figure 2.9, page 15),

- **an RX unit**

that is capable of receiving and storing the transmitted data in real-time on hard-disk arrays as well as controlling the overall measurement procedure via a single, fully automatized, script (see Section 2.7, page 29),

- **a network bridge**

that allows the RX unit to actually control the TX unit via a wireless point to point LAN connection over distances of up to 80 km with a maximum latency of 2 ms [83] (this being fast enough for quasi-realtime feedback, see Section 2.8, page 30),

- **a cluster of PCs**
to evaluate the data collected by the RX unit off-line in MATLAB effectively¹ (see Section 2.5, page 20),
- **GPS units and rubidium frequency standards**
at the transmitter and receiver site to allow for accurate timing and frequency synchronization if necessary [84, 85],
- **cabling**
to connect and control the required PCs, webcams, antennas, linear guides, lights, GPS units, and radio frequency switches,
- **and a host of additional accessories**
as shown in Figure 3.3 and the many boxes therein.

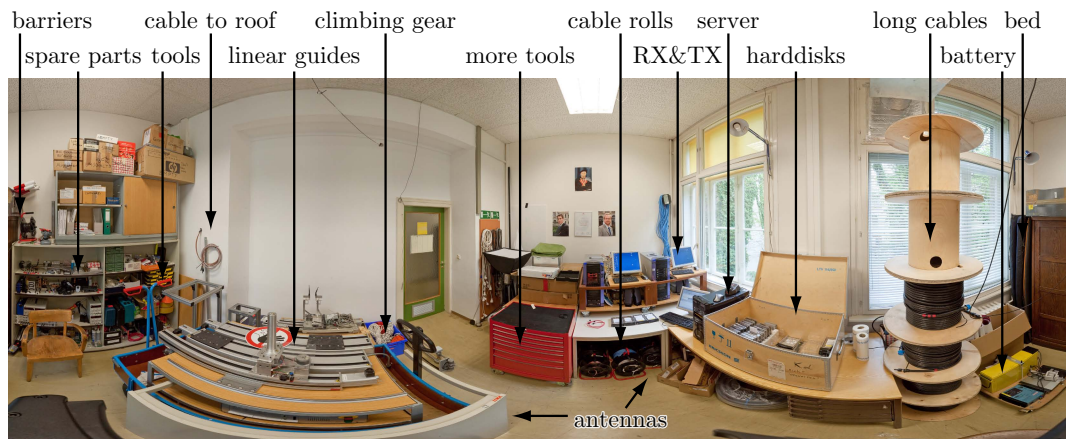


Figure 3.3: The complete Vienna MIMO Testbed stored in a room.



Figure 3.4: For carrying out a measurement campaign, the testbed and a small PC cluster is transported in a van.

¹ And efficiently in terms of total time and manpower needed to (a) write the programs for evaluation and (b) evaluate the data.

3.2. Transmitter

As shown in Figure 3.5, the transmitter consists of a personal computer (A1), a PCI plug-in board for digital to analog conversion (B1:6), a radio frequency frontend (C1:7), antennas (C9), accessories such as webcams (A12), devices for synchronization (S1:10) (see Section 3.4, page 41), power supplies (A14), an uninterruptible power supply (A15), a power set (A16), and a lot of cabling (C6, A8, A9, A13, S2, S9, and A17:19).

In the transmit PC, operated using Windows 2003 Server (A2), baseband data samples are pre-generated using MATLAB (A3) to be stored on RAID flash hard-disks (A4) and/or the internal memory for fast access (A5) by the PCI plug in board (B1:6).

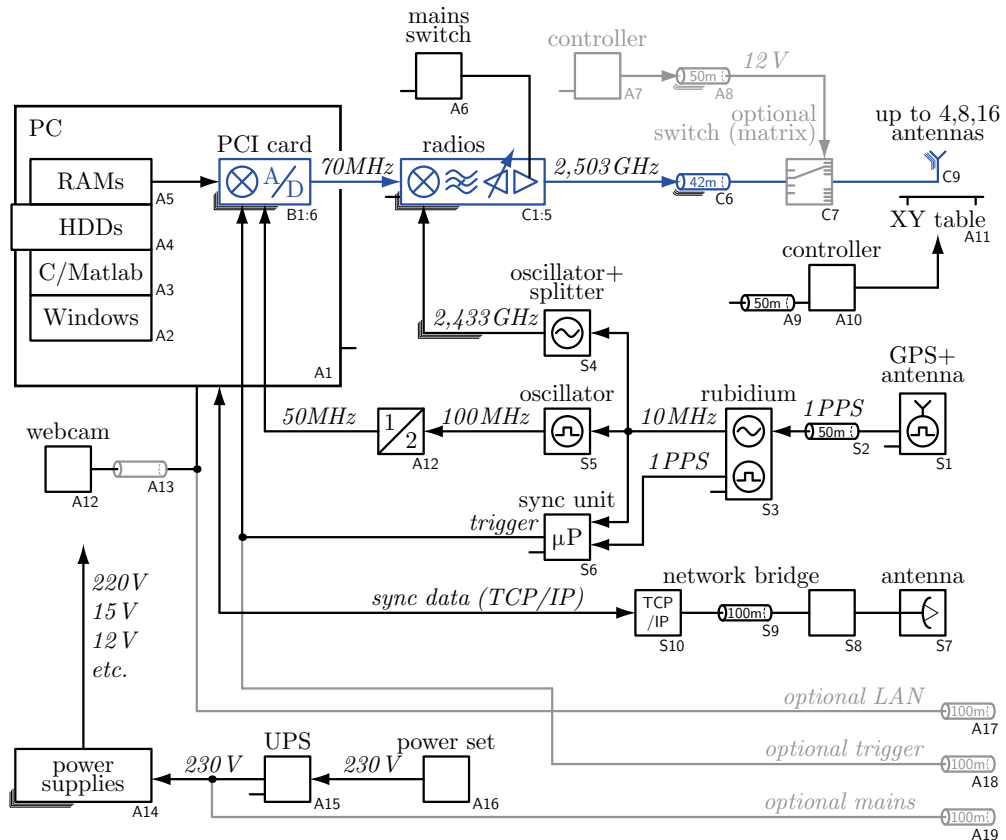


Figure 3.5: The TX Unit (real-time parts in blue). The open connections are USB or RS232 control connections to the transmit PC.

As pointed out in Figure 3.6, when data is to be transmitted, the previously stored samples are copied to FIFOs (B1), real-time interpolated to 200 MSample/s (B2&B3), digitally upconverted to a center frequency of 70 MHz (B4&B5), and finally converted to the analog domain (B6). See [4, 28] for further details.

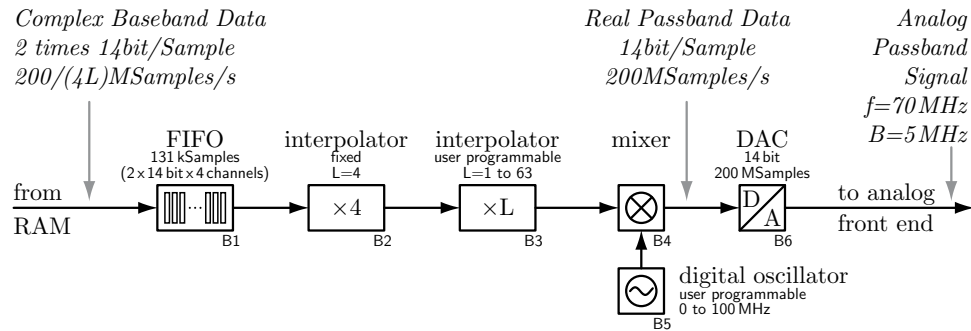


Figure 3.6: The TX Unit, digital signal processing.

Designing the radio frequency hardware for upconverting the 70 MHz intermediate frequency signal to 2.5 GHz is a straightforward task (see [36, 37]). As shown in Figure 3.7, the signal is attenuated (C1), mixed to 2.5 GHz (C2), variably attenuated to be able to generate different transmit powers (C3), filtered (C4), power amplified (C5), guided by cables to the roof (C6), optionally switched to different antennas (C7), guided to the antennas (C8), and finally transmitted (C9).

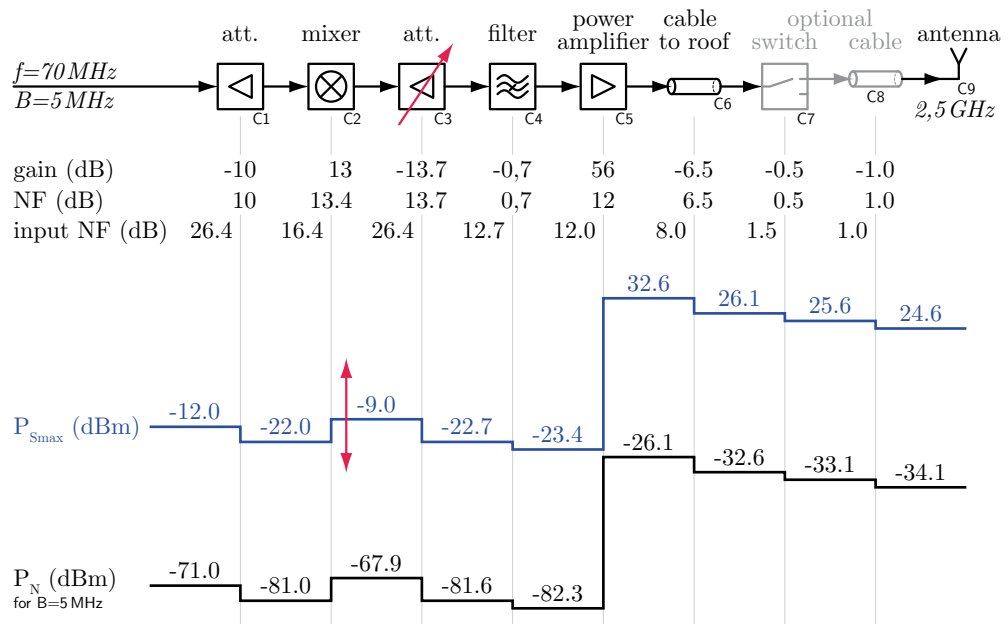


Figure 3.7: Power level plan of the transmitter.

3.3. Receiver

At the receiver, see Figure 3.8, the transmitted signal is received by up to four antennas (D1), guided (D2) to the receive filter (D3), low noise amplified (D4), re-attenuated (D5) (or guided over long distances if the previous part (D1:4) is mounted on a mast top), re-filtered (D6), mixed down to 70 MHz (D7), re-filtered once more (D8), and finally amplified to the signal level required by the analog to digital converters (D9). See [36, 37] for further details.

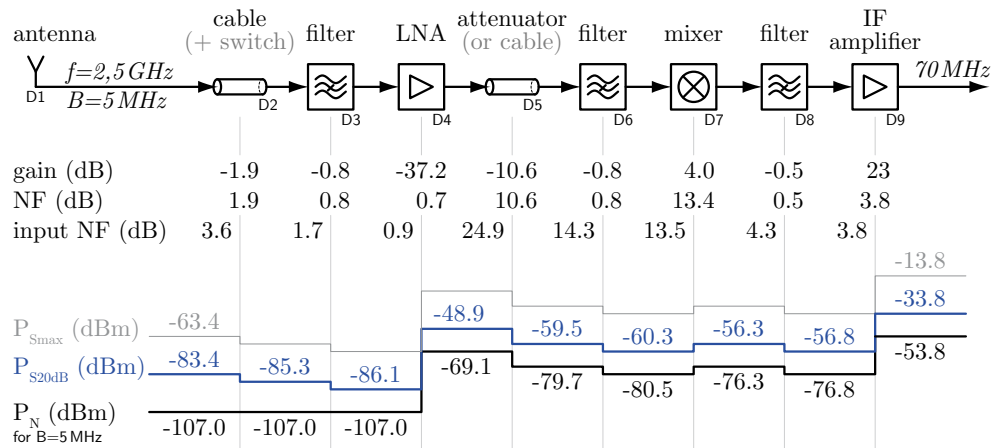


Figure 3.8: Power level plan of the receiver.

As shown in Figure 3.9, the signal is then converted to the digital domain (E1), mixed down to baseband (E2&E3), digitally decimated (E4), and buffered in FIFOs (E5). See [4, 28] for further details.

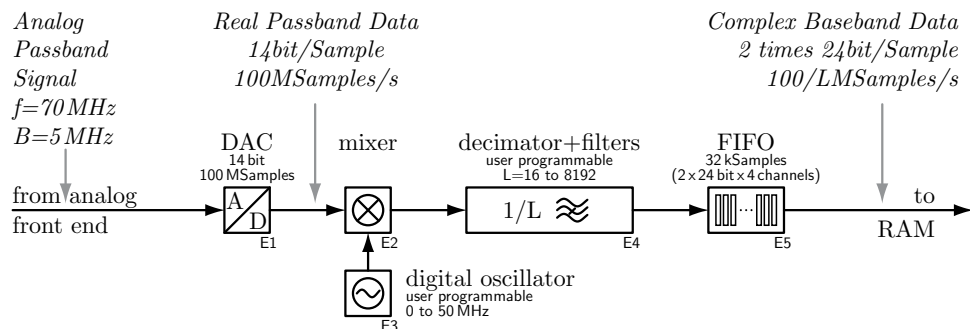


Figure 3.9: The RX Unit, digital signal processing

The RX unit, see Figure 3.10, is set up in a very similar fashion to the transmitter. It consists of a personal computer (F2), the parts previously described for receiving a signal (D1:9, E1:5), accessories such as webcams (F18), devices for synchronization (S1:10) (see Section 3.4, page 41), power supplies (F16), an uninterrupted power supply (F15), a battery (A13), a DC/AC converter (A14) for mobile use, and again, extensive cabling (D2, S2, S9, F10:12, F17).

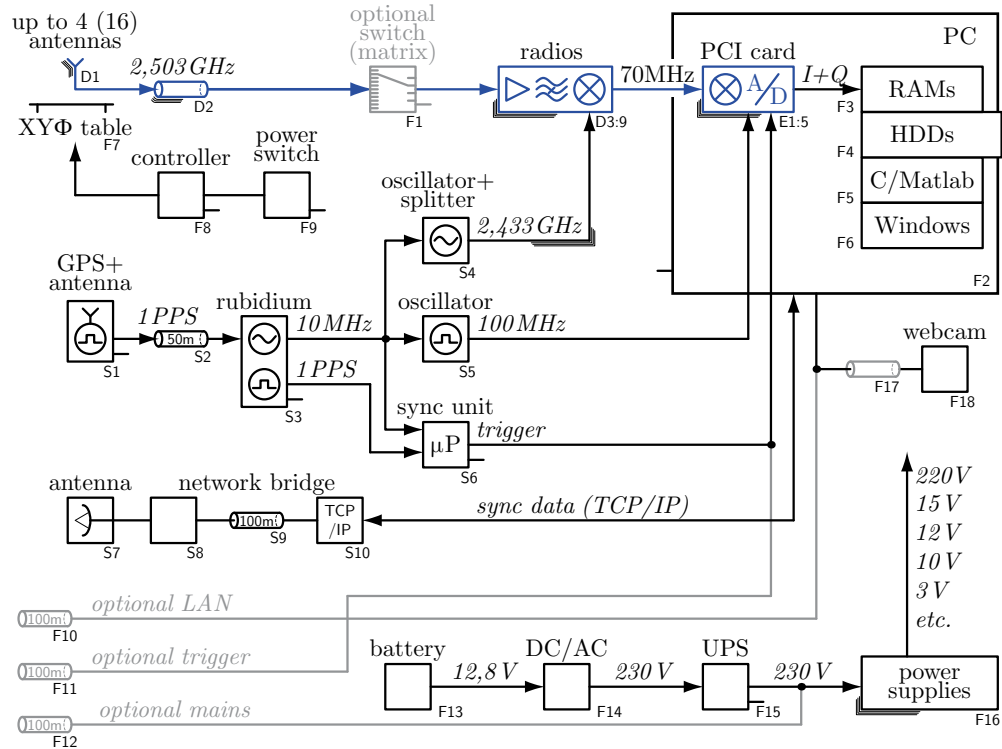


Figure 3.10: The RX Unit (real-time parts in blue).

In the personal computer, the received data samples stored in the FIFOs (E5) of the PCI plug in board are either directly copied to the hard-disks (F4) or copied to MATLAB (F5) for fast feedback calculation. In the latter case, the resulting optimal block to be transmitted is fed back to the transmitter via a network bridge (S7:S10). This network bridge is also used for remote control of the transmitter operation in general.

The measured power consumption of the receiver is about 250 watts, in other words, a decent 47 kg heavy battery (F13) can supply the whole set-up with the energy required for approximately five hours.

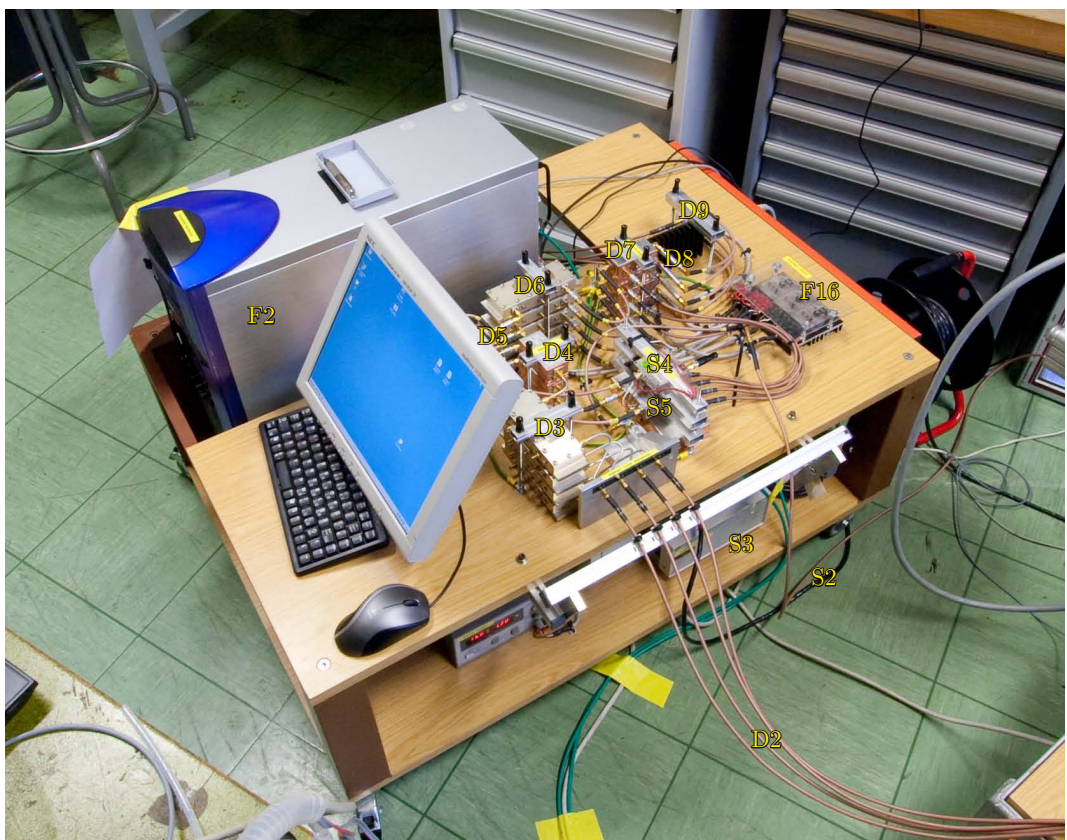
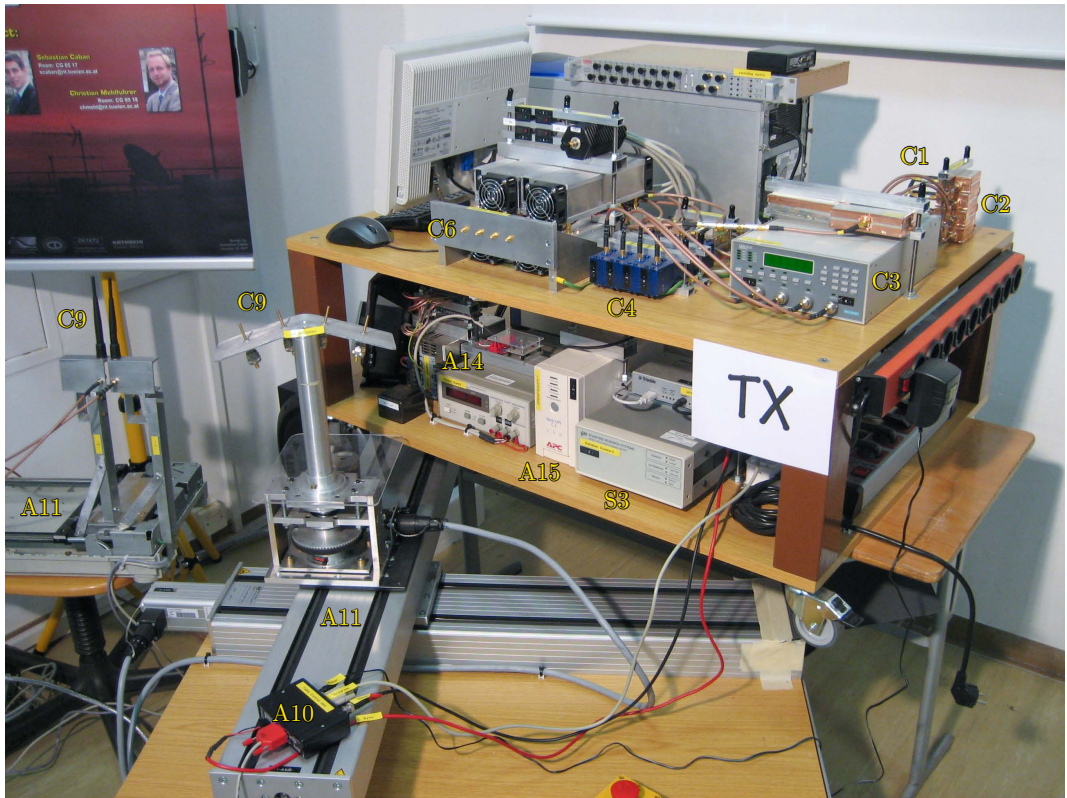


Figure 3.11: The transmitter (top) and the receiver (bottom).

3.4. Synchronization

As there is (in general) no cable connection between the TX and the RX unit, some sort of synchronization is needed to ensure that the blocks of data are transmitted (at the TX site) and received (at the RX site) at the same time. Furthermore, it should optionally be possible to synchronize the frequency of the internal clocks of the TX unit to those of the RX unit. This is all achieved as follows (see Figure 3.12):

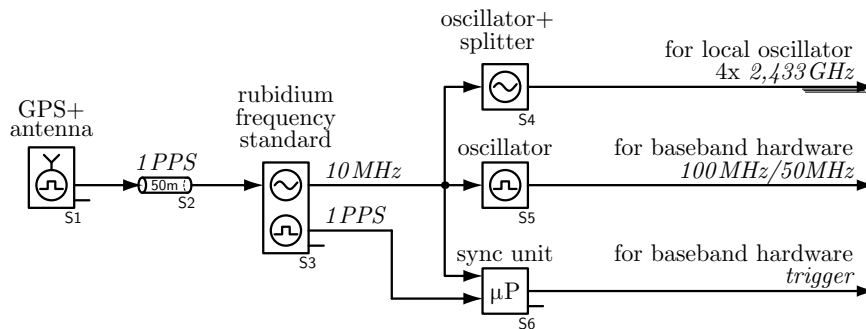


Figure 3.12: Synchronization units at the TX *and* RX site (both equal). The open connections are USB or RS232 control connections to the transmit PC.

Locked to geostationary satellites, a GPS (S1) at the TX site outputs one pulse per second (PPS), as does a second GPS (S1) at the RX site. The starting time of these pulses differs by up to ± 20 ns (see Figure 3.14, page 42).

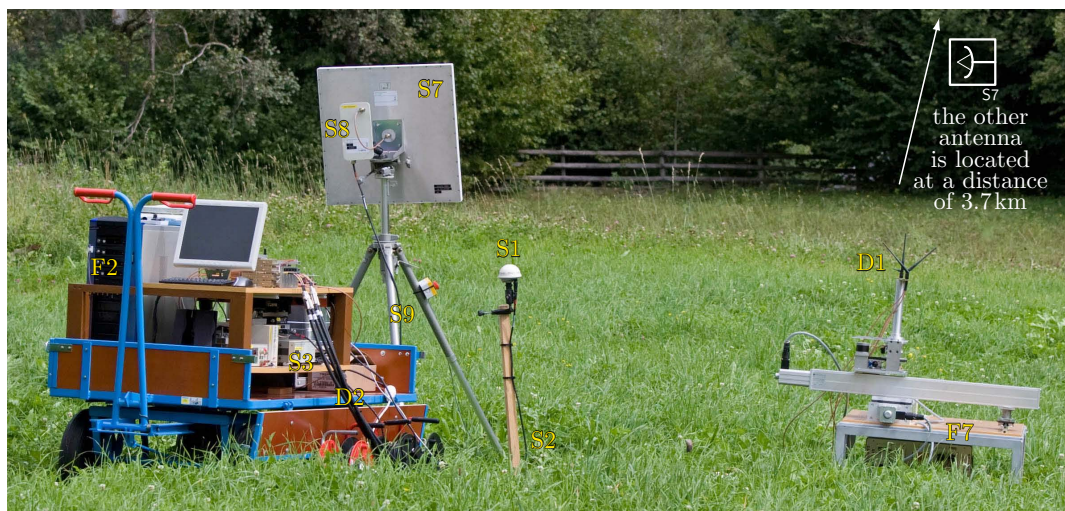


Figure 3.13: Network bridge and synchronization at the receiver site.

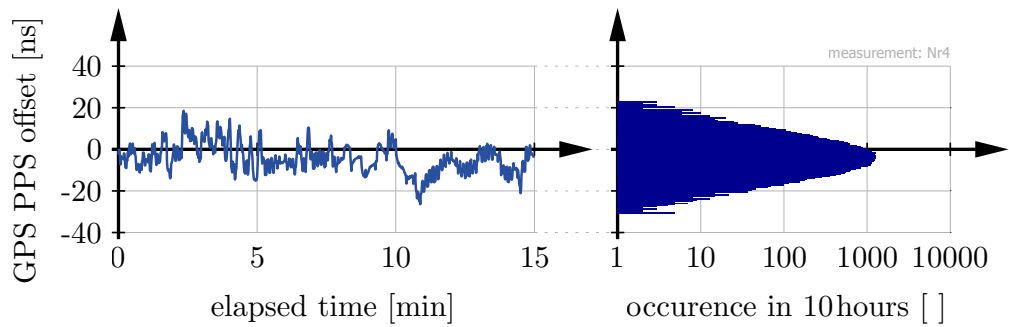


Figure 3.14: Measured PPS output offset between the two GPS units (S1).

In the next step, the long-term-stable PPS pulses are short-term-stabilized by a rubidium frequency standard (S3) (see Figure 3.15).

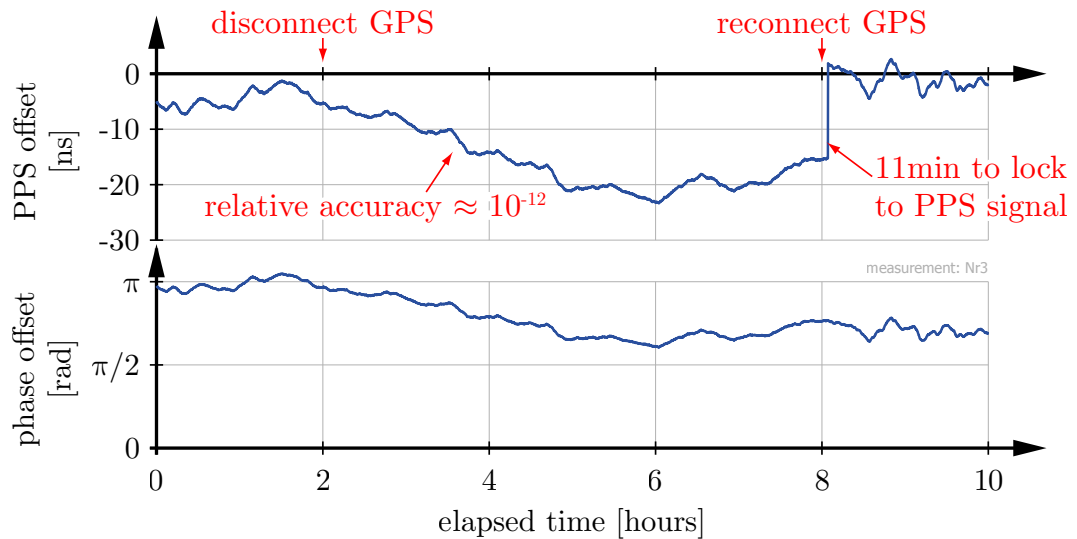


Figure 3.15: Top: measured PPS output offset between the two rubidium frequency standards (S3). Bottom: measured phase difference between the two 2.433 GHz low phase-noise local-oscillators (S4). At the beginning of the experiments, the rubidiums (S3) are locked to the GPS units (S1), disconnected at time=2 h, and connected again at time=8 h. Note that prior to the experiment, the rubidiums and GPS units were only heated up and locked for about 20 minutes—the resulting accuracy is still sufficient to carry out measurements (A symbol is typically about 200 ns long.).

The resulting PPS signal is forwarded to a self-built synchronization unit (S6). This unit basically consists of a counter which runs at a frequency of 10 MHz (provided by the rubidium). At the beginning of each measurement, this counter is reset at the TX and the RX site at exactly the same time by the use of the PPS signal and handshaking via the network bridge (S7:S10).

During the measurement, the TX site then just has to tell the RX site at which counter-value it should receive the transmitted data. See [7] for further details.

The 10 MHz output of the rubidium is also used to lock a 2.433 GHz low phase-noise oscillator (S4) that is used to mix the 70 MHz intermediate frequency signal to 2.503 GHz (C2 in Figure 3.7, page 37) and back (D7 in Figure 3.8, page 38). Another 100 MHz oscillator (S5) is used to provide the PCI plug in boards (B1:6 in Figure 3.5, page 36, and E1:5 in Figure 3.10, page 39) with a stable reference clock.

Since the rubidium (S3), the 2.433 GHz oscillator (S4), and the 100 MHz oscillator (S6) can be used without a reference input as free running devices, all measurements can be carried out with/without external synchronization (or optionally by using a tuneable oscillator with a given frequency offset).

3.5. Possible Pitfalls

3.5.1. Digital Baseband Hardware

Our experience over the years has shown that it takes a considerable amount of time and manpower to get even the most basic demo programs to work. Reasons for this are:

- missing, misleading, or carelessly written and not updated **manuals**, pinout documentation, and sample programs coming with off-the-shelf products,
- a lack of **support** or extremely long support-answer times, not only when buying from low-cost vendors,
- **compatibility** problems between different versions of hardware and software,
- and **stability** problems. Even a demo program provided by the manufacturer that initially appears to run smoothly may reveal astonishing and unforeseen instabilities if executed over several weeks.

One has to be careful that for marketing reasons:

- bandwidths and transfer **speeds** proclaimed by hardware manufacturers usually represent **pure marketing** numbers. Busses are often not able

to transfer bus-clock times bus-width bits on a permanent basis but only in burst mode.

- It also sometimes happens that **different features** proclaimed for a product cannot be achieved at the same time, but only on an **either-or basis**. For example, a synchronous transfer is only possibly at a lower speed, the proclaimed higher speed only works in asynchronous mode.

Another problem that arises with digital baseband hardware is that products are sometimes sold *not* including the possibility to flexibly reprogram them as advertised—and this fact is not obvious to the customer:

- Typically, **firmware** can be used in its delivered form but **cannot be modified**. In order to modify it, additional licenses and tools are required, costing considerable additional amounts of money.
- The **software** included with the product may also be **limited** “on purpose” in its functionalities (for example, it will work on one FPGA but not on two). The unlock keys required imply additional expenditure often overlooked at the date of purchase.
- And even if the software keys are not limited, one has to be careful that all the **documentation needed to modify** the firmware is included and does not have to be purchased additionally. In such situations one may find oneself performing the programming and development work that has already been paid for.

3.5.2. Tool and Component Selection

One also has to bear in mind that the *specific* software tools sold with a product require other *specific* software packages—in a *specific* version—to operate.

- It often happens that errors found are corrected in newer software versions, but this also implies that all the other specific **software packages have to be updated** in order to work correctly—a vicious circle that consumes a lot of time and money since it is common for other software packages from other vendors to also be affected.
- It has been reported that companies “charge for maintenance,” which means that one has to pay special attention to whether charge-free bug-fixes are included in the delivered software.

- In addition, highly specialized software **tools** used to program hardware **do not**, unfortunately, often **work reliably**.
- Due to poor documentation and the endless number of possibilities why bugs could occur, tracking, reporting, and getting these errors fixed is usually an endless challenge. Therefore, one should consider only using extensively tested “**standard tools**”, for example: TI Development Environment or Xilinx ISE, instead of spending money on tools that seem to save time at first glance, but afterwards turn out to be error prone.

Baseband hardware is often sold on a module basis in complete packages. The hardware develops so rapidly that hardly any company has the time to extensively test its hardware and prepare well-written manuals and source codes. The best way to deal with these problems is to buy from the company with the best support. A fast and competent support often makes the difference between achieving anticipated goals or not.

In multiple antenna architectures, special emphasis has to be put on “synchronous” operation:

- It must be possible to **synchronize the digital signal paths** used for different antennas, even if they are spread among several chips or modules. Memories, interpolators, filters, and digital mixers may not allow for this, especially if dedicated hardware is used instead of FPGAs.
- Because they are just scaled SISO solutions, many MIMO solutions offered do not allow for a **synchronous radio frequency oscillator** for analog up/down mixing—even if advertised.
- One has to make sure that the word “synchronous” really means “equal in phase and frequency without any jitter” if used in product advertising brochures. Failure in synchronicity may result in dramatic performance loss compared to perfectly synchronous transmission.

3.5.3. Analog RF Front-Ends

When it comes to analog front-ends (for example, analog upconverters, filters, amplifiers), the opposite is true. On the one hand it is extremely difficult to buy the hardware needed, since very few products exist (most only as components rather than complete). One has to buy everything on a per module basis sometimes even from different suppliers. On the other hand, once the hardware has been obtained, components can be set up and get working relatively

quickly. Some very expensive measurement equipment is, however, required in order to check if the hardware is working within the desired specifications or not. There are usually no hidden costs afterwards, no software tools needed, no carelessly written manuals and demo applications. On the downside, analog high frequency hardware is hardly ever flexible. Once one changes the center frequency, one has to rebuy most of the hardware—in the digital domain, this only requires the modification of some bits.

Therefore, when buying a new analog RF frontend, it is very important to choose the “proper” center frequency:

- It is a lot easier and cheaper to obtain hardware for free **ISM bands** (for example, 2.4 GHz, or 5.2 GHz). Other bands (1.5 GHz, 2 GHz, 3.5 GHz, 5.8 GHz) are sufficiently close to draw the right conclusions for the experiments.
- Choosing a frequency within a free ISM band implies that other interferers such as cordless computer peripherals, WLAN, Bluetooth, and microwave ovens may inherently influence every single measurement. If this **unpredictable interference** is desired, a transmit frequency within an ISM band should be chosen.

3.5.4. Cost

As pointed out, setting up a testbed requires a considerable amount of money, manpower, and —most important— time, but in many cases, this may be still more economical than, for example, buying an extremely expensive but rather inflexible channel sounder.

A high quality channel sounder costs typically between 300 k€ and 1 M€, the hardware for a good testbed (100 k€) plus four person-years for setting it up may add up to 250 k€—still considerably cheaper. Furthermore, it allows one to perform more research than just extracting channel coefficients, and also to test transmissions over the air with the signals that will be applied in the final product.

The main downside of a testbed, however, is the time needed to set everything up and get it working². This makes testbeds very suitable for basic research,

² As a rule of thumb this time cannot be reduced to less than a year because of delivery times and unforeseeable problems.

where time to market is usually not the primary factor, but often inappropriate for other purposes. Companies, on the other hand, are well recommended to continuously put effort into testbeds in order to constantly have them available and not to start from scratch every time a new product design cycle is started. Note also that *if* a testbed is set up and working, it may allow for measurements to be carried out within minutes, especially when the data is processed off-line in tools like MATLAB. Intelligent consideration of similar experiments, which can utilize the testbed without time consuming hardware modifications, can enable “lost” time to be easily made up.

3.5.5. Matlab Code and Testbeds

Once a MATLAB code has been proven to work well in simulation, a testbed can clarify whether the algorithms are suitable for real over-the-air communications. Unfortunately, using MATLAB code with a testbed is not a simple process. There are many things that have to be taken into account. For the simple case of off-line processing in MATLAB these are, for example:

- MATLAB simulations often operate **in the discrete baseband** only. Therefore, transmit and receive filters, interpolators, etc. have to be added.
- Interpolating to a fixed, given hardware sample-rate may also introduce impractical interpolation factors (for example, 3.84 MHz (UMTS) to 100 MHz sampling) requiring interpolation filters with extreme length. Alternatively, decreasing and optimizing the filter complexity may result in a lengthy project in its own right.
- MATLAB simulations often assume **perfectly synchronized signals**. In measurements, one now has the choice to:
 - synchronize transmitter and receiver perfectly (typically by cables)
 - nearly perfectly synchronize them using rubidium frequency standards and GPS receivers (which may be required if, for example, the receiver is mounted in a car)
 - use special training sequences prior to the transmitted data (which may only be possible in static scenarios)
 - implement proper synchronization algorithms.

Several of these options may even be used together for all required synchronizations (for example, local oscillator frequency, timing, and block start).

In some cases, perfect synchronization may be the method of choice to avoid all undesired effects (for example, for reference purposes to test the performance loss of proper synchronization algorithms). Even the first famous MIMO experiments carried out were using cables for synchronizing transmitter and receiver clocks [77]. In other cases, implementing proper synchronization algorithms in the receiver may deliver a better view of the reality. Unfortunately, this is not always possible, for example if only a limited number of blocks is available and synchronization requires averaging over long periods of time.

- **The channel is never known** to the receiver. Therefore, channel estimation cannot be omitted as often the case in MATLAB simulations. Fortunately, in quasi-static scenarios, long training sequences can be used to nearly perfectly estimate the channel (for reference purposes).
- **For many (optimal) receiver algorithms the noise variance also has to be estimated** at the receiver. However, the simple trick of measuring the noise variance in the absence of transmitting signals may often save coding time and provides accurate estimates regardless of the modulation scheme used.

Once it is working properly, a testbed (plus subsequent off-line processing of the received data in MATLAB) is a very powerful and swift method for evaluating algorithms using realistic over-the-air transmissions. One has the choice of measuring the absolute performance of a transmission scheme or of comparing two transmission schemes relative to each other. It is particularly easy to measure the relative difference between two types of receivers because

- The same stored receive data can be evaluated, thus making the comparison fair.
- Debugging is also made easier, because the received data remains equal.
- The number of channel realizations can be significantly reduced since for measuring relative performance, compared to absolute performance, a much smaller number of realizations measured is sufficient.
- Systematic errors in relative performance measurements play a less dramatic role than in absolute performance measurements.

3.6. Summary, Issues, and Criticism

The testbed presented in this chapter perfectly meets the specifications required by the quasi-real-time measurement procedure described in Chapter 2. It consists of a TX unit and an RX unit comprising moveable and rotatable antennas, a network bridge, GPS units, rubidium frequency standards, extensive cabling, and a host of accessories, as well as a cluster of evaluation PCs.

Of course, one could say that our testbed is —besides many others [147–189]— just another approach to building a piece of “publishable” MIMO measurement hardware. Therefore, the engineering part of Chapter 3 was kept short, whilst still describing all the parts of our testbed before listing possible issues regarding testbed design in general.

On the other hand, only very few groups nowadays are continuously producing results based on testbeds due to the extremely time consuming efforts involved and the required educational profile ranging from computer science through telecommunication engineering and electrical engineering to even mechanical engineering in many cases. What actually differentiates our approach from others is the quantity of efficiently produced measurement results [1–3, 6–9, 11–16, 18, 19, 22–25] showing more than scatter plots, estimated transfer functions, or estimated mutual information.

Even after being continuously redesigned for over five years, our testbed is still far from perfect:

- The interpolator (B3) in Figure 3.6, page 37, is not synchronous for the four channels. By interpolating the data already in MATLAB this error can be minimized, at the cost of longer data transfer times and smaller possible block sizes. Unfortunately this design flaw in the PCI plug in boards cannot be corrected.
- The synchronization units employed ((S6) in Figure 3.12, page 41) require some communication with the host PC that is —especially if high load is put on the CPU— delayed by the non real-time capable Windows operating system. If such an unforeseen delay occurs, the data is not received at the same time as it is transmitted. Fortunately, the synchronization units can perfectly detect such delays; the transmission is then repeated. If the CPU now has to calculate the feedback, nearly all transmissions fail, therefore increasing transmission time. Two possible ways of solv-

ing this problem are to calculate the feedback on only one of the two CPU cores (which is what we do), or to redesign the synchronization unit (which is what we plan to do).

Despite these two hard to correct issues, the testbed appears to work flawlessly so far.



Figure 3.16: The Vienna MIMO Testbed transmitting MIMO HSDPA from a cowshed in the Alps in Austria.

4. On the Influence of Antenna Spacing

Transmit and receive diversity have emerged as an effective means of achieving higher throughput in wireless communication systems. Unfortunately, correlation between the different propagation paths of a MIMO link reduces the achievable link capacity. Low transmit antenna spacing, as demanded by today's ever smaller devices, is one major cause of such undesired interdependence. The lower the spacing, the worse the radio link performance, but the smaller the base-station/hand-held can be.

Although this phenomenon is well understood in quality, the open question remains for exact quantitative behavior, that is, how does the throughput of a realistic communication system change over antenna spacing?

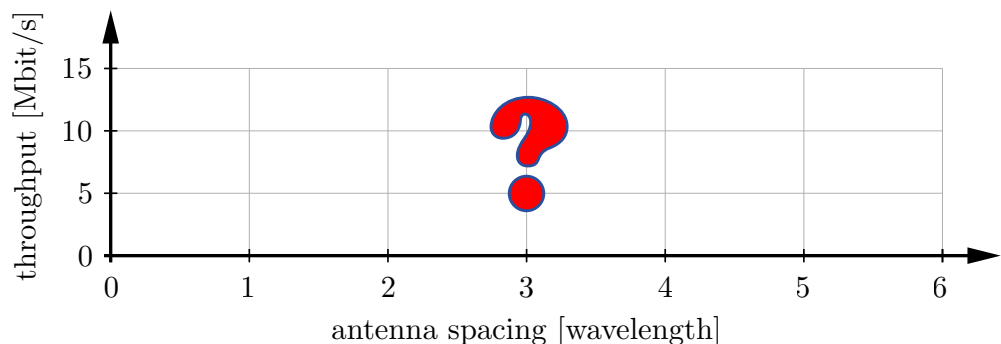


Figure 4.1: No result could be found in the literature that relates antenna spacing to the throughput of a realistic communication system.

4.1. Indoor – Un-coded Single Carrier

Measuring indoors with a MIMO testbed is a well established experience [147–189]. Nevertheless, the perfectly static, interference-free, and convenient conditions are the perfect playground for pre-testing any major experiment. Especially in a cellar —shielded by some meters of sand, concrete, and stone— even the slightest flaw in an experiment can be easily unveiled.

The same holds true for investigating un-coded narrow band single carrier transmissions. Such transmissions do not exist in isolated form in practice, although they may in some way be part of a bigger (for example, coded, multicarrier) system. We therefore tested all our equipment and scripts thoroughly using very basic modulation techniques and comparing with well known theoretical results before moving on to more sophisticated standards such as HSDPA in the next section.

4.1.1. Existing Research

To our knowledge, the influence of antenna spacing on the BER over SNR performance of 2×1 and 2×2 space-time coding schemes has never been systematically studied either theoretically or by indoor/outdoor measurements. However, there are some results that relate antenna spacing, correlation, and capacity. This provides us with an expectation for the BER over SNR performance of the radio link at small antenna distances:

Utilizing 2-D shooting and bouncing ray-tracing, [62] concludes for indoor scenarios a significant drop in capacity for spacings smaller 5λ . Also in [66] and [67], a significant drop in capacity for spacings smaller than 4λ is predicted by using a multipath cluster channel fading model. Leading to similar results, other theoretical papers such as, for example, [71] and [72] also ignore the fact that small inter-element antenna spacing will cause mutual coupling¹. The same is true for multiplexed channel sounding of MIMO channels using a single transmit and receive antenna. Used for example in [69] and [65], this simplification —often referred to as “virtual antenna arrays”— also neglects the interaction between the two transmit antennas. In [64], the angle of arrival is obtained by true 4×4 MIMO channel sounding, which is then used to calcu-

¹ That is, “current induced on one antenna produces a voltage at the terminals of nearby elements” [70].

late the power angle spectrum, and then the spatial correlation as a function of antenna spacing.

Using a geometrically based statistical channel model, particular emphasis is placed on mutual coupling in [63]. A curve of capacity versus antenna distance with and without mutual coupling is derived. Full capacity is reached at about 0.3λ and greater. Reference [70] accounts for mutual coupling effects by full-wave electromagnetic antenna simulations and leads to the same results. These results are explained by the fact that coupling changes the antenna patterns *individually* as the antennas are moved closely to each other. Therefore, a decorrelating effect is observed, usually referred to as pattern diversity. Also [68] takes mutual coupling into account to theoretically show that capacity is decreased substantially if the spacing gets closer than 0.5λ .

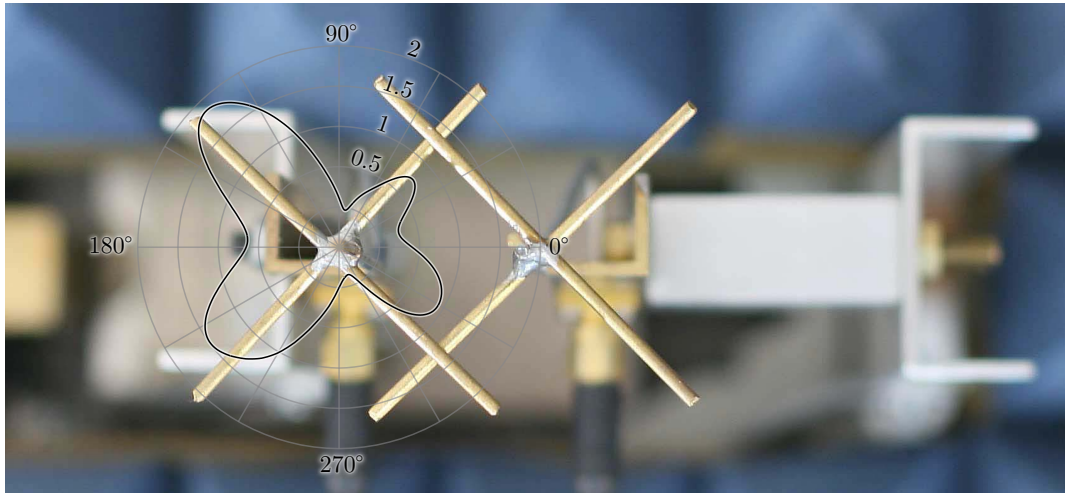


Figure 4.2: Simulated antenna pattern of the set-up shown in Figure 4.3. When the antennas are spaced close together (0.2λ in this case), their pattern is no longer omnidirectional.

There are also some channel sounding experiments where four antennas have been actually (rather than virtually) placed at distances as low as 0.2λ [59–61]. The papers conclude that capacity does not degrade until 0.2λ and explain this by mutual coupling effects. In [75], the same results are achieved by a completely different approach; namely, MIMO systems were measured and characterized in a so-called reverberation chamber that represents the isotropic multipath environment. To sum up, taking mutual coupling into account, spacings of 0.2 to 0.5λ should be sufficient to reach nearly full capacity. But does this hold true for a “real” 2×1 or 2×2 transmission and which code does actually perform best?

4.1.2. Experiment I, 2×1 Indoor

In this first experiment, we compare the uncoded BER over SNR performance of a 2×1 Alamouti coded transmission to ordinary SISO transmission. We will show that down to transmit antenna distances of 0.12λ , an SNR gain of 5 dB is achieved.

Therefore, at a data rate of 500 ksymbol/s, we transmit a 4QAM modulated and root raised cosine filtered (roll-off=0.22) signal from two transmit antennas (see Figure 4.3) to a single receive antenna. We measure indoors between different office rooms located about 30 m apart on the same floor.

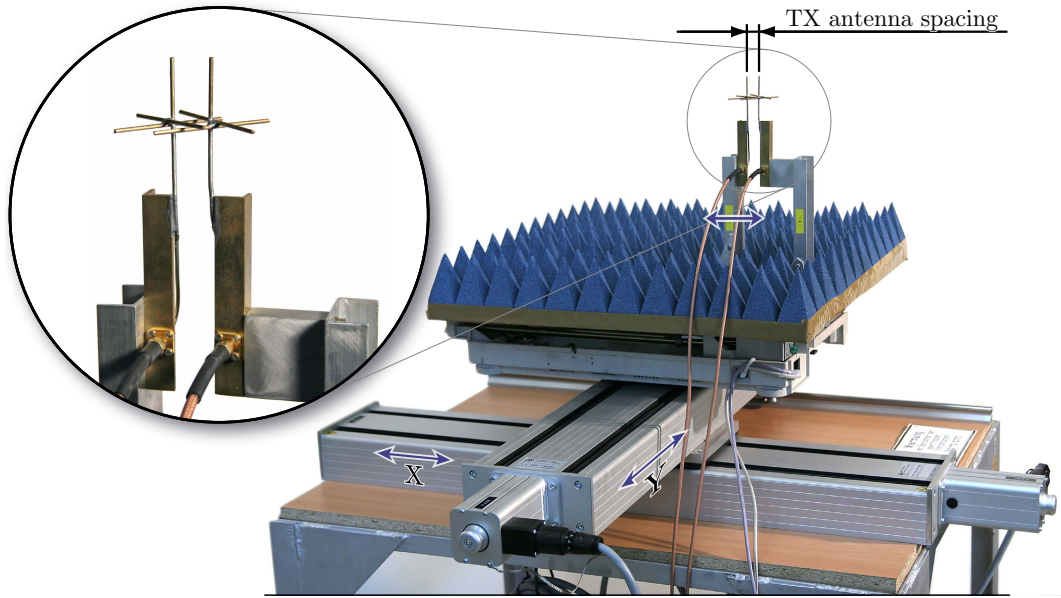


Figure 4.3: Transmit antennas used for the 2×1 measurements.

First, we transmit 100 SISO symbols plus sufficient training on the left transmit antenna, followed by 100 Alamouti coded symbols plus sufficient training on both transmit antennas, and finally, 100 SISO symbols plus training on the right transmit antenna (see Figure 4.4).

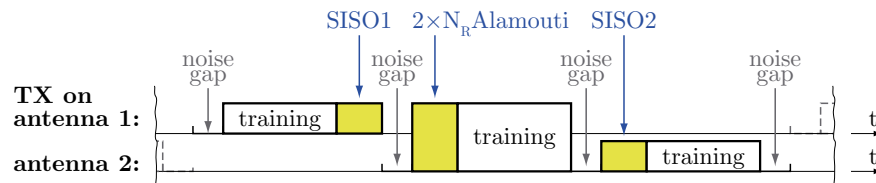


Figure 4.4: Basic transmit block used for the 2×1 measurements.

Each of these three transmissions is separately decoded at the receiver, leading

to an estimated SNR and BER each. We then repeat the whole transmission for six different SNRs (by attenuating the transmit signal), 50 different antenna spacings (we mounted the left of the two transmit antennas on a linear guide), 17×17 different xy-positions of the transmit antenna (achieved by using an xy-positioning table), and 17×17 different xy-positions of the receive antenna (achieved by using a second xy-positioning table). The resulting $3 \times 6 \times 50 \times 17^2 \times 17^2 \approx 75$ million blocks are then subject to averaging over all $17^2 \times 17^2$ transmit and receive table positions.

Results

For each of the 50 different transmit antenna spacings, the measurement procedure described above leads to a “SISO1”, a “SISO2”, and an “Alamouti” BER over TX power² curve (see Figure 4.5).

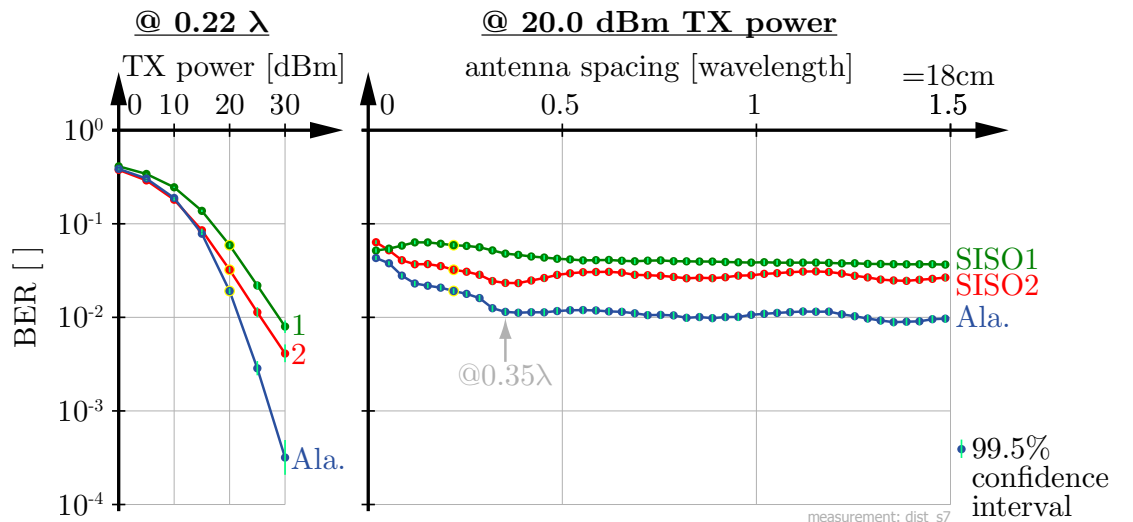


Figure 4.5: BER performance of SISO and 2×1 Alamouti.

The right-hand side of Figure 4.5 shows the BER achieved at a transmit power level of 20 dBm for different antenna distances. The BER remains almost constant down to distances of 0.35λ , after which it increases significantly. Notably, this increase is not due to antenna correlation but due to mutual coupling between the antennas that destroys the antenna matching, changes the beam-patterns, and alters the power actually radiated. Therefore, the SNR at the receiver is not constant over antenna distance when keeping the

² We measure the TX power at the input of the TX antennas.

transmit power fixed at, for example, a level of 20 dBm (see Figure 4.6). Also note the significantly different average signal powers received from the two transmit antennas.

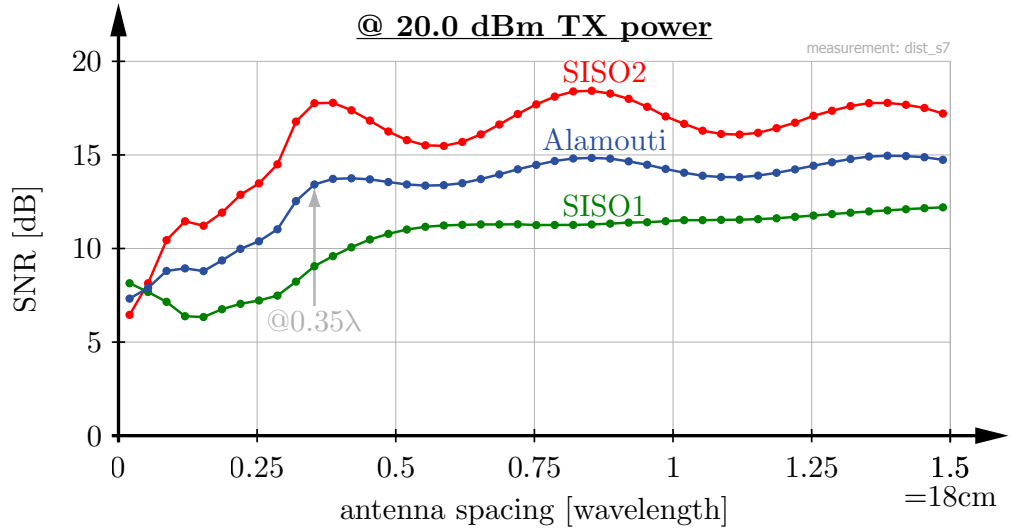


Figure 4.6: SNR achieved (TX power=const) over antenna spacing.

Because of these highly different average signal powers, it makes a difference if curves are plotted over TX power or SNR at the receiver (see Figure 4.7).

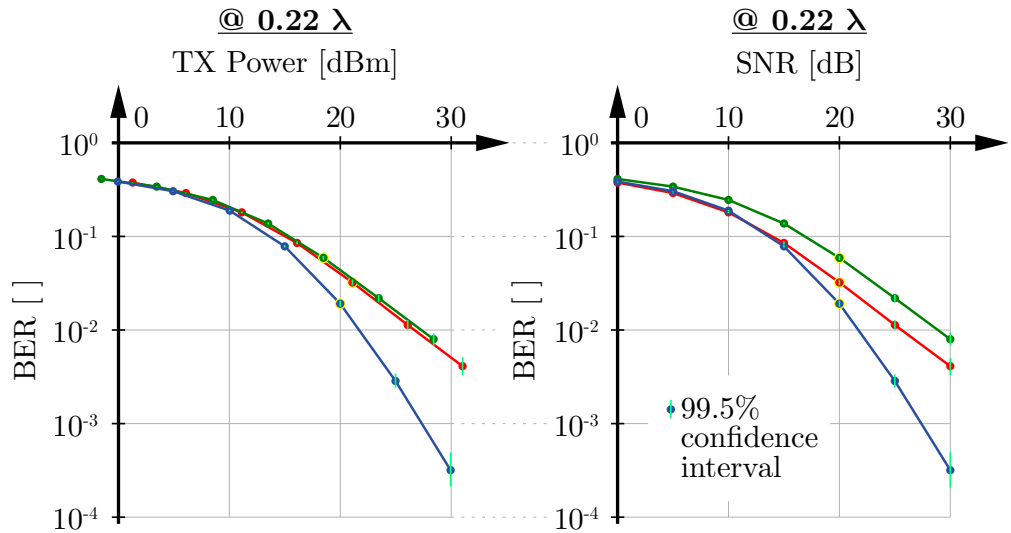


Figure 4.7: BER performance over TX Power vs. BER performance over SNR.

To visualize the performance degradation caused by correlation, we spline-interpolated all BER over SNR curves obtained to calculate the SNR required to achieve a target BER of 1% (see Figure 4.8).

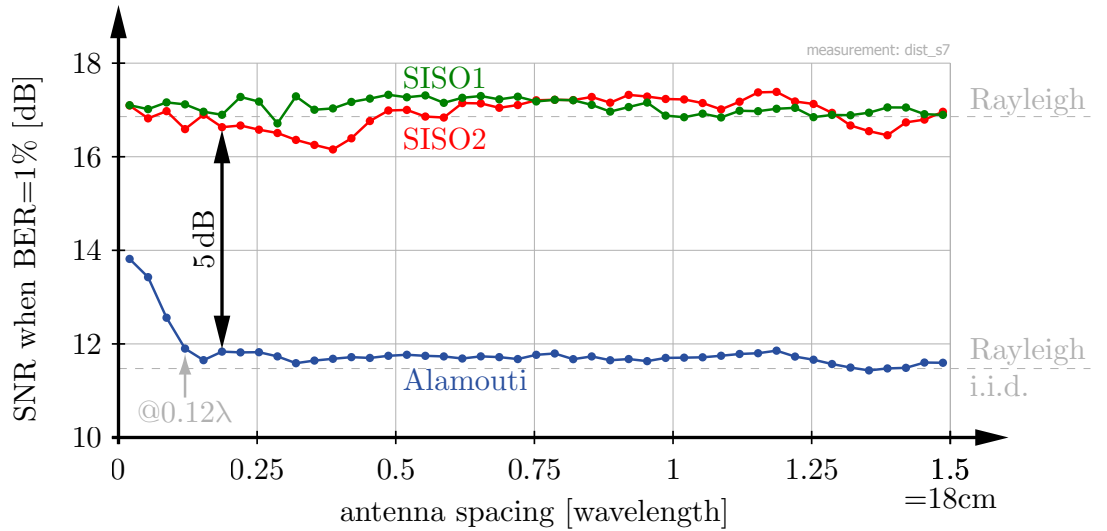


Figure 4.8: SNR required for 1% BER over antenna spacing.

As expected, we observe that the performance of the SISO links remains — apart from fluctuations in the scenario — almost equal over all measured antenna spacings at Rayleigh like conditions. Down to spacings of 0.12λ , the Alamouti link also achieves approximately the performance of a Rayleigh i.i.d. channel. The same behavior could be observed for different scenarios measured, with the Alamouti link losing performance somewhere between 0.1λ and 0.2λ . We confirmed our measurements using a $\lambda/4$ -monopole common-ground-plane antenna (similar to the second antenna shown in Figure 4.10) with a fixed antenna spacing of 0.2λ . We also used a rotation-unit to check if the results remain similar for different orientations (broadside, etc.) of the transmit antenna array.

4.1.3. Experiment II, 2×2 Indoor

In this second experiment, we evaluate the uncoded BER over receive antenna distance performance of various 2×2 single carrier schemes, namely: spatial multiplexing, a linear dispersion code, the Golden Code, and Alamouti coding. We will show that even at very small antenna distances, a significant gain compared to an ordinary 1×2 SIMO transmission can be measured.

As with the previous 2×1 measurement, we transmit the following basic transmit block on two transmit antennas.

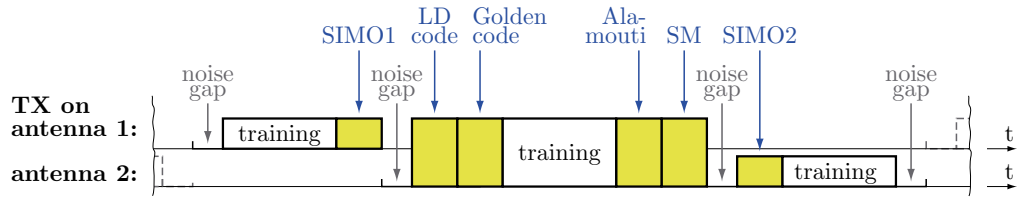


Figure 4.9: Basic transmit block used for the 2×2 measurements.

The yellow blocks in Figure 4.9 indicate the six different data blocks transmitted. To make the comparison fair

- each block incorporates exactly 64 bits of data,
- lasts for exactly $160 \mu\text{s}$ ($=400 \text{ kbit/s}$),
- and is transmitted at the same total power (sum of the power fed into both antennas).

The six blocks are coded as follows:

- I: *SIMO 1*: 16 symbols, 16-QAM modulated, transmitted on Antenna 1.
- II: *Linear Dispersion code*: 32 symbols, linearly dispersed in space and time according to the number theory enhanced space-time codes presented in [76].
- III: *Golden Code*: 32 Golden coded symbols. The Golden Code is a 2×2 full-rate, full-diversity, space-time code with non-vanishing determinants [73, 74].
- IV: *Alamouti*: 16 symbols, 16-QAM modulated and then Alamouti space-time coded [58].
- V: *Spatial Multiplexing*: 32 symbols, where 16 symbols each are 4-QAM modulated to be transmitted independently on Antenna 1 and Antenna 2, respectively [77].
- VI: *SIMO 2*: The same as SIMO 1 in item I, but the signal is transmitted on antenna 2 instead.

At the receiver, the incoming data samples were first synchronized by the use of the training sequences (shown in gray in Figure 4.9). These 4-QAM modulated, 511 sample-long training sequences were then also used to estimate the channel almost perfectly. In addition, the position of the data blocks relative to the training was also constantly permuted during the experiment³.

³ The technique of randomization does not compensate for estimation errors but gives all received blocks an equal chance of having a well estimated channel. See also [43, p.128].

Finally, maximum likelihood symbol detection is required at the receiver to achieve competitive performance. For the Alamouti code, this ML receiver can be implemented using a matched filter, whereas for the LD Code and the Golden Code a sphere decoder is required. This sphere decoder has to search over a maximum number of 256 possible transmit symbol vectors since four 4-QAM symbols are encoded in one block.

Each of the six data blocks was decoded separately at the receiver, leading to an estimated SNR and BER for each one. We then repeated the whole transmission frame for 14 different SNR values, 30 different antenna spacings, 9×9 different xy-positions of the transmit table, and 9×9 different xy-positions of the receive table. In addition, the receive antenna was also rotated between 0 and 360 degrees (uniformly distributed) during the measurement.

All $6 \times 14 \times 30 \times 9^2 \times 9^2 \approx 17$ million blocks were then subject to averaging over all $9^2 \times 9^2$ transmit and receive table positions. The averaged BER over SNR results were subsequently spline-interpolated to obtain the SNR required for a BER of 1%, for each transmission scheme and antenna distance.

The measurement of a scenario took about 10 hours, mainly because of the time needed to move the antennas. A further 10 hours were needed to process the 600 GB of baseband data samples received, in a cluster of 15 PCs, by MATLAB.

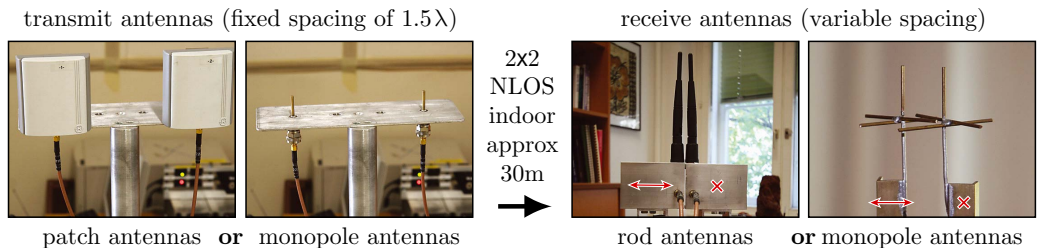


Figure 4.10: Antennas used in the 2×2 measurements.

Results

In total, 21 different indoor-scenarios were measured within a timeframe of two weeks, in and between different floors of an office building, using different antennas (see Figure 4.10). Surprisingly, the measurement results presented below showed no essentially change between the different scenarios.

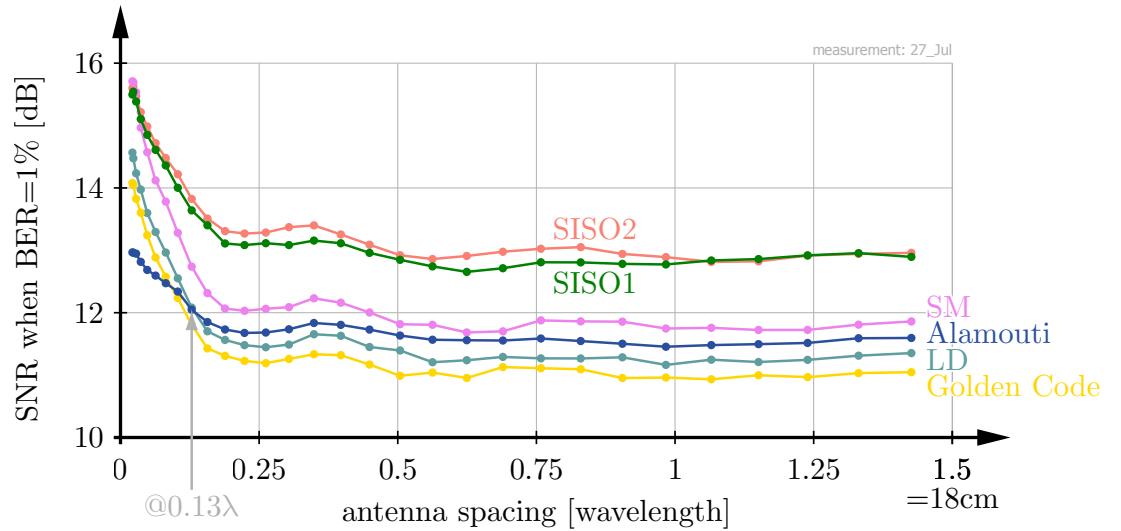


Figure 4.11: SNR required for 1% BER over antenna spacing. Exemplary result using the right TX and RX antenna in Figure 4.10.

- At an antenna distance greater than 0.13λ (0.1 to 0.4λ in other scenarios), the Golden Code outperformed all the other transmission schemes, which means that a 0.2 to 1 dB smaller average SNR was required at the receiver to obtain an average BER of 1% .
- Only at very small antenna distances was the Golden code outperformed by the Alamouti code. Note that the curve of the Alamouti code crosses the other curves at an antenna spacing of 0.13λ (0.1 to 0.4λ in other scenarios).
- But even when the antennas are not too closely spaced, the Alamouti code still performs nearly as well as the Golden Code or the LD code.
- In all scenarios measured, the LD code and the Alamouti code showed a similar level of performance for antenna distances greater than 0.4λ .
- Using two transmit antennas instead of a single one always led to a significant increase in performance.
- If the black RX rod antennas shown in Figure 4.10 were tilted slightly (to change the polarization), the performance did not degrade any further for small antenna distances. In fact, with this tilt, the antennas could no longer be placed close enough together to observe any decrease in performance (see Figure 4.13).

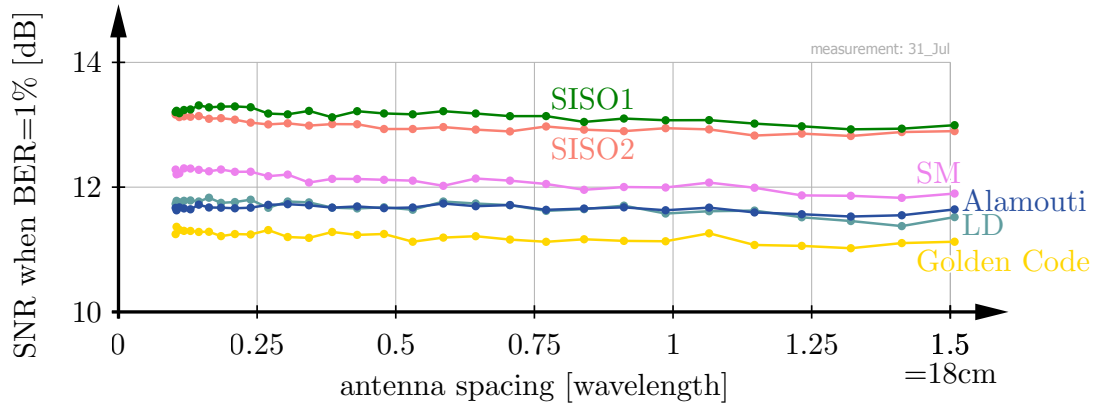


Figure 4.12: Exemplary result with tilted RX rod antennas.

Note that it makes a huge difference (up to 5 dB) if the curves presented in for example Figure 4.13 are plotted using “average transmit power required for a BER of 1 %” instead of “average SNR required at the receiver for a BER of 1 %” (see Figure 4.12).

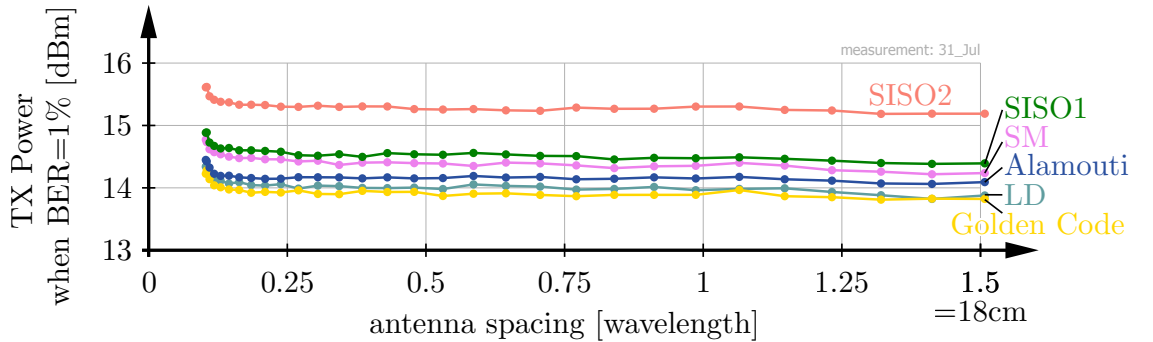


Figure 4.13: Same as 4.12 but for TX power.

This difference is due to the following reasons:

- Firstly, because mutual coupling effects and antenna mismatch losses⁴ attenuate the transmitted signal, especially at very small antenna distances.
- Secondly, real channels are not Rayleigh i.i.d., that is, the average power received from TX antenna one and antenna two differed by up to 4 dB, depending on the scenario.

⁴ For a fixed antenna distance, losses due to antenna mismatch can be eliminated by correctly matching the antennas. For variable antenna distances, this is not possible within reasonable bounds of time and effort.

- Thirdly, facing real channels that are not Rayleigh i.i.d., it turns out that the average receive power of the LD code is higher than that of the other 2×2 schemes.

Figure Figure 4.14 exemplarily shows the relationship between SNR at the receiver and antenna spacing. In all scenarios, the three effects described above could be observed to a greater or less extent.

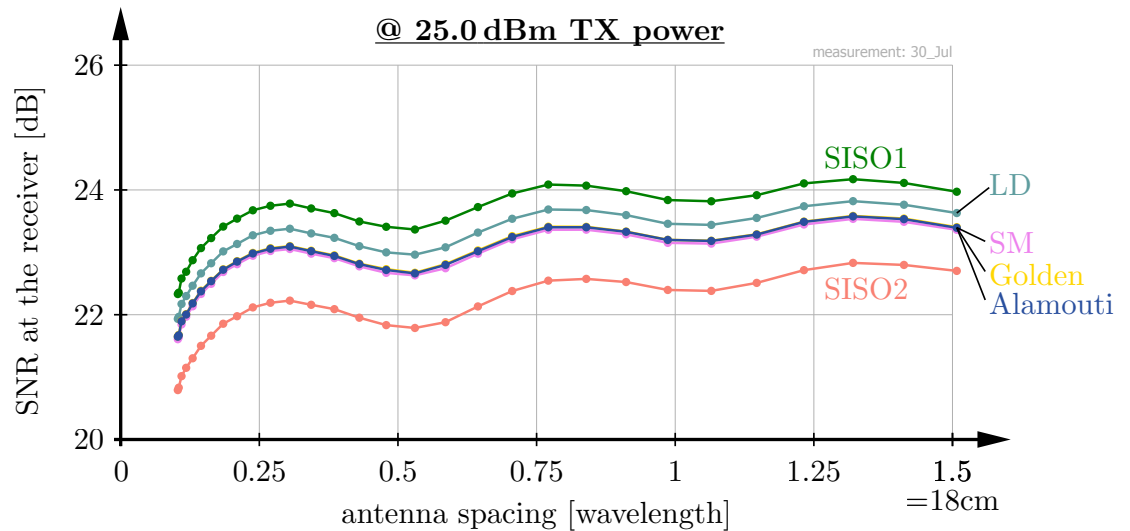


Figure 4.14: SNR achieved (TX power=const) over antenna spacing. Exemplary result using the right TX and the left RX antenna in Figure 4.10.



Figure 4.15: The receiver employing moveable (x,y) and rotate-able (Φ) rod antennas that can be changed in distance (distance).

4.2. Outdoor – HSDPA

In the following section we want to examine, by measurements, the impact of transmit antenna spacing on the throughput (rather than BER or capacity) of such a HSDPA transmission.

Consider the following set-up:

- An urban outdoor environment
- A 2×2 MIMO HSDPA transmission [120]
- Realistic flat panel base station antennas at the TX site [86, and Appendix C, page 117]
- Realistic printed monopole antennas at the RX site [118, 119]

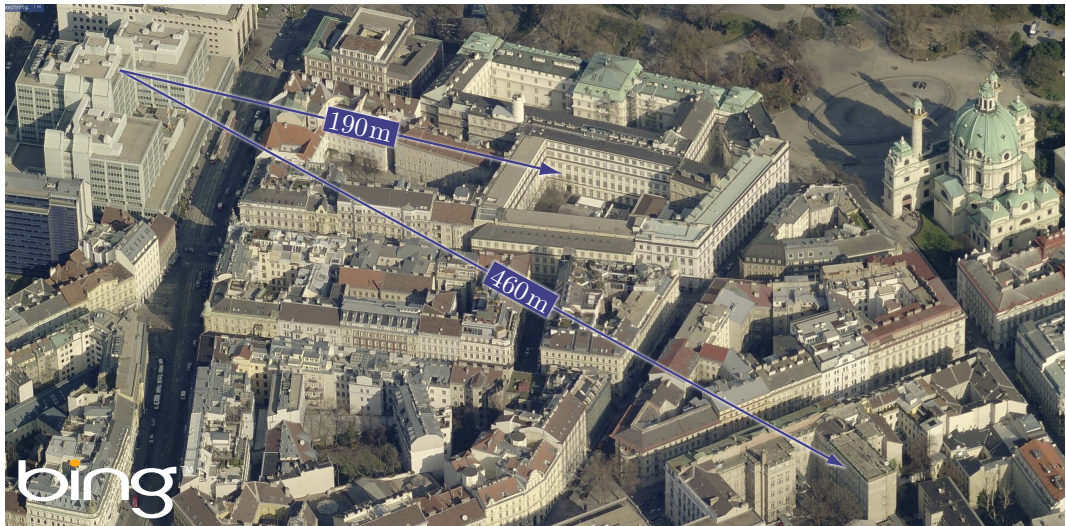


Figure 4.16: Urban scenarios measured [82].

4.2.1. Existing Research

To our knowledge, no results (measurement or simulation) exist that

- relate TX antenna spacing to the physical layer throughput of a standardized MIMO mobile communication system.
- relate TX antenna spacing to the throughput (or a similar performance metric⁵) of a MIMO closed-loop radio link in general.

⁵ Note that capacity is —although an interesting and very important performance metric— an upper performance bound. Neither does uncoded BER say much about the performance actually achieved by a system.

- investigate TX antenna spacing in an outdoor scenario using realistic TX and RX antennas to investigate MIMO transmissions (and not, for example, dipoles at the TX site).
- For the special case of 2×2 HSDPA considered in the following, no closed-loop throughput measurement result exist over transmit power, let alone antenna distance. See [34, Section 1.3, Chapter 3 Overview] for an in depth literature research.

Note that results relating antenna spacing, correlation, and capacity have already been extensively discussed in Section 4.1.1, page 52.

4.2.2. Experiment III, 190 m Urban

In the following, we will report on 2×2 HSDPA physical layer throughput measurements that were carried out for various TX antenna distances between 0.6 and 7.7λ . Transmitter and receiver are placed 190 m apart (see Figure 4.16, page 63) in the inner city of Vienna. The direct path from the TX to the RX antennas is blocked by the building the RX unit is located in. The resulting non line-of-sight connection (see Figure 4.17, page 65) is characterized by a low root-mean-square delay spread of $0.5 \mu\text{s}$, which equals to 1.9 UMTS chip durations⁶ [34].

TX Antennas – Flat Panel 2X-Pol Antennas

At the base-station, we employ KATHREIN 800 10629 [86] 2X-pol panel antennas with a half-power beam width of $80^\circ/7.5^\circ$ and a total down tilt of 16° ($= 10^\circ$ mechanical + 6° electrical). The antennas are placed on the roof of a tall building in the center of Vienna, Austria, right adjacent to other base stations, making the measurement results obtained very realistic and representative for a mobile communication system (see Figure 4.17, page 65).

Note that the Kathrein 800 10629 antennas used in the following experiments are laboratory samples that will most probably be replaced by a more advanced design in the near future. (See Appendix C, page 117, for a detailed list of specifications.)

⁶ The chip duration in UMTS is 260 ns.

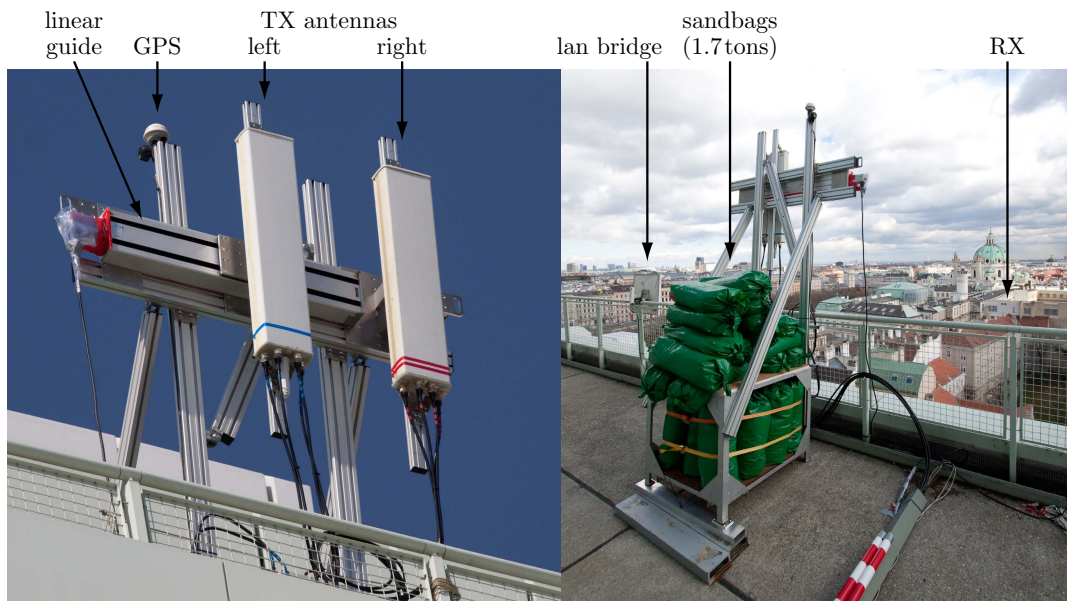


Figure 4.17: The TX antennas employed.

Each of these two 2X-pol antennas has four connectors, two for $+45^\circ$, and two for -45° polarization. The two equally polarized elements are separated by 0.6λ . Thus we were able to measure with two equally polarized TX antenna elements at distances from 0.6 to 7.7λ (see Figure 4.18). The critical issue here is that, in order to make the comparison fair, the right-hand “/”-antenna elements of both antennas have to yield the same average path loss (and antenna pattern) at an antenna distance of 1.4λ . Careful selection and tuning of the base station antennas is therefore required.

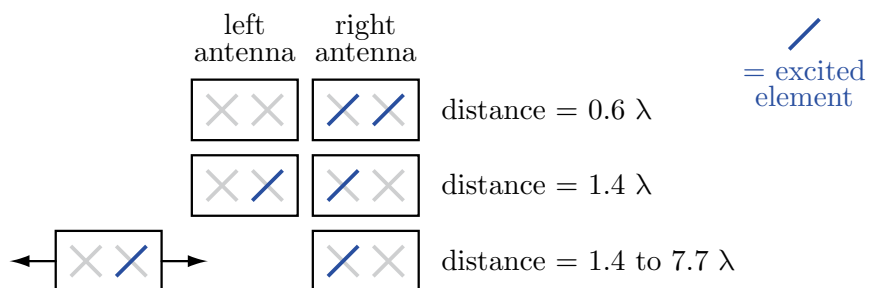


Figure 4.18: Changing the distance between 0.6 and 7.7λ .

When comparing 2×2 transmissions over equally polarized versus cross polarized elements at the TX antenna, the same problem arises. Here the trick is to measure the comparison on the same elements as shown in Figure 4.19, page 66.

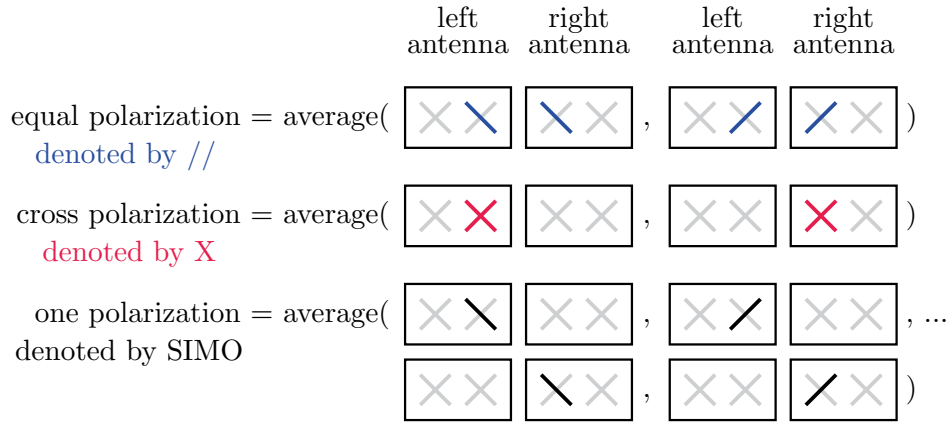


Figure 4.19: Comparing equal with cross polarization and SIMO.

RX Antennas – Printed Monopole Antennas

At the mobile phone site, we utilize two low-cost printed monopole antennas [118, 119], which are based on the generalized Koch pre-fractal curve. Due to their low cost and small size, such antennas are very realistically built into a mobile handset or a laptop computer. In order to exploit polarization diversity and a good separation between the two spatial data streams, differently polarized antenna elements are employed. In the following, we only present data measured with RX antennas 1 and 2 (see Figure 4.20).

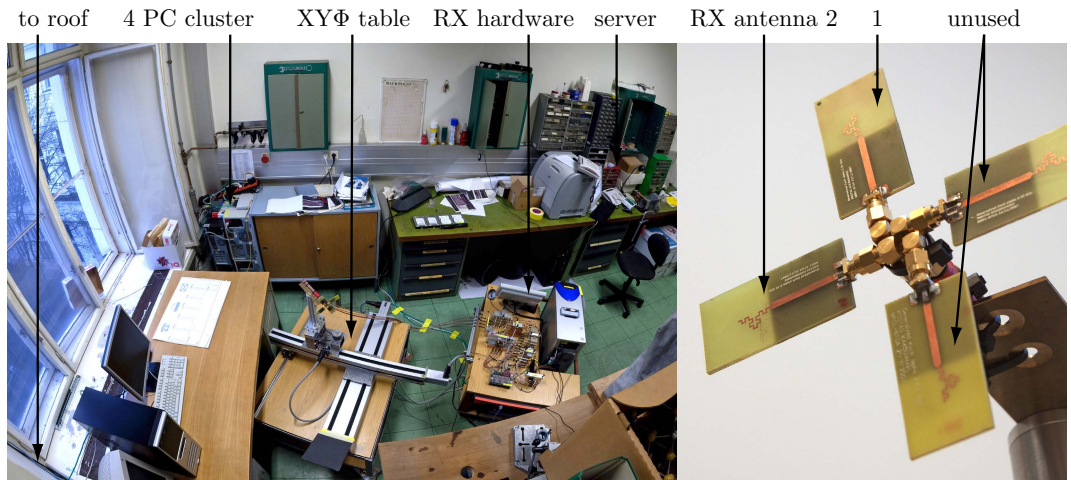


Figure 4.20: The RX antennas employed.

The receive antennas are mounted on an XYΦ-positioning table in order to be able to generate the channel realizations from which we average the performance of the scenario.

Performance Metric – HSDPA Throughput

The High Speed Downlink Packet Access (HSDPA) mode [120] was introduced in Release 5 of UMTS to provide high data rates to mobile users. This is achieved by several techniques [126–129] such as fast link adaptation [124], fast hybrid automated repeat request [125], and fast scheduling. In contrast to the pure transmit power adaptation performed in UMTS, fast link adaptation in HSDPA adjusts the data rate and the number of spreading codes depending on a so-called channel quality indicator feedback. MIMO HSDPA [130], recently standardized in Release 7 of UMTS, further increases the maximum downlink data rate by spatially multiplexing two independently coded and modulated data streams. Additionally, channel-adaptive spatial precoding is implemented at the basestation. The standard defines a set of precoding vectors where one of them is chosen based on a so-called precoding control indicator feedback obtained from the user equipment.

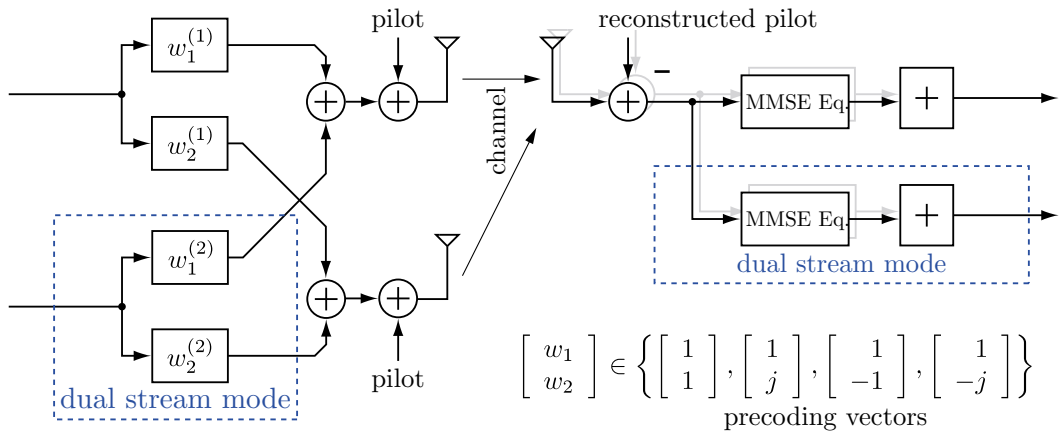


Figure 4.21: TxAA and D-TxAA MIMO HSDPA.

In the measurements, we restrict ourselves to the single-user case due to the hardware effort required for multi-user measurements. Another reason for choosing only the single-user case for the measurements is that multi-user scheduling for HSDPA is still a topic in research [140–142]. We furthermore restrict our investigations to slow fading, that is, the channel is assumed to be constant during the transmission of several subframes. This restriction is required by our measurement procedure for measuring retransmissions and feedback (see Section 2.8, page 30).

In the following measurements we compare six different 2×2 HSDPA transmission modes:

1// One Stream, Equally Polarized TX Antennas:

The so-called closed loop Transmit Antenna Array (TxAA) [121] uses strongly quantized precoding at the transmitter to increase the signal to interference and noise ratio (SINR) at the user equipment. In the case of the Category 16 user equipment, the maximum transport block size in this single-stream mode is 25 558 bits transmitted in one subframe of length 2 ms. Thus, the maximum data rate in single-stream mode is 12.779 Mbit/s.

1or2// One or Two Streams, Equally Polarized TX Antennas:

In 2007, the 3GPP standardized D-TxAA (Double Stream Transmit Antenna Array) [78], the first true MIMO extension in UMTS. D-TxAA is downward compatible with TxAA and equals TxAA when the SINR at the user equipment is low. At larger SINRs, D-TxAA switches to dual stream mode and transmits two independently coded HSDPA [122] data streams. Thus, in TxAA a single stream is always transmitted and in D-TxAA either single-stream or double-stream transmission —whichever is better— is used.

Switching between single and dual stream mode, the encoding rate, and the modulation alphabet are determined by the Channel Quality Indicator feedback. Depending on the channel conditions and the type of receiver implemented, the user equipment calculates an appropriate feedback value in order to achieve a block error ratio of 10 % [121]. In dual stream mode, the maximum transport block size of one stream is equal to 27 952 bits allowing for a maximum overall data rate of 27.952 Mbit/s.

2// Two Streams, Equally Polarized TX Antennas:

In addition we also implemented a mode —non existent in reality— that behaves like D-TxAA, but always forces the transmission to use two streams, even if one stream would have performed better.

1X One Stream, Cross Polarized TX Antennas

As **1//**, but using cross polarized TX antenna elements (see Figure 4.19, page 66).

1or2X One or Two Streams, Cross Polarized TX Antennas

As **1or2//**, but using cross polarized TX antenna elements.

2X Two Streams, Cross Polarized TX Antennas

As **2//**, but using cross polarized TX antenna elements.

SIMO 1×2 HSDPA

In order to be able to correct for different average path losses we also consecutively transmit 1×2 HSDPA from every transmit antenna to both receive antennas (see Figure 4.19, page 66).

Measurement Procedure

In Figure 2.22, page 31, we showed how a “single” HSDPA data frame is transmitted. To infer the average throughput performance (as shown for example in Figure 4.22, page 70) of this specific urban scenario we carry out the following fully automatized steps:

- We consecutively transmit all $3 (//) + 3 (\times) + 1 (\text{SIMO}) = 7$ schemes under investigation as described above (the curves in Figure 4.22, page 70). Due to required feedback, possible retransmissions (see Figure 4.22, page 70), and averaging (see Figure 4.19, page 66), we actually transmit $[1 (\text{feedback}) + 1 + 2 (\text{retransmissions})] \times [2 \times 3 (//) + 2 \times 3 (\times) + 4 (\text{SIMO})] = 4 \times 16 = 64$ blocks of HSDPA data.
- We repeat all the above for 11 different transmit power levels (the left x-axis in Figure 4.22). To achieve this, we attenuate the transmit signal before it enters the power amplifier.
- We repeat all the above for 12 transmit antenna spacings (the right x-axis in Figure 4.22). As shown in Figure 4.18, 11 of these are created by moving the left antenna, whilst the 12th is created by switching the left antenna elements.
- We repeat all the above for 303 different receive antenna positions, which are created by moving the RX antennas using the fully automated $XY\Phi$ positioning shown in Figure 4.20. To minimize large scale fading effects, we measure positions that are uniformly distributed within an area of $3 \times 3 \lambda$. Correlation between the different positions is minimized by this systematic sampling approach, maximizing the distance between all positions measured.

Measuring all these $(1+1+2) \times (2 \times 3 + 2 \times 3 + 4) \times 11 \times 12 \times 303 = 639\,939$ HSDPA blocks took about two days. Meanwhile, a self programmed cluster software parallelized the off-line evaluation of the received data samples (about 900 Gigabytes) on a position-by-position basis (see also Section 2.5, page 20). We positioned the necessary cluster server and four PCs directly next to the receiver since the wireless-LAN network available at the site did not allow

for transferring the data back to our institute in reasonable time (see Figure 4.20).

During the measurement we instantly collected all the calculated results from the cluster in order to average the throughput observed over the positions measured. Several tests were carried out in order to validate the results. For example, we checked for measurement outliers or interference that should not exist (see Section 2.4.4, page 18).

Plotting the Results

Figure 4.22 presents the outcome of the measurement procedure as described above. In the left graph, the averaged (over 303 positions) HSDPA throughput is plotted versus transmit power for a TX antenna element spacing of 3.9 wavelengths (about 47 centimeters). The right-hand graph shows exactly the same measured data, but versus antenna element spacing for a fixed TX power of 24.6 dBm. Therefore, the two yellow points in the left-hand graph equal the two yellow ones in the right-graph graph.

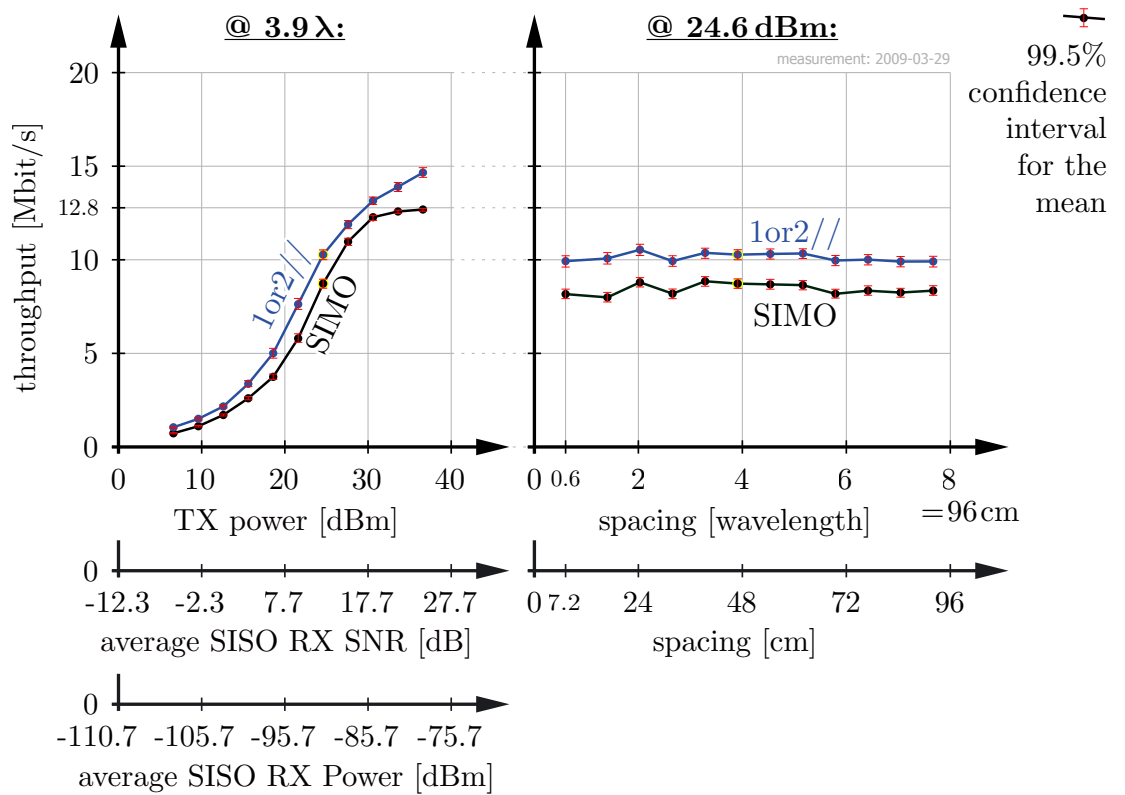


Figure 4.22: Measured average throughput.

In the left-hand graph, the throughput curves are plotted over total transmit power⁷. Two additional x-axes show the average received SIMO SNR and average received SIMO signal power. The reason why we plot the throughput over transmit power is the following: all MIMO schemes in HSDPA utilize adaptive precoding at the transmitter that effectively increases the received power and thus also the SNR while the total transmit power is the same as in the SIMO transmission. If the throughputs were plotted over SNR, rather than over transmit power, the relative position of the curves would change. The additional x-axes (average SISO RX SNR and average SISO RX Power) are thus only shown as a reference to indicate the approximate SNR and receive power ranges.

Finally, we investigate the precision of the measurement by means of bootstrapping methods [38]. In both graphs, the vertical red lines represent the 99.5% BCa bootstrap confidence intervals for the mean⁸, and the corresponding horizontal lines the 0.25% and 99.75% percentiles. Note that the RX antenna position remains unchanged while measuring different schemes at different transmit power levels. This leads to smooth curves in the left-hand graph and *relative* positions of the curves that are more precise than the confidence intervals for the *absolute* positions might suggest.

Correcting for the Average Path Loss

Looking back at the right-hand graph in Figure 4.22, page 70, we observe that the `1or2//` as well as the SIMO performance exhibit small variations over TX antenna element spacing, while the SIMO performance at least should remain constant. The corresponding confidence intervals suggest that this change is not due to an imprecise measurement (otherwise we could just measure at more RX antenna positions). Actually, moving the left antenna seems to slightly change the scenario, leading to slightly different fading at the receiver site. The trick now is to correct for this undesired effect that adds some undesired disturbance to our desired result, namely, the performance over antenna element spacing.

Returning to the right-hand graph in Figure 4.22, we clearly observe that the

⁷ Since we cannot easily measure the power actually radiated by the TX antenna, we define the TX power as the power actually fed into the TX antenna (measured directly at its connectors).

⁸ See Section 2.6.2, page 24.

average throughput of the `lor2//` transmission might be highly correlated with the corresponding averaged SIMO transmission. In fact, for example, for a TX power of 24.6 dBm, the correlation coefficient⁹ between the SIMO throughput and the `lor2//` throughput values turns out to be 0.92¹⁰. Figure 4.23 shows the corresponding scatter plot.

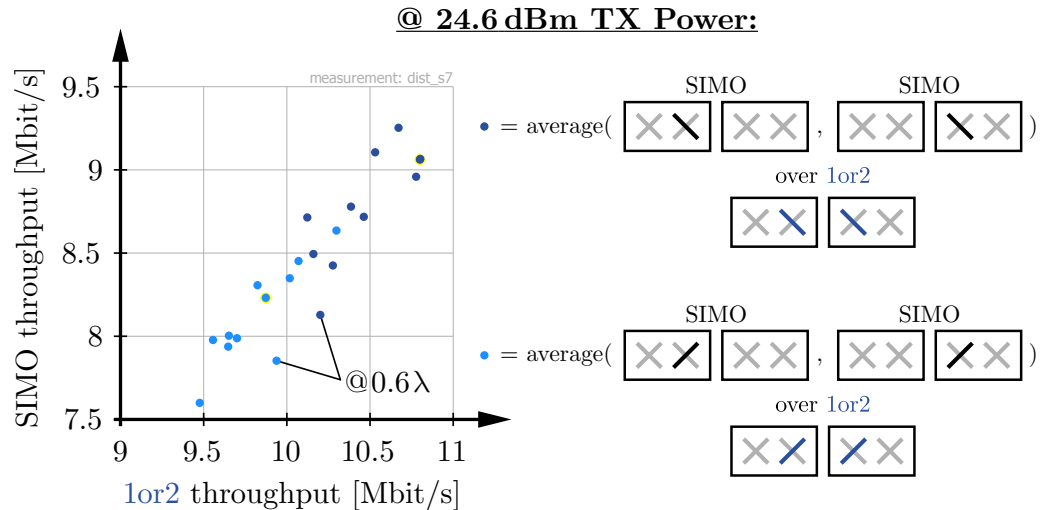


Figure 4.23: Scatter plot for $\pm 45^\circ$ polarization and 11 different antenna spacings. SIMO versus `lor2//` average throughput.

Since the $+45^\circ$ and -45° polarization measurements averaged to the `lor2//` curve receive a different average path loss, the two polarizations are drawn separately versus the averaged corresponding SIMO transmissions (11 points each). Note the two points obtained at an antenna element spacing of 0.6λ that were measured using different antenna elements at the TX site (see Figure 4.18, page 65). Without these points the correlation turns out to be 0.95, with a 95% BC_a bootstrap confidence interval of [0.91, 0.97].

Postulating that the SIMO performance does not change over antenna distance, we can now use the SIMO measurement to correct for the average path loss in all other measured curves. As shown in Figure 4.24, we do so by simply subtracting¹¹ the corresponding SIMO throughput-change measured at

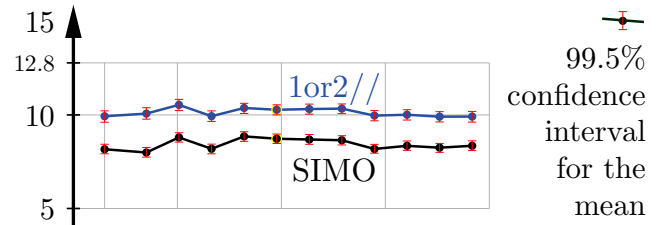
⁹ Note that “correlation measures association. But association is not causation” [52, p.150].

¹⁰The 95% BC_a bootstrap confidence interval for the correlation coefficient is [0.83, 0.97].

¹¹Performing a linear regression on the data presented in Figure 4.23, page 72, the regression coefficient turns out to be 0.98 with a 95% BC_a bootstrap confidence interval of [0.83, 1.17]. For more information on how to use supplementary (so-called “concomitant”) observations that are correlated with the observations of interest see [47, p.48].

the same antenna elements. Note that the corresponding BCa confidence intervals even decrease in size due to the high degree of correlation between the curves.

Before correction:



After correction:

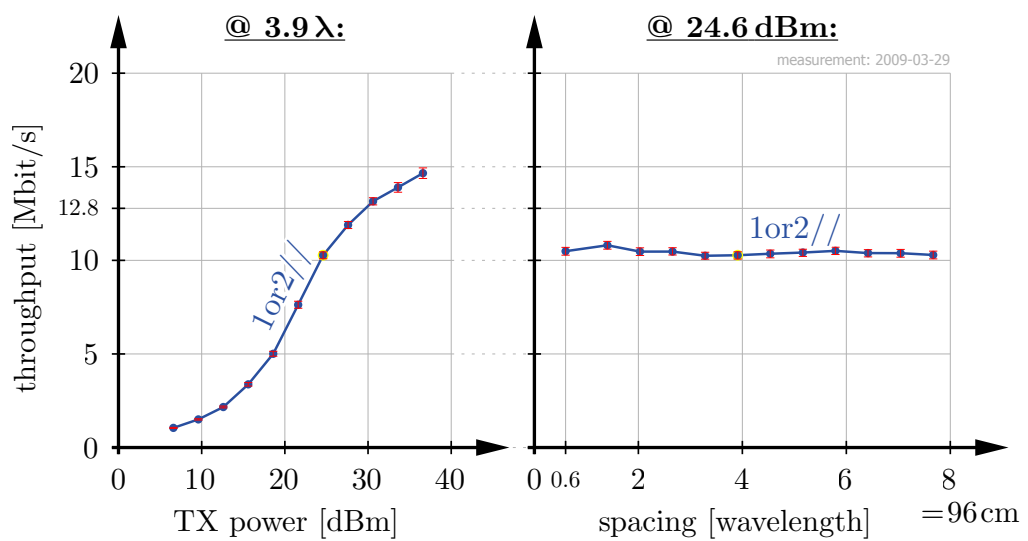


Figure 4.24: Throughput from Figure 4.22 corrected by average path loss.

Results for Equal Polarization

After applying the correction method described above, we can now proceed to investigate the results obtained. Figure 4.25, page 74, shows the average throughput for 1, 1or2, and 2 HSDPA data streams when utilizing equally polarized antenna elements at the TX site.

We observe the following for this particular scenario:

- Transmitting one stream (1//) works as well as transmitting one or two streams (1or2//) when employing equal polarizations. In other words, it seems that beamforming is far more efficient than spatial multiplexing (2//) in this scenario.
- Only at transmit power levels exceeding 27.6 dBm does transmitting two streams become advantageous, because the one stream mode saturates

at its theoretical maximum of 12.8 Mbit/s.

- For antenna distances greater than 5λ , two streams work better than one stream at some RX antenna positions, making the $1or2//$ stream mode work slightly better than the $1//$ stream mode¹².

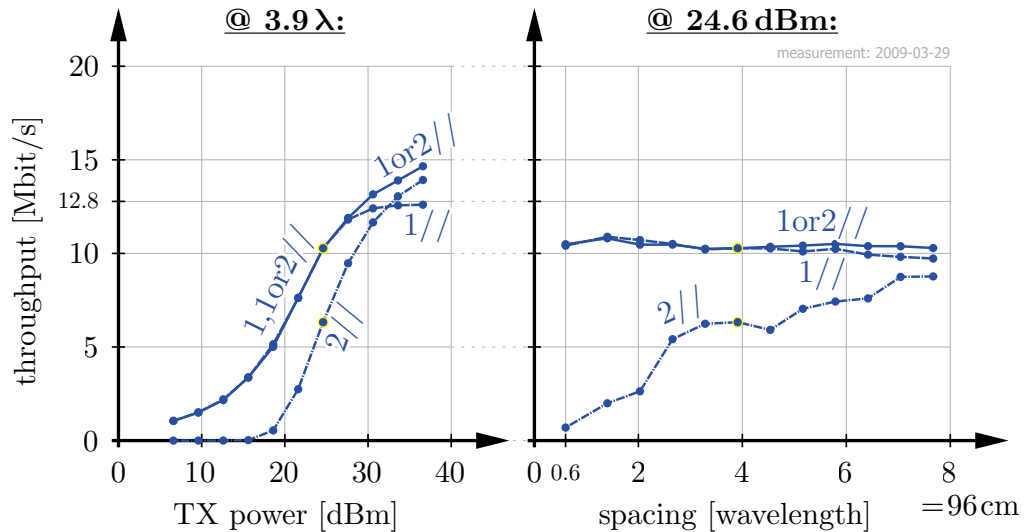


Figure 4.25: 1, 2, and 1&2 data streams, equal polarization.

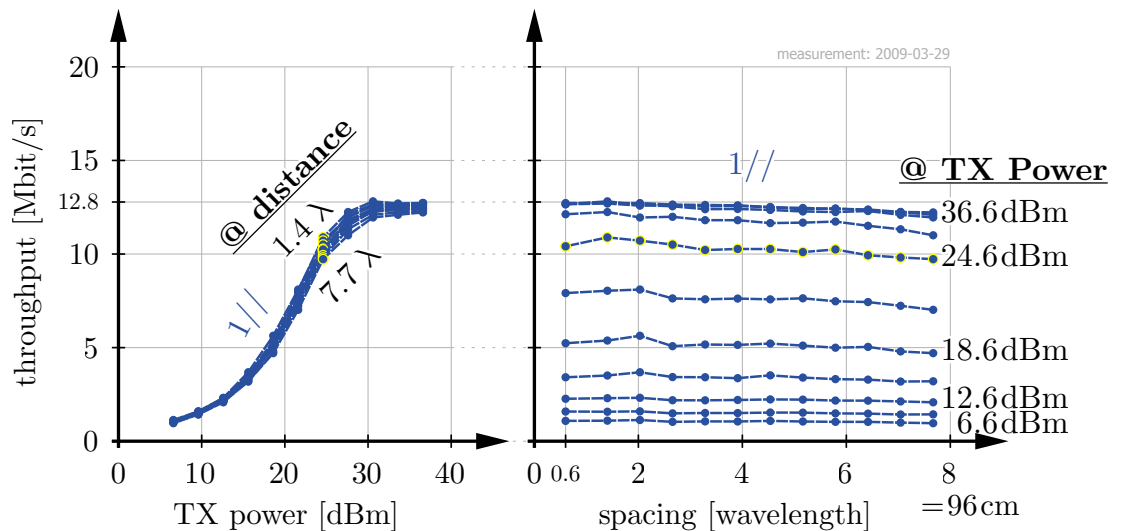


Figure 4.26: 1 data stream (= TxAA), equal polarization.

¹²In theory, as the $1//$ stream mode is a subset of the $1or2//$ mode, the former can never work better. In practice, however, estimation errors occur and the scenario may change slightly between these two consecutive transmissions.

Figure 4.26 shows the performance of HSDPA employing 1 data stream at equal polarization:

- The 1// stream mode saturates at its theoretical maximum of 12.8 Mbit/s—that is, error free transmission when employing the highest possible modulation alphabet.
- A slight, but significant, decrease in throughput is observed when the TX antenna element separation is increasing. In other words, beamforming works slightly better at small antenna element spacings.

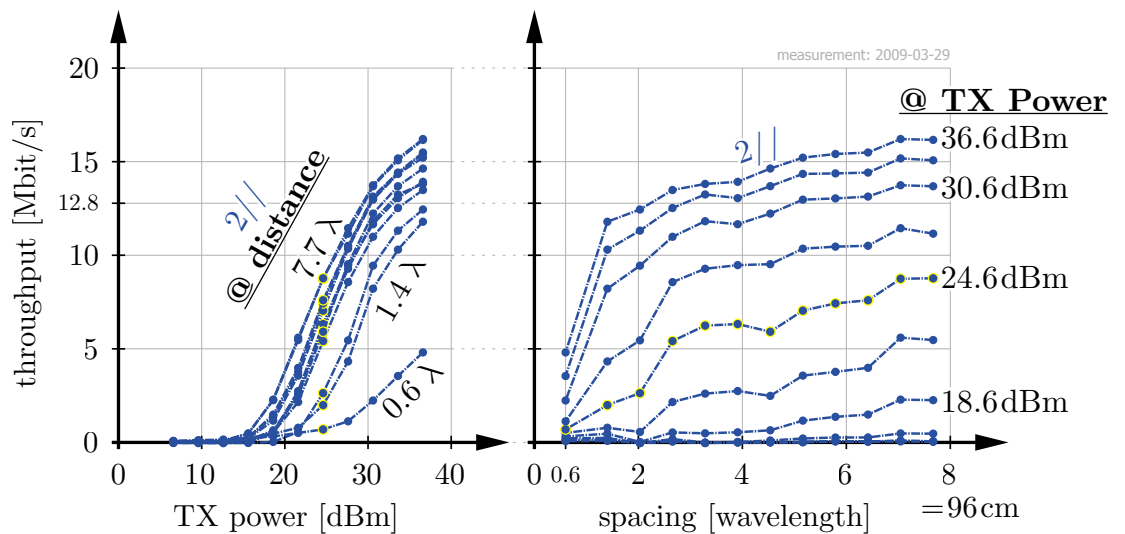


Figure 4.27: 2 data streams, equal polarization.

Figure 4.27 shows the performance of HSDPA when forcing 2 data streams at equal polarization:

- The performance of the 2-stream mode is highly dependent on the TX antenna element spacing.
- The two antenna elements could not be placed far enough apart (due to mechanical limitations in our set-up) in order to obtain any further gains from an increased element spacing.
- Because the 2-stream mode does not exist in a real HSDPA system, its poor performance at low antenna distances is covered by the excellent performance of the 1-stream mode as shown in Figure 4.28, page 76,.

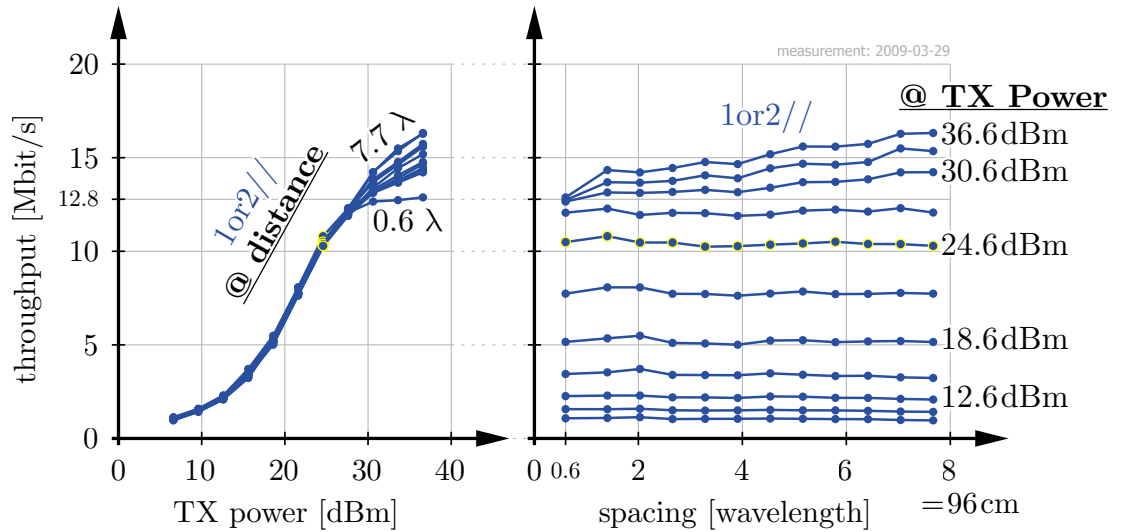


Figure 4.28: 1 or 2 data streams (= D-TxAA), equal polarization.

Figure 4.28 shows the performance of HSDPA when either one or two streams (whichever is better on a position by position basis) are transmitted.

- At lower TX powers, the performance remains constant over TX antenna element spacing.
- At higher TX powers, the performance increases over antenna element spacing because the 1-stream mode is saturated.

Results for X Polarization

Figure 4.29 shows the same measurement as Figure 4.25, page 74, but employing cross polarized antennas at the transmitter. The spacing between the two excited elements is always zero, although the antennas are still moved during the measurement (see Figure 4.19, page 66). We observe the following:

- The performance does not significantly change over “equivalent // spacing” since the spacing between the excited elements is always zero.
- There is a significant gain from employing D-TxAA (1or2-streams), even at low transmit powers.
- Only at very low transmit powers (≤ 12.6 dBm) does the single stream mode (beamforming) perform as well as when 1or2 streams are used.

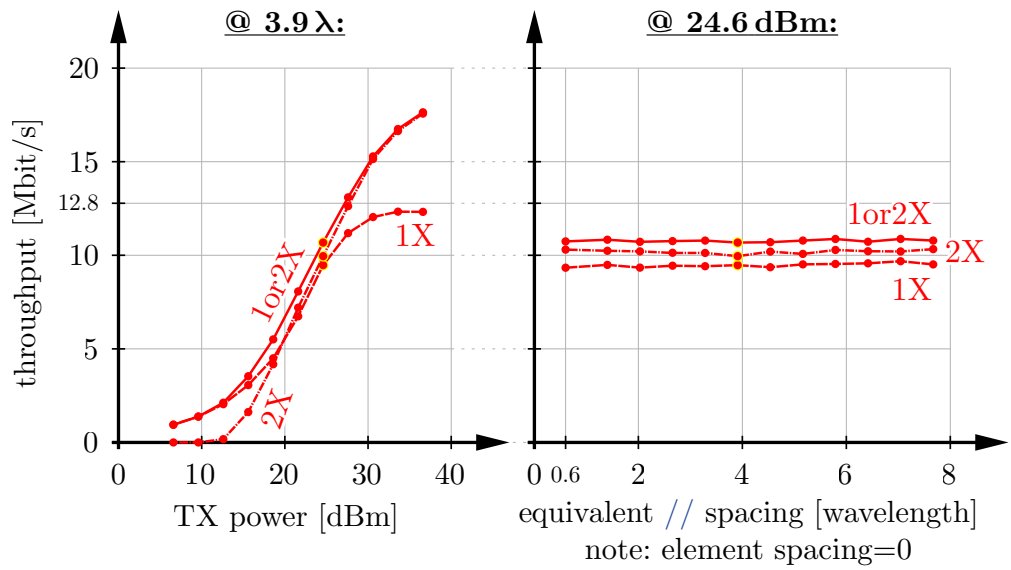


Figure 4.29: Results for cross polarization.

Because the results for equal and cross polarization are obtained by measuring on the same antenna elements (see Figure 4.19, page 66), we are now able to directly compare the results in Figure 4.30. We averaged the cross polarized measurements to one single point plotted at an element spacing of 0λ . The SIMO curve is constant over distance per definition because of the correction technique applied (see Section 4.2.2, page 71).

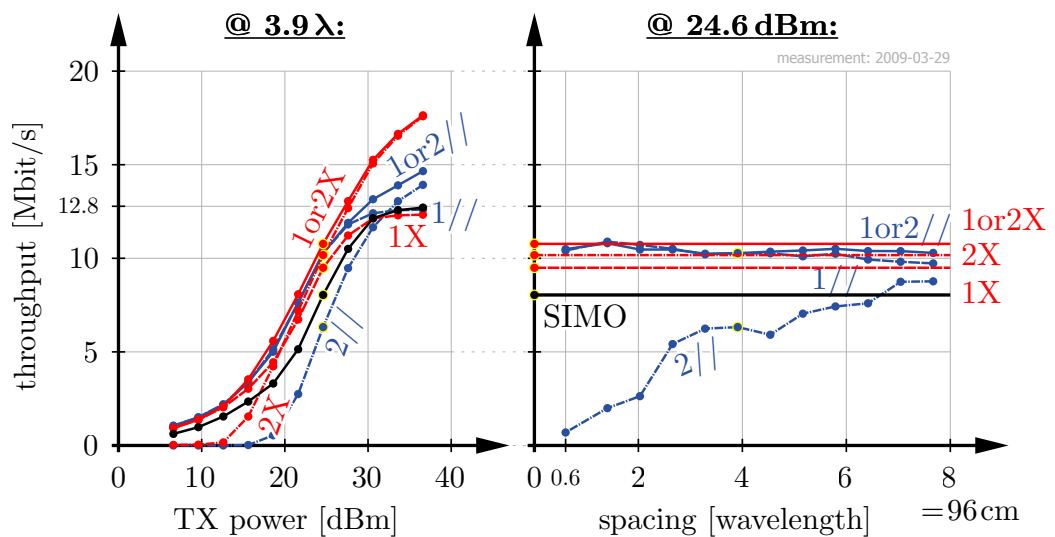


Figure 4.30: Comparing equal to cross polarization.

- Regardless of the TX antenna element spacing employed, there is a significant gain from using more than one antenna element at the TX site. In other words, MIMO always works better than SIMO.
- For D-TxAA (1or2 streams), cross polarized antennas at the transmitter yield a higher throughput than equally polarized antennas¹³.
- Interestingly, TxAA (1 stream – beamforming) works better with equally polarized antennas¹⁴.

In the following two subsections, we will now compare the results obtained with measurements carried out previously:

4.2.3. Experiment IV, 460 m Urban

Looking back at Figure 4.16, the transmitter is still placed on the roof of the same building in the inner city of Vienna, Austria. The receiver is now placed 460 m away in the topmost floor of an office building. The direct path is blocked by a copper roof and the adjacent buildings, resulting in a non line of sight connection with a very large root mean square delay spread of 1 μ s (equal to 3.8 UMTS chip durations¹⁵) [34]. This scenario was chosen as an extreme example (while still being realistic) due to the high degree of scattering at the cell border.

TX Antennas – Flat Panel X-Pol Antennas

At the transmitter, we utilize two Kathrein 800 10438 [86, and Appendix C, page 117] X-pol antennas ($\pm 45^\circ$ polarization, half-power beam width $65^\circ/5^\circ$, total down tilt 6°), see Figure 4.31. Unfortunately, these X-pol panels only allow for measuring down to antenna element spacings of 1.3λ . That is the reason why we employed XX-pol antennas in Experiment III (Section 4.2.2, page 64), which was carried out some time later.

¹³In practice, employing two equally polarized antennas at the transmitter is cheaper, provided that there is sufficient room at the base-station.

¹⁴This fact has also been observed in other measurements that we have carried out throughout the last year.

¹⁵The chip duration in UMTS is 260 ns.

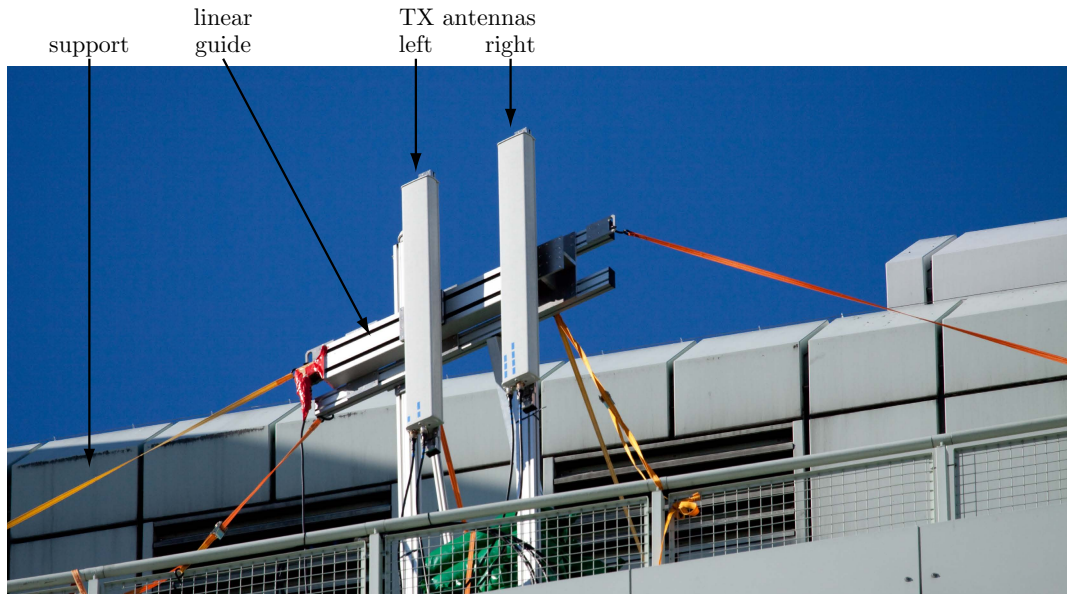


Figure 4.31: The TX antennas employed.

RX Antennas – Printed Monopole Antennas

At the receiver, we employ the same printed monopole antennas as in Experiment III. We also place them on an $XY\Phi$ positioning table in order to create 930 different channel realizations (see Figure 4.32).

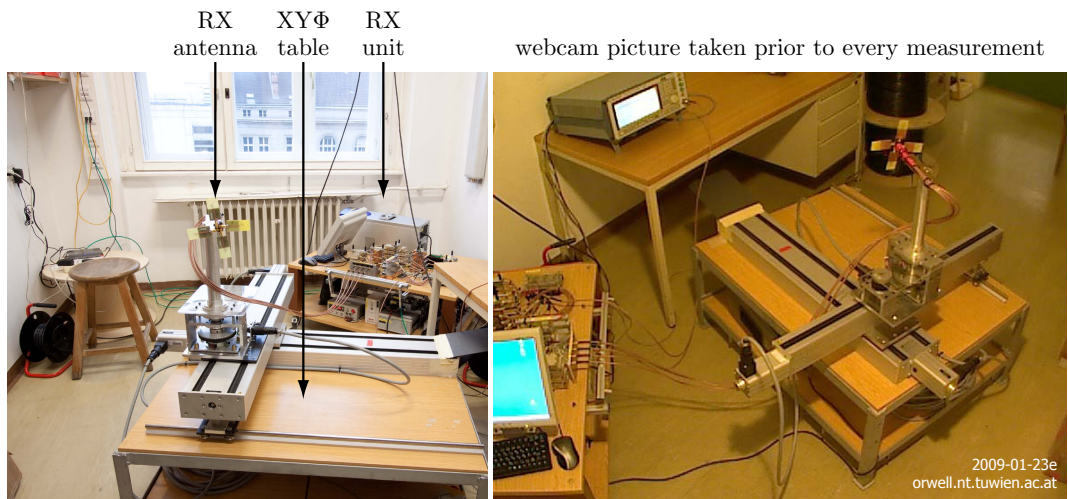


Figure 4.32: The RX unit employed.

The right-hand side of Figure 4.32 shows the webcam picture that is taken prior to every measurement for documentation purposes.

Results

Unfortunately, we have no measurement results available over TX power, the 2//, and the 2X mode¹⁶. However, we are able to reconstruct most of Figure 4.30 for this old scenario (see Figure 4.33);

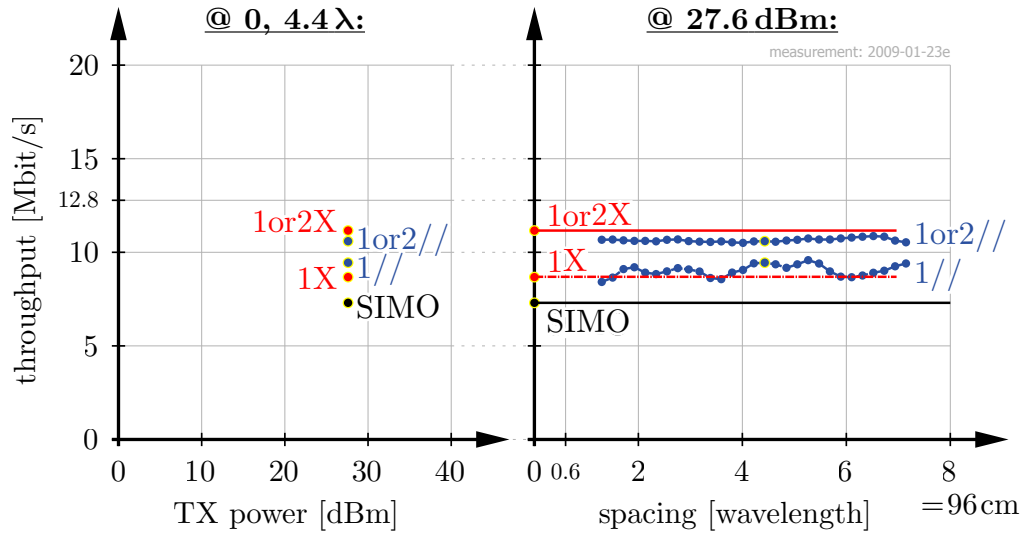


Figure 4.33: Throughput obtained in the 460 m urban scenario.

- D-TxAA (1or2 streams) works significantly better than TxAA (1 stream) in this scenario, regardless of the TX antenna element spacing employed. We believe that this is a result of the greatly increased scattering compared to the last experiment¹⁷.
- For D-TxAA (1or2 streams), it is better to employ cross polarized TX antennas. For TxAA (1 stream), it is better to employ equally polarized TX antennas.
- In any case, employing MIMO yields significantly higher throughputs than SIMO.

4.2.4. Experiment V, 5.7 km Alpine Valley

After investigating a scenario with a very large angular spread in Experiment IV, we now consider the other extreme of transmitting HSDPA in the Drau

¹⁶In Experiment III we corrected the flaws of Experiment IV.

¹⁷The root mean square delay spread doubled from 0.5 μ s to 1 μ s.

valley in Austria. In this scenario, the TX antennas are placed immediately adjacent to existing base station antennas on one side of the valley. The RX unit is located at a distance of 5.7 km (no obstacles in between) inside a house on the opposite side of the valley.

RX Antennas – Rod Antennas

At the RX unit, we utilize standard Linksys WiFi-Router rod antennas¹⁸ (see Figure 4.34). They are placed indoors in non-line-of-sight to the transmitter. The whole set-up is characterized by a short mean root-mean-square delay spread of about 1 chip (260 ns) and a single major propagation path because the receive signal mainly enters through a window next to the transmit antennas (see Figure 4.34).

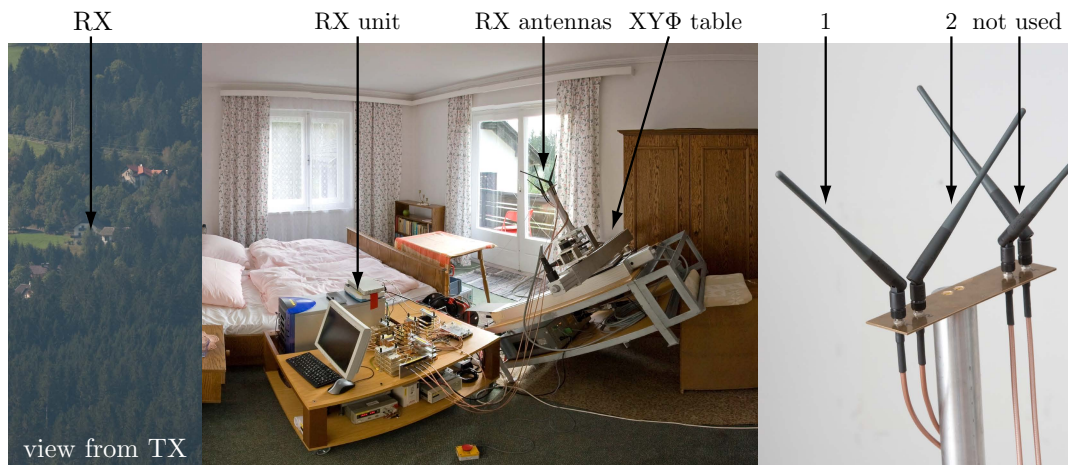


Figure 4.34: RX unit and antennas employed.

Additionally to this set-up, we also investigated RX antenna positions in different rooms where the TX antennas can and cannot be seen from the window. We also placed the RX unit outside, in the middle of a hayfield, with direct line-of-sight to the transmitter (see Figure 4.35, page 82). In all measured set-ups, the results obtained did not change significantly, apart from a variation in the average path loss that only shifts the throughput curves in Figure 4.38, page 83 to the left and right.

¹⁸Usually, very cheap antennas are employed at the mobile site. We paid 2 € per antenna.

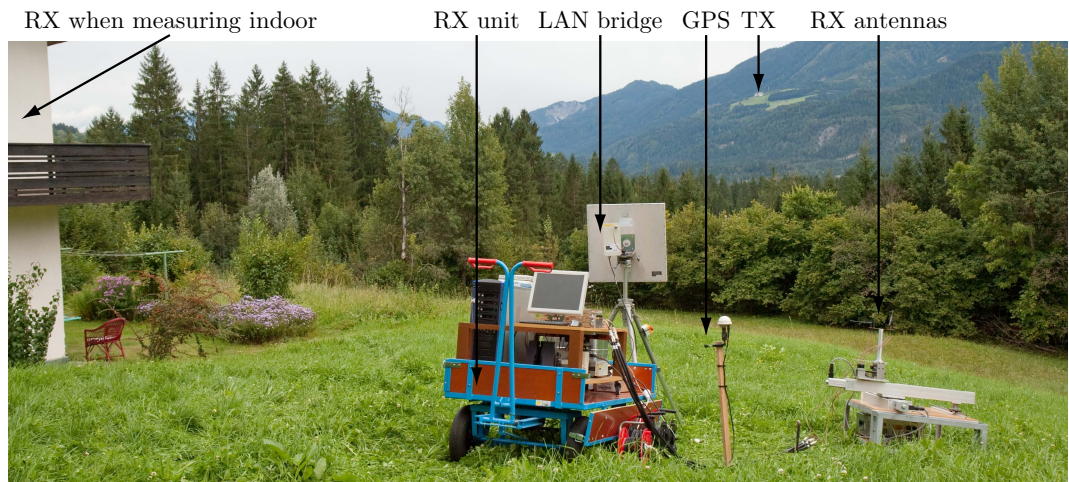


Figure 4.35: RX unit employed in the middle of a hayfield.

TX Antennas – Flat Panel 2X-Pol Antennas

At the base-station, we utilize two Kathrein 800 10543 [86, and Appendix C, page 117] 2X-pol flat panel antennas ($2 \times \pm 45^\circ$ polarization, half-power beam width $60^\circ/6.5^\circ$, down tilt 6°), see Figure 4.36. The corresponding TX unit is placed inside a cowshed immediately adjacent to the antennas, protected by a tent.

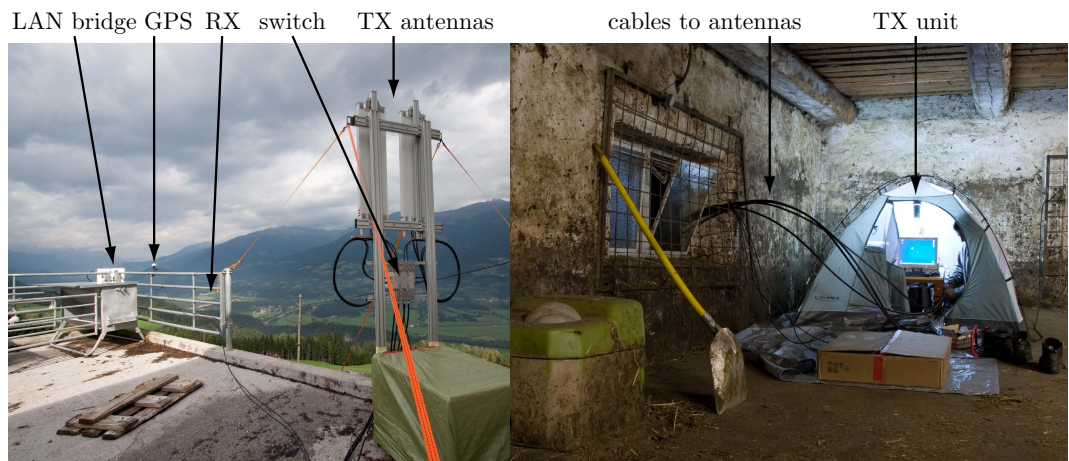
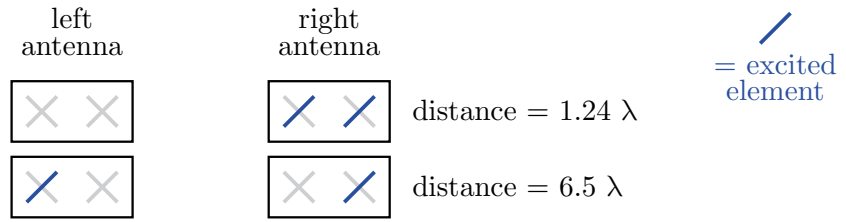


Figure 4.36: TX unit and antennas employed.

We create different antenna element spacings by switching one of the two excited elements from one antenna to the other (see Figure 4.37)¹⁹.

¹⁹As the results of this experiment will show, there is no need to employ a linear guide to move the TX antennas.


 Figure 4.37: Changing the distance between 1.24 and 6.5λ .

The averaging required to compare equal with cross polarization is still carried out as shown in Figure 4.19, page 66.

Results

Measuring 196 RX antenna positions for two different TX antenna element spacings we obtain the results shown in Figure 4.38.

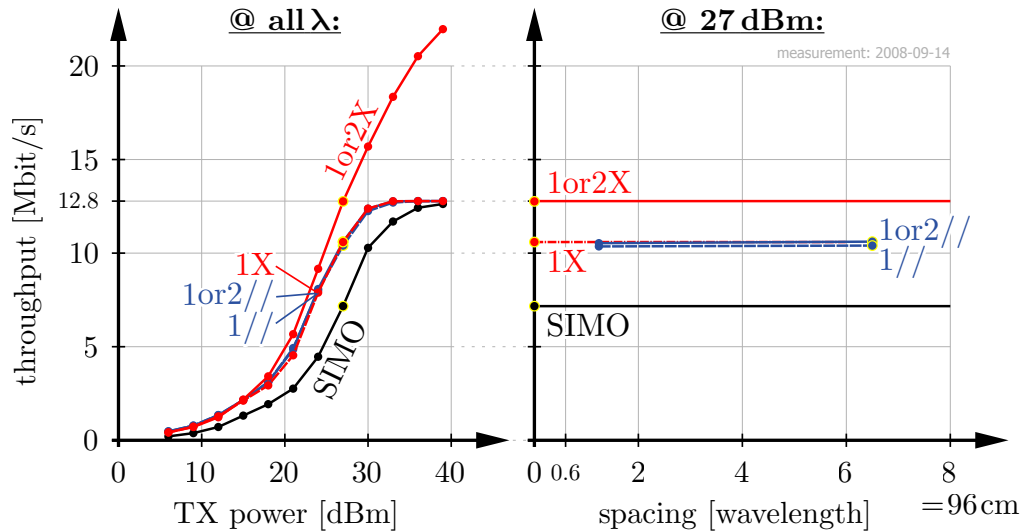


Figure 4.38: Throughput obtained in the 5.7 km Alpine valley scenario.

- Employing equal polarizations, D-TxAA (1or2 streams) works *exactly* as good as TxAA (1 stream) for both antenna element spacings measured. Looking deeper into the data evaluated we see that in D-TxAA, the two stream mode is never selected for transmission (because the one stream mode is always believed to work better).
- Employing cross polarization, D-TxAA (1or2 streams) works significantly better than TxAA (1 stream).
- In any case, employing MIMO yields significantly higher throughputs than SIMO.

4.3. Summary and Criticism

In this chapter, we have presented measurement results showing the influence of transmit antenna spacing on the average performance of a radio transmission. In particular, we have investigated the over transmit antenna spacing performance of HSDPA in three substantially different scenarios. Applying the measurement techniques presented in Chapter 2 allowed for straightforwardly inferring the average performance of these scenarios from a sample of about 300 receive antenna positions measured. The testbed presented in Chapter 3 supported the measurement process appropriately and flawlessly whilst the results obtained are consistent and precise showing no contradiction with what the literature suggests. In other words, a job well done.

The “presumably easiest” next step still to be taken is the investigation of the same questions regarding UMTS LTE²⁰. We can say ‘easiest’, because it seems to be just another straightforward extension of the measurement techniques already applied but have to say ‘presumably’ because there are always issues hidden amongst the details.

From a scientific point of view, however, the measurements presented in this chapter are *just* the beginning because they do only reflect a small (yet still interesting) snapshot of reality, namely three scenarios. What would be of even more interest now is a general view of reality—namely, how transmit antenna spacing in general influences the throughput of an HSDPA transmission. The large sample²¹ of different scenarios required for this inference is, unfortunately, beyond the reach of a small research group such as ours.

The other question of even greater scientific interest also lies outside the scope of this thesis: *Why* does the performance over transmit antenna spacing change as the measurements show? Or even more general: *What property* of the scenario causes the performance to change over transmit antenna spacing and *in what way*?

Question after question that can now be investigated for the first time, since very precise measurement data is available.

²⁰Long Term Evolution, see page 98.

²¹Preferably a random, rather than a judgement sample, as is now the case.

5. On Antenna Switching

Simulations usually assume that the individual SISO links of a full MIMO system suffer from the same average path loss. However in reality, this is typically not the case¹, especially for differently polarized and/or orientated antennas.

In this chapter, we will provide a new throughput-based antenna selection criterion that considers the entire system design rather than only the channel state information. We present measurement results in terms of physical layer throughput over transmit power. In addition to diversity gains, we clearly see gains due to the selection of, for example, differently polarized or orientated antennas. In terms of SNR, the results show a gain of several decibels, depending on the number of antennas selected.

5.1. Motivation

One of the main reasons for the slow introduction of MIMO technologies in commercial wireless systems is the required increment in complexity and hardware costs. While antenna elements are cheap and usually small, each one

¹ Over the last three years we have tried to create measurement set-ups with nearly equal average path losses between all TX and RX antennas. This was done so as to be able to compare our measurement results with existing simulation results. Although the use of, for example, rotation units and omnidirectional antennas helped to a certain extent, we were never really “successful” because a realistic scattering environment is highly unsymmetrical.

requires a complete radio frequency (RF) chain (low-noise amplifier, frequency down-converter, analog to digital converter, filters, and so on). Unfortunately, RF hardware is expensive compared to the cost of digital hardware. Also, introducing new hardware consumes more energy, which is very inconvenient for today's hand-held mobile devices.

Antenna subset selection is a promising technique that reduces the MIMO hardware complexity problem. Antenna subset selection adaptively chooses a specific subset of all available antennas, for example, an $N_t \times N_r$ system can be constructed while only $L_t \times L_r$ complete RF chains are used at the same time ($L_t < N_t$ and $L_r < N_r$). The antenna subset selection is based on a "selection criterion" depending on the application. It has been shown that under most circumstances, antenna selection systems can achieve the same diversity gains as full-complexity systems. On the downside, antenna selection systems suffer from a loss in array gain (mean SNR gain) but this loss can be avoided by preprocessing in the RF chain [87–89, 115, 117].

5.2. Existing Research

Antenna subset selection has been intensively studied during recent years (see [90–97] and references therein). Most published work usually assumes perfect knowledge of the channel at both the transmitter and the receiver sides under the assumption of a flat fading channel model with independent and identically distributed fading at each antenna. In [92], the problem of channel frequency selectivity is jointly addressed with some practical issues such as channel estimation errors and hardware non-idealities. The receive antenna subset selection is extensively studied in [98–102]. Besides the general subset selection overview, [103, 104] deal with the subset selection problem both at the transmitter and the receiver sides. As mentioned before, most of the available literature addresses the problem from a theoretical point of view and rarely focuses on common practical issues such as antenna coupling effects, noisy estimate of the channel and hardware non-idealities. However, some studies focus on more realistic channel models and consider the subset selection problem for frequency-selective channels when frequency-domain equalizers are used (see [103], and references therein), or when only noisy channel estimates are available [105, 106]. Another interesting and new advantage of subset selection is the possibility of reducing the complexity of MIMO-OFDM precoded systems [107].

In order to take advantage of the diversity available in MIMO systems, there is also some previous work on subset selection based on the maximization of channel capacity [108, 109]. During the last years, MIMO-OFDM systems have become very popular due to their ability to exploit the benefits from both MIMO and OFDM systems. For this reason subset selection has also been studied in such systems, specifically in indoor environments and existing wireless communication standards [110–112].

Despite all this previous work, however, very little attention has been paid to real scenario measurements and/or selection criteria that take into account the effects of practical implementations. In [113], a subset selection implementation applied to IEEE 802.11a is presented. In [111], the performance of transmit and receive antenna subset selection for MIMO-OFDM based on measured indoor correlated and frequency selective channels is studied in detail. The results obtained are compared with those computed using channel models. The comparison reports that the capacity gain predicted from the simulated channels is significantly lower than that achievable over real channels. The study also provides useful information about the antenna effects. Antenna subset selection has also been applied to the proposed IEEE 802.11n standard [114]. Finally, in [115] a complete list of practical issues related to subset selection are emphasized, for example RF preprocessing, subset selection training, RF mismatch, non idealities in selection or the antenna subset selection in OFDM systems. Also, measurement-based capacity analysis for indoor environments is provided.

5.3. Receive Antenna Selection

Diversity via multiple receive antennas is a direct extension of traditional diversity ideas. The receiver sees several versions of the transmit signal, each one experiencing a different fade and noise. The classic extension of selection combining to receive antenna subset selection is to select the L_r receive antennas with the highest SNR among the N_r available. For that we need to know *all* individual branch SNRs that can be determined by sounding the full MIMO channel in a time multiplexed manner. When more than one antenna is selected, maximum ratio combining (MRC) can be performed among L_r out of N_r antennas. Using this approach, antenna subset selection can extract most of the diversity of the full system without requiring all N_r RF chains.

When the wireless channel has sufficient degrees of freedom, the data streams transmitted from multiple antennas can be separated, thus leading to parallel data paths. The capacity of the radio channel increases under these conditions with $\min(N_t, N_r)$, that is, linearly with the number of antennas. In a multiple antenna system with N_t transmit and N_r receive antennas, the complex-valued channel matrix \mathbf{H} is of dimension $N_r \times N_t$. When antenna subset selection at the receiver side is used, a subset of L_r out of N_r antennas is selected. It is straightforward to see that the equivalent problem consists in building a matrix $\tilde{\mathbf{H}}$ with dimensions $L_r \times N_t$ from the full matrix \mathbf{H} . The selection usually requires all possible paths to be sounded using the available RF chains at the receiver. This can be achieved in $\lceil \frac{N_r}{L_r} \rceil$ sounding operations. After that, the selection criterion has to be applied in an exhaustive search among all $\binom{N_r}{L_r}$ different receive antenna combinations. For example, selecting one out of four receive antennas requires four sounding operations and evaluating the selection criterion four times, whereas selecting two out of four receive antennas demands only two sounding operations but six selection criterion evaluations.

5.3.1. Antenna Selection Based on System Throughput

In the literature, different selection criteria have been proposed based on specific properties of the channel such as channel capacity, eigenvalue spread, and so on. However, most of these antenna subset selection methods do not take the transmission system into account. For example, eigenvalue-based or capacity-based selection methods only look at the coefficients of the wireless channel. However, an optimum selection criterion for a specific transmission system such as HSDPA also has to consider —apart from the channel coefficients— the properties of the transmit signal and the receiver. We therefore propose the utilization of analytic expressions of the post-equalization SINR as the criterion for selecting the subset of receive antennas. The SINR is obtained directly from the estimated wireless channel and can be mapped to the physical layer throughput using a look-up table [11]. It is shown in [11] that maximizing the SINR also maximizes the throughput. It is important to note that this antenna selection criterion is not only limited to HSDPA [116]. It can be used in any situation in which it is possible to describe the physical layer throughput by means of analytic expressions depending on the channel coefficients and the type of receiver implemented.

5.3.2. Hardware Aspects of Antenna Selection

Ideal hardware is widely considered in the literature of antenna selection. Nevertheless, taking into account the actual features of the additional hardware required, the promised gains of antenna subset selection will be reduced *a priori*. Particular attention should be paid to the RF switch. *Ideal* switches do not deteriorate the noise figure of the receiver and work instantaneously, without any delay. However, these features cannot be completely fulfilled in practice. The attenuation of typical switches varies between a few tenths of a decibel and several decibels, depending on the switch size and the required switching speed. Typical settling times of RF switches are of the order of microseconds, corresponding to a duration of several symbols in current wireless communication systems.

The losses caused by the RF switches at the receiver side are difficult to compensate. One possible approach consists of installing the switch after the low-noise amplifier, but this requires as many low-noise amplifiers as receive antennas, thus reducing the benefits provided by antenna selection. However, the HSDPA system under consideration is an interference limited system rather than a noise limited one. This means that although the receiver noise figure is increased by the switch insertion loss, the final system throughput will not be degraded.

From the hardware point of view, sequentially sounding the full MIMO channel is a challenging task. Particularly in systems in which the base stations do not continuously transmit pilot symbols, it can take a long time until the full MIMO channel is acquired. While the full MIMO channel state information is not available, antenna selection cannot be applied, which typically leads to a loss in spectral efficiency. Fortunately, in HSDPA the base stations are always transmitting pilot channels, and the user equipment is therefore able to continuously perform channel sounding over the N_r antennas even when it is not receiving data. As soon as the user equipment is notified by the base station of a new incoming data block, it can use the previously obtained channel information to select the optimum subset of antennas. This “instantaneous best selection” of course requires no significant change of the channel for several subframes (a few milliseconds). If the channel changes faster than this, the antennas can be selected according to the average throughput of the most recent subframes (in the order of hundreds). In the results we will refer to this selection as the “average best throughput selection”. As a consequence of

the above, the proposed throughput-based antenna subset selection technique is especially suitable for HSDPA because the required training stage can be easily implemented.

Last, but not least, another frequently ignored problem is noisy channel estimation which can lead to a suboptimal subset selection and, consequently degrade the performance. Fortunately, antenna selection is quite robust to imperfect channel estimates [117].

5.4. Experiment VI - Urban 460m

In order to measure HSDPA throughput with antenna subset selection, a non line of sight urban scenario featuring rich scattering is selected (the same as that presented in Section 4.2.3, page 78). At the basestation, we employ a Kathrein 800 10543 [86, and Appendix C, page 117] 2X-pol basestation panel antenna ($2 \times \pm 45^\circ$ polarization, half-power beam width $58^\circ/6.2^\circ$, down tilt 6°). We place it on the roof of a tall building in the center of Vienna (see Figure 4.16, page 63). The receive antennas are located at an approximate distance of 460 m inside an office room.



Figure 5.1: RX antennas employed.

Results for $1 \times N_r$ HSDPA

Firstly, we transmit from a single TX antenna element to one, two, or all four receive antennas employed. Three sets of curves are plotted in Figure 5.2 below:

- The black leftmost curve shows the average throughput achieved when all four receive antennas are used (no selection).
- The set of red curves was measured with two out of four receive antennas selected.
- The set of blue curves was measured selecting only one out of four possible antennas at the receiver.

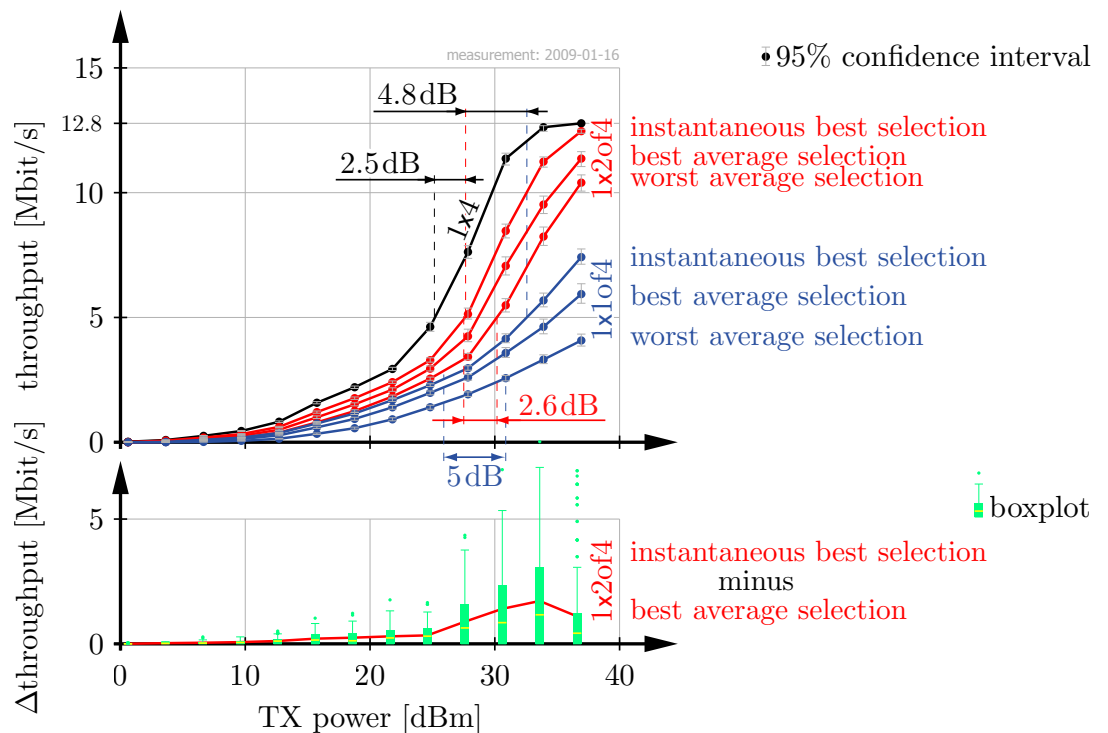


Figure 5.2: $1 \times N_r$ TxAA HSDPA (single stream) throughput measured.

The following three different curves are plotted for each set measured:

- “Instantaneous best selection”:
For each channel realization (created by moving the RX antennas), the RX antenna combination offering the highest throughput is chosen in accordance with the SINR expressions calculated in [11]. When throughput-based antenna subset selection is employed, this is an upper bound for the achievable performance that can be reached if the channel

is exactly known for every realization. Since in HSDPA the channel can be sounded continuously, a performance close to this upper bound can easily be achieved in reality.

- “Best average selection”:
The RX antenna combination offering the best throughput for all measured channel realizations is selected. This means that for a chosen transmit signal power, the average throughput for each antenna combination is evaluated and then the best of them is selected. This approach is especially suitable when the channel coherence time is short. Note that in a real HSDPA system, the average throughput can be calculated permanently by sounding the channel.
- “Worst average selection”. The same as in the previous case, but the antenna combination that produces the worst performance is selected. This selection method represents the worst case scenario that could occur if no antenna subset selection is performed at all (lower bound).

Note that the 15 to 30 dBm transmit power region is the most adequate for comparing the different throughput curves. For higher transmit powers, no higher modulation and coding schemes are available to exploit the channel capacity, and therefore saturation occurs.

Again, we investigate the precision of the measurement by means of bootstrapping methods [38]. In both graphs, the gray vertical lines represent the 95% BCa confidence intervals for the mean, and the corresponding horizontal lines the 2.5% and 97.5% percentiles. Note that the RX antenna position remains unchanged while measuring different schemes at different transmit power levels. This leads to smooth curves and *relative* positions of the curves that are more accurate the confidence intervals for the *absolute* positions suggest.

Let us now take a closer look at the results for one transmit antenna presented in Figure 5.2, page 91.

- The difference between the 1×4 full system and the 1×2 (out of 4) instantaneous best selection is approximately 2.5 dB, expressed in terms of TX power required to achieve the same throughput. This can be explained by the additional array gain of the four receive antenna system.
- The 1×2 (out of 4) scheme presents a TX power gain of up to 4.8 dB with respect to the 1×1 (out of 4) system. This is due to the array gain offered by the 1×2 (out of 4) system and, additionally, due to the ability

to exploit all available diversity.

- The maximum observed gain offered by antenna subset selection (2.6 dB and 5 dB) is the difference between the “instantaneous best selection” and the “worst average selection” curves.

The lower part of Figure 5.2 shows the difference between the “instantaneous best selection” and the “best average selection”. Average gains of up to 2 dB are observed, while instantaneous gains may be much higher.

Results for $2 \times N_r$ HSDPA

In Figure 5.3, the average throughput is plotted for the case of two TX antenna elements transmitting in single stream mode. Again, the red curves show the cases when two receive antennas are selected whilst the blue curves correspond to one selected RX antenna. As in the single transmit antenna system, large gains in throughput or in SNR are observed when antenna subset selection is employed.

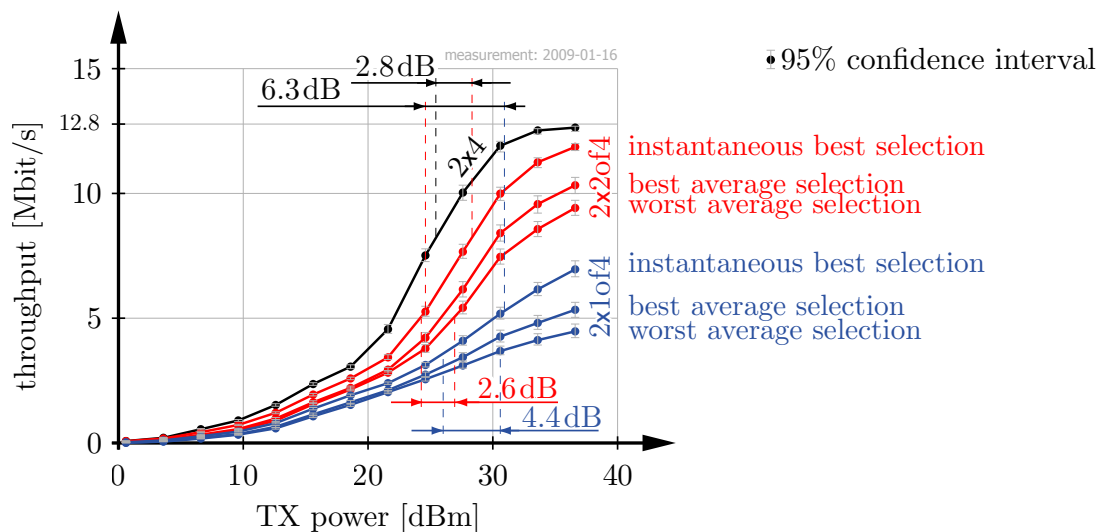


Figure 5.3: $2 \times N_r$ TxAA HSDPA (single stream) throughput measured.

5.5. Summary and Criticism

In this chapter, we first presented a new antenna selection criterion applicable to HSDPA and other mobile communication systems. We based this new criterion on signal to interference noise ratio expressions describing the behavior of the whole radio link including the receiver, rather than using only

channel state information. We furthermore emphasized the suitability of antenna selection to HSDPA because most of the implementation issues can be overcome.

To demonstrate the performance of our approach, we have carried out measurements in a non line-of-sight urban outdoor scenario. The results presented in terms of system throughput show large throughput increases when using antenna selection. In terms of TX power required to achieve the same throughput, the observed gains are between 2.6 and 5 dB, depending on the HSDPA scheme and the number of antennas selected.

Nonetheless, we omitted two important issues in the performance evaluation presented. Firstly, continuously receiving HSDPA data packets on different antennas in order to obtain knowledge about the channel consumes energy that may not be affordable at the hand-held. Secondly, switching between different receive antennas takes time. While this delay does not affect the throughput in the case of the “best average selection”, the throughput of the “instantaneous best selection” has to be corrected by the switching time needed. Consequently, an optimal switching rate can be defined.

6. Conclusion and Outlook

Building a testbed is an “easy” task that many have succeeded in [147–189]. *Using* a testbed to produce scientific results¹ on a large scale is a different matter altogether, especially when resources are limited:



Figure 6.1: Receiving the Vodafone Prize in 2006.

As from 2004 I have devoted myself to developing measurement techniques for characterizing the performance of MIMO systems under real-world conditions. After setting up a MIMO testbed in 2005 [4, 5, 17, 20, 21, 26, 27], I have compared the uncoded [16, 18] and coded [19] performance of measured indoor multiple antenna radio links with theoretical results presented in the literature.

¹ Scientific output is usually measured in terms of papers per year. Whether this metric is a meaningful one is —of course— another story, which I will not discuss here.

Using the experience gained, I have started to investigate the influence of antenna spacing on the performance of MIMO radio links [3]. Even more sophisticated measurement procedures have provided a precise picture of how the performance of several commonly used coding schemes degrades when the transmit antenna distance decreases [13]

After successfully carrying out large numbers of indoor measurements, I have completely redesigned the measurement equipment used in order to support outdoor experiments. This allowed me to investigate MIMO HSDPA [12, 15] and MIMO WiMAX [2, 14] in a realistic urban scenario (namely the fourth district of Vienna) where the transmit antennas were mounted 16 meters above the roof of my institute. Unlike the types of measurement campaign usually carried out, I did thereby not sound the MIMO channel (to store the channel coefficients for later use) *but* transmitted actual data packets in order to evaluate the throughput instantly at the receiver site. This takes time and requires a number of iterations but —on the upside— delivers novel, close-to-reality results [23–25].

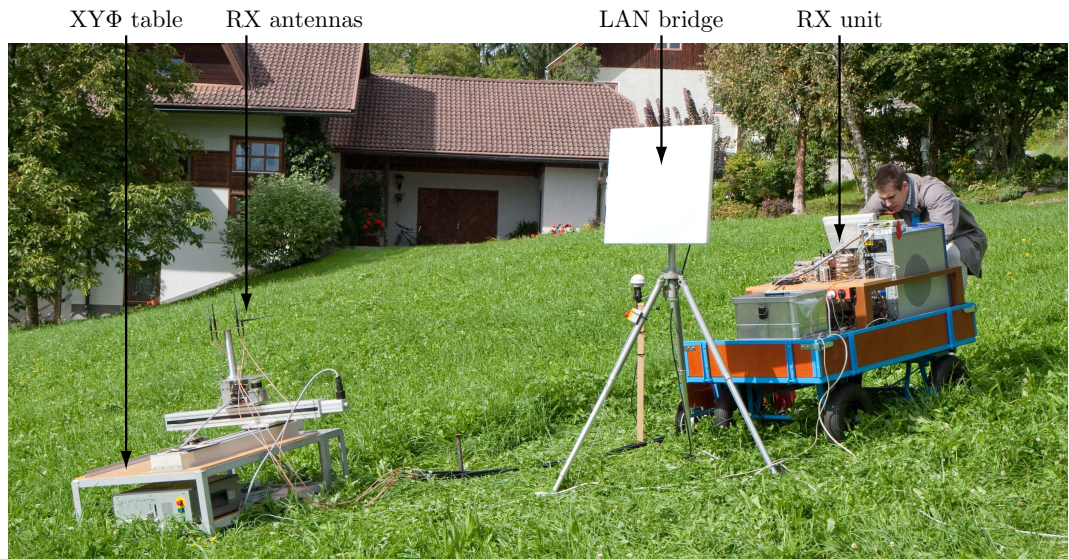


Figure 6.2: Employing the receiver in the middle of a hayfield.

The next step was to move all the measurement equipment to an Alpine valley in order to perform the measurements in a realistic, non-urban outdoor scenario [11]. The new, harsh outdoor conditions required me to further improve the measurement techniques applied. In particular, synchronizing the TX to the RX unit over a distance of 5.7 km for several weeks without being able to use a cable turned out to be a key problem that called for an innovative so-

lution [7, Chapter 2, Chapter 3]. This latest complete redesign of the testbed now enables me to not only measure easily at distances up to 80 km but also in non-static environments, for example, in a car on the highway [10]. In addition, it allows for the precise measurement of the impact of frequency offsets introduced by the radio frequency hardware [6].

The next obvious step was to move back to the city of Vienna in order to compare the results obtained in the Alps with the more scattering urban environment encountered near to my office [1]. New measurements investigating HSDPA throughput [9] over TX antenna rotation [7] and RX antenna switching [8, Chapter 5] were soon carried out.

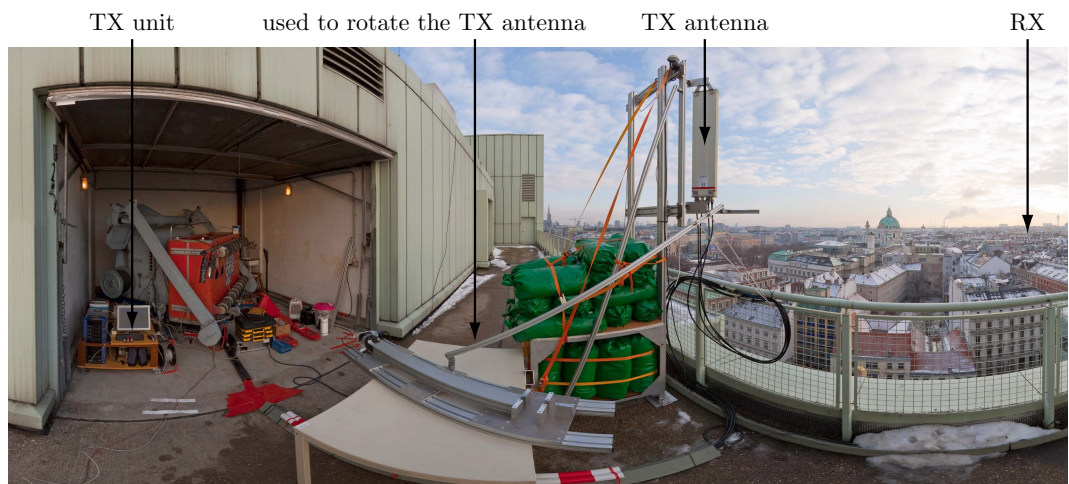


Figure 6.3: Realistic set-up.

The final major step was to investigate the influence of antenna spacing on an HSDPA transmission using realistic flat panel X-pol antennas at the transmit site [Chapter 4, to be published].

Now, 6 Journals, 16 conference papers, and 4 talks later, there seems to be no doubt that the quasi-realtime-approach featured by the Vienna MIMO Testbed is a real success. However, the question as to how to continue from here remains open.

The “presumably easiest” next step to be taken is the investigation of the same questions regarding UMTS LTE. We can say ‘easiest’, because it seems to be just another straightforward extension of the measurement techniques already applied but have to say ‘presumably’ because there are always issues hidden amongst the details.

LTE - The Next Challenge

In December 2008, the specification of the so-called LTE (Long Term Evolution) system was completed. The targets for downlink and uplink peak data rate requirements were set to 100 Mbit/s and 50 Mbit/s, when operating in a 20 MHz spectrum allocation [136]. In LTE, the first version already supports up to four transmit antennas. Initial performance evaluations show that the throughput of the LTE physical layer and MIMO enhanced HSDPA is approximately the same [131–135]. However, LTE has several other features of which the most important ones for future research (and realistic performance evaluations) are briefly explained below.

The LTE downlink transmission scheme is based on orthogonal frequency-division multiple access (OFDMA), which converts the wide-band frequency selective channel into multiple flat fading subchannels. The flat fading subchannels have the advantage that—even in the case of MIMO transmission—optimum receivers can be implemented with reasonable complexity, in contrast to HSDPA. OFDMA additionally allows for frequency domain scheduling, typically trying to assign only “good” subchannels to the individual users. This offers large throughput gains in the downlink due to multi-user diversity [143, 144]. Another feature of LTE is the X2-interface between base stations. This interface can be used for interference management with the goal of decreasing inter-cell interference. The standard only defines the messages exchanged between the base stations while the algorithms and the exact implementation of the interference mitigation remain vendor specific and are currently topics of great scientific interest, see for example [137–139].

During the last year, a MATLAB-based LTE physical layer downlink simulator was developed at the Institute of Communications and Radio Frequency Engineering, Vienna University of Technology [145, 146]. Using this simulator, a measurement-based performance evaluation of LTE can be carried out in an initial step similar to that done for WiMAX in this thesis (simply by transmitting all possible transmit data blocks over the same channel). However, since LTE also supports hybrid automatic repeat requests and many different MIMO modes with adaptive precoding, the mini-receiver approach used for the HSDPA performance evaluation is more suitable. For this approach, an analytical model of the physical layer (similar to the one for HSDPA [11]) has to be developed and verified. While it is quite straightforward to develop such

a model for linear receivers, it is challenging for non-linear receivers, such as for example sphere decoding. Such a verified model of the LTE physical layer is also the basis for meaningful system level simulations.

As explained above, LTE was developed as a multi-user system. The multi-user scheduling in the base station modifies the channel statistics the individual users are experiencing. (For example, by serving a user only with subchannels with a high SNR.) As channel statistics have a great impact on receiver performance, multi-user scheduling has to be considered for a realistic performance evaluation. Since the effort for testbed measurements in which multiple users are simultaneously connected to a single base station is beyond our reach, the following method can be applied for such measurements. Firstly, we measure a host of different receiver locations in order to calculate the corresponding user feedback values. Secondly, when performing the “real” throughput measurement at different receiver locations, the scheduler is not only provided with the current user feedback but also with the previously recorded feedback values of the other users. Nevertheless, this method only allows for measuring the performance of one user connected to a single base station.

The X2 interface between base stations allows the management of inter-cell interference. Directly measuring interference management algorithms requires the use of many base stations simultaneously. In order to decrease the hardware effort but still obtain meaningful results, the in our current opinion most realistic performance evaluation of such algorithms is to first successively record the channels between several base stations and a single user. The measured channel coefficients can then be used in the LTE physical layer simulator to investigate the interference management algorithms.

If interference aware receivers are to be tested, the signals received from different base stations can be recorded in a first step (by physically repositioning the only base station we have) and then added up in the digital domain during the actual measurement.

In other words, there is still an enormous amount of work ahead.

A. Bibliography

A.1. Self References

A.1.1. Authored Book Chapters

- [1] C. Mehlführer, S. Caban, and M. Rupp, “**MIMO HSDPA throughput measurement results,**” in *HSDPA/HSUPA Handbook*, B. Furht and S. Ahson, Eds. CRC Press, 2009, submitted.

A.1.2. Authored Journals

- [2] C. Mehlführer, S. Caban, and M. Rupp, “**Experimental evaluation of adaptive modulation and coding in MIMO WiMAX with limited feedback,**” *EURASIP Journal on Advances in Signal Processing*, vol. 2008, Article ID 837102, 2008, doi: 10.1155/2008/837102.
http://publik.tuwien.ac.at/files/pub-et_13762.pdf
- [3] S. Caban and M. Rupp, “**Impact of transmit antenna spacing on 2x1 Alamouti radio transmission,**” *Electronics Letters*, vol. 43, no. 4, pp. 198–199, Feb. 2007.
http://publik.tuwien.ac.at/files/pub-et_12278.pdf
- [4] S. Caban, C. Mehlführer, R. Langwieser, A. L. Scholtz, and M. Rupp, “**Vienna MIMO Testbed,**” *EURASIP Journal on Applied Signal Processing*, vol. 2006, Article ID 54868, 2006, doi: 10.1155/ASP/2006/54868.
http://publik.tuwien.ac.at/files/pub-et_10929.pdf
- [5] M. Rupp, C. Mehlführer, S. Caban, R. Langwieser, L. W. Mayer, and A. L. Scholtz, “**Testbeds and rapid prototyping in wireless system design,**” *EURASIP Newsletter*, vol. 17, no. 3, pp. 32–50, Sept. 2006.
http://publik.tuwien.ac.at/files/pub-et_11232.pdf

A.1.3. Authored Papers

- [6] Q. Wang, S. Caban, C. Mehlführer, and M. Rupp, “**Measurement based throughput evaluation of residual frequency offset compensation in WiMAX,**” in *Proc. 51st International Symposium ELMAR-2009*, Zadar, Croatia, Sept. 2009.
- [7] S. Caban, C. Mehlführer, G. Lechner, and M. Rupp, “**Testbedding MIMO HSDPA and WiMAX,**” in *Proc. 70th IEEE Vehicular Technology Conference (VTC2009-Fall)*, Anchorage, AK, USA, Sept. 2009.
http://publik.tuwien.ac.at/files/PubDat_176574.pdf

- [8] J. A. García-Naya, C. Mehlführer, S. Caban, M. Rupp, and C. Luis, “**Throughput-based antenna selection measurements,**” in *Proc. 70th IEEE Vehicular Technology Conference (VTC2009-Fall)*, Anchorage, AK, USA, Sept. 2009.
http://publik.tuwien.ac.at/files/PubDat_176573.pdf
- [9] C. Mehlführer, S. Caban, and M. Rupp, “**MIMO HSDPA throughput measurement results in an urban scenario,**” in *Proc. 70th IEEE Vehicular Technology Conference (VTC2009-Fall)*, Anchorage, AK, USA, Sept. 2009.
http://publik.tuwien.ac.at/files/PubDat_176321.pdf
- [10] T. Zemen, S. Caban, N. Czink, and M. Rupp, “**Validation of minimum-energy band-limited prediction using vehicular channel measurements,**” in *Proc. 17th European Signal Processing Conference (EUSIPCO 2009)*, Glasgow, Scotland, UK, Aug. 2009.
http://publik.tuwien.ac.at/files/PubDat_176572.pdf
- [11] C. Mehlführer, S. Caban, M. Wrulich, and M. Rupp, “**Joint throughput optimized CQI and precoding weight calculation for MIMO HSDPA,**” in *Conference Record of the Fourtysecond Asilomar Conference on Signals, Systems and Computers, 2008*, Pacific Grove, CA, USA, Oct. 2008.
http://publik.tuwien.ac.at/files/PubDat_167015.pdf
- [12] C. Mehlführer, S. Caban, and M. Rupp, “**Measurement based evaluation of low complexity receivers for D-TxAA HSDPA,**” in *Proc. of the 16th European Signal Processing Conference*, Lausanne, Switzerland, Aug. 2008.
http://publik.tuwien.ac.at/files/PubDat_166132.pdf
- [13] S. Caban, C. Mehlführer, L. W. Mayer, and M. Rupp, “**2x2 MIMO at variable antenna distances,**” in *Proc. of the IEEE Vehicular Technology Conference (VTC 2008 Spring)*, Singapore, May 2008, doi: 10.1109/VETECS.2008.276.
http://publik.tuwien.ac.at/files/pub-et_12543.pdf
- [14] C. Mehlführer, S. Caban, and M. Rupp, “**An accurate and low complex channel estimator for OFDM WiMAX,**” in *3rd International Symposium on Communications, Control and Signal Processing (ISCCSP 2008)*, pp. 922–926, St. Julians, Malta, Mar. 2008.
http://publik.tuwien.ac.at/files/pub-et_13650.pdf
- [15] M. Rupp, S. Caban, and C. Mehlführer, “**Challenges in building MIMO testbeds,**” in *Proc. of the 13th European Signal Processing Conference (EUSIPCO 2007)*, Poznan, Poland, Sept. 2007.
http://publik.tuwien.ac.at/files/PubDat_112138.pdf
- [16] M. Wrulich, S. Caban, and M. Rupp, “**Testbed measurements of optimized linear dispersion codes,**” in *Proc. of the ITG Workshop on Smart Antennas*, Feb 2007.
http://publik.tuwien.ac.at/files/pub-et_12313.pdf
- [17] L. W. Mayer, M. Wrulich, and S. Caban, “**Measurements and channel modeling for short range indoor UHF applications,**” in *Proc. of the European Conference on Antennas and Propagation, EuCAP 2006*, Nov 2007.
http://publik.tuwien.ac.at/files/pub-et_11470.pdf
- [18] S. Caban, C. Mehlführer, A. L. Scholtz, and M. Rupp, “**Indoor MIMO transmissions with Alamouti space-time block codes,**” in *Proc. of the 8th International Symposium on DSP and Communication Systems, DSPCS 2005*, Noosa Heads, Australia, Dec.

2005.

<http://publik.tuwien.ac.at/files/pub-et.9815.pdf>

- [19] C. Mehlführer, S. Caban, M. Rupp, and A. L. Scholtz, “**Effect of transmit and receive antenna configuration on the throughput of MIMO UMTS downlink**,” in *Proc. of the 8th International Symposium on DSP and Communication Systems, DSPCS 2005*, Noosa Heads, Australia, Dec. 2005.
<http://publik.tuwien.ac.at/files/pub-et.10269.pdf>
- [20] C. Mehlführer, S. Geirhofer, S. Caban, and M. Rupp, “**A flexible MIMO testbed with remote access**,” in *Proc. of the 13th European Signal Processing Conference (EUSIPCO 2005)*, Antalya, Turkey, Sept. 2005.
<http://publik.tuwien.ac.at/files/pub-et.9732.pdf>
- [21] E. Aschbacher, S. Caban, C. Mehlführer, G. Maier, and M. Rupp, “**Design of a flexible and scalable 4x4 MIMO testbed**,” in *Proc. of the 11th IEEE Signal Processing Workshop (DSP 2004)*, pp. 178–181, Taos Ski Valley, NM, USA, Aug. 2004.
<http://publik.tuwien.ac.at/files/pub-et.8758.pdf>

A.1.4. Authored Talks

- [22] S. Caban, C. Mehlführer, J. A. García-Naya, C. Luis, and M. Rupp, “**Testbed-based evaluation of WiMAX and HSDPA**,” Invited Talk: COMONSENS Meeting, Santander, Spain, July 2009.
- [23] C. Mehlführer and S. Caban, “**Outdoor WiMAX throughput measurements**,” Talk: SARG Meeting, Stanford University, CA, USA, Oct. 2008.
http://publik.tuwien.ac.at/files/PubDat_167679.pdf
- [24] M. Rupp, S. Caban, and C. Mehlführer, “**Measurements of MIMO HSDPA and WiMAX transmissions**,” in *Proc. of the 15th International Conference on Systems, Signals and Image Processing, IWSSIP 2008*, p. Keynote Lecture, Bratislava, Slovakia, July 2008.
<http://publik.tuwien.ac.at/files/pub-et.13801.pdf>
- [25] M. Rupp, S. Caban, and C. Mehlführer, “**“Testbedding” MIMO HSDPA versus WiMAX**,” Talk at ITG Fachtagung, Vienna, Austria, Oct. 2008.
http://publik.tuwien.ac.at/files/PubDat_166753.pdf
- [26] S. Caban, R. Langwieser, C. Mehlführer, E. Aschbacher, W. Keim, G. Maier, B. Badic, M. Rupp, and A. L. Scholtz, “**Design and verification of a flexible and scalable 4x4 MIMO testbed**,” Workshop on MIMO Implementation Aspects at RAWCON 2004, Atlanta, GA, USA, Sept. 2004.
<http://publik.tuwien.ac.at/files/pub-et.9210.pdf>
- [27] S. Caban and C. Mehlführer, “**Do you MIMO?**” Workshop mit Vodafone-Stiftungspreisträgern 2006, Dresden, Germany, 2006.
<http://publik.tuwien.ac.at/files/pub-et.11068.pdf>

A.2. Theses by Researchers Involved

- [28] S. Caban, “**Development and setting up of a 4x4 real-time MIMO testbed,**” Master’s thesis, Vienna, Austria, 2005.
http://publik.tuwien.ac.at/files/pub-et_9754.pdf
- [29] C. Mehlführer, “**Implementation and real-time testing of space-time block codes,**” Master’s thesis, Vienna, Austria, 2004.
http://publik.tuwien.ac.at/files/pub-et_8438.pdf
- [30] S. Geirhofe, “**Design and real-time measurement of equalization schemes for HSDPA,**” Master’s thesis, Vienna, Austria, 2005.
http://publik.tuwien.ac.at/files/pub-et_9592.pdf
- [31] A. Roca, “**Implementation of a WiMAX simulator in simulink,**” Master’s thesis, Vienna, Austria, 2007.
http://publik.tuwien.ac.at/files/pub-et_12498.pdf
- [32] L. W. Mayer, “**Wideband 4x4 MIMO over the air transmission at 2.45 GHz,**” Master’s thesis, Vienna, Austria, 2005.
http://publik.tuwien.ac.at/files/pub-et_10521.pdf
- [33] R. Langwieser, “**Entwicklung von HF-Baugruppen für ein ein MIMO Echtzeit-Übertragungssystem,**” Master’s thesis, Vienna, Austria, 2004.
http://publik.tuwien.ac.at/files/pub-et_8413.pdf
- [34] C. Mehlführer, “**Measurement-based performance evaluation of WiMAX and HSDPA,**” Ph.D. dissertation, Technische Universität Wien, Institut für Nachrichtentechnik und Hochfrequenztechnik, Sept. 2009, supervisors Markus Rupp and Thomas Kaiser.
- [35] S. Caban, “**Testbed-based evaluation of mobile communication systems,**” Ph.D. dissertation, Technische Universität Wien, Institut für Nachrichtentechnik und Hochfrequenztechnik, Sept. 2009, supervisor: Markus Rupp.

A.3. Recommended Books by Other Authors

- [36] A. Behzad, **Wireless LAN Radios**, 1st ed. Wiley & Sons, 2007. ISBN: 0471709646.
- [37] A. Luzzatto and G. Shirazi, **Wireless Transceiver Design**, 1st ed. Wiley & Sons, 2007. ISBN: 047006076X.
- [38] B. Efron and D. V. Hinkley, **An Introduction to The Bootstrap (CRC Monographs on Statistics & Applied Probability 57)**, 1st ed. Chapman & Hall, 1994. ISBN: 0412042312.
- [39] A. M. Zoubir and D. R. Iskander, **Bootstrap Techniques for Signal Processing**, 1st ed. Cambridge University Press, 2004. ISBN: 052183127X.
- [40] A. C. Davison and R. J. Tibshirani, **Bootstrap Methods and Their Application (Cambridge Series in Statistical and Probabilistic Mathematics, No 1)**, 1st ed. Cambridge Univ Press, 1999. ISBN: 0521574714.

- [41] R. Fisher, **The Design of Experiments**, 1st ed. New York: Wiley, 1935.
- [42] C. R. Hicks, **Fundamental Concepts in The Design of Experiments**, 4th ed. John Wiley & Sons, 1993. ISBN: 003097710X.
- [43] R. L. Mason, R. F. Gunst, and J. L. Hess, **Statistical Design and Analysis of Experiments**, 2nd ed. Wiley-Interscience, 2003. ISBN: 0471372161.
- [44] F. X. Schumacher, **Sampling Methods in Forestry and Range Management**, 1st ed. Duke University, 1942.
- [45] A. Lindner, **Planen und Auswerten von Versuchen**, 1st ed. Birkhauser, 1953.
- [46] T. H. Naylor, **The Design of Computer Simulation Experiments**, 1st ed. Symposium on the Design of Computer Simulation Experiments, Duke University, 1968. ISBN: 0822302322.
- [47] D. Cox, **Planning of Experiments**, 1st ed. John Wiley & Sons, 1958.
- [48] W. G. Cochran, **Sampling Techniques**, 3rd ed. Wiley, 1977. ISBN: 047116240X.
- [49] D. Hawkins, **Identification of Outliers**, 1st ed. Springer, 1980. ISBN: 041221900X.
- [50] B. Vic and T. Lewis, **Outliers in Statistical Data**, 1st ed. Wiley, 1980. ISBN: 0471995991.
- [51] R. P. Haining, **Spatial Data Analysis In The Social And Environmental Sciences**, 1st ed. Cambridge University Press, 1993. ISBN: 0521448662.
- [52] D. Freedman, R. Pisani, and R. Purves, **Statistics**, 4th ed. Norton, 2007. ISBN: 0393930432.
- [53] J. P. C. Kleijnen, **Statistical Techniques in Simulation**, 1st ed. Dekker, 1974. ISBN: 082476157X.
- [54] J. M. Hammersley and D. C. Handscomb, **Monte Carlo Methods**, 1st ed. LinkChapman and Hall, 1979. ISBN: 0412158701.
- [55] C. E. Shannon, A. D. Wyner, and N. J. A. Sloane, **Claude E. Shannon: Collected Papers**, 2nd ed. John Wiley & Sons Inc, 1993. ISBN: 0780304349.
- [56] Merriam-Webster, **The Merriam-Webster Dictionary**, 1st ed. Merriam Webster Inc, 2005. ISBN: 087779636X.
- [57] A. D. McNaught and A. Wilkinson, **Compendium of Chemical Terminology: IUPAC Recommendations: Gold Book**, 2nd ed. IUPAC International Union of Pure and Applied Chem, 1997. ISBN: 0865426848.

A.4. Journals and Papers by Other Authors

- [58] S. Alamouti, "A simple transmit diversity technique for wireless communications," *IEEE Journal on Selected Areas in Communications*, vol. 16, issue 8, pp. 1451–1458, Oct. 1998. <http://ieeexplore.ieee.org/iel4/49/15739/00730453.pdf>
- [59] V. Jungnickel, V. Pohl, and C. Helmolt, "Capacity of MIMO systems with closely spaced antennas," *IEEE Communications Letters*, vol. 7, no. 8, pp. 361–363, Aug. 2003. <http://ieeexplore.ieee.org/iel5/4234/27419/01220269.pdf>
- [60] V. Jungnickel, V. Pohl, and C. Helmolt, "Experiments on the element spacing in multi-antenna systems," in *Proc. VTC Spring 2003*, vol. 2, pp. 1124–1126, April

2003. <http://ieeexplore.ieee.org/iel5/8574/27185/01207802.pdf>
- [61] V. Pohl, V. Jungnickel, T. Haustein, and C. Helmolt, "Antenna spacing in MIMO indoor channels," in *Proc. VTC Spring 2002*, vol. 2, pp. 749–753, May 2002. <http://ieeexplore.ieee.org/iel5/7859/21638/01002587.pdf>
- [62] J. Lv, Y. Lu, Y. Wang, H. Zhao, and C. Y. Han, "Antenna spacing effect on indoor MIMO channel capacity," in *Proc. Asia-Pacific Microwave Conference 2005*, pp. 1–3, Dec. 2005. <http://ieeexplore.ieee.org/iel5/10688/33746/01606620.pdf>
- [63] T. Svantesson and A. Ranheim, "Mutual coupling effects on the capacity of multielement antenna systems," in *Proc. ICASSP 2001*, vol. 4, pp. 2485–2488, May 2001. <http://ieeexplore.ieee.org/iel5/7486/20357/00940505.pdf>
- [64] A. Intarapanich, P. Kafle, R. Davies, A. Sesay, and J. McRory, "Spatial correlation measurements for broadband MIMO wireless channels," in *Proc. VTC Fall 2004*, vol. 1, pp. 52–56, Sept. 2004. <http://ieeexplore.ieee.org/iel5/9623/30410/01399919.pdf>
- [65] J. Medbo, F. Harrysson, H. Asplund, and J. Berger, "Measurements and analysis of a MIMO macrocell outdoor-indoor scenario at 1947 MHz," in *Proc. VTC Spring 2004*, vol. 1, pp. 261–265, May 2004. <http://ieeexplore.ieee.org/iel5/9530/30201/01387954.pdf>
- [66] Z. Guangze and S. Loyka, "Performance study of MIMO systems in a clustered multipath channel," in *Proc. CCECE 2004*, vol. 1, pp. 453–456, May 2004. <http://ieeexplore.ieee.org/iel5/9317/29618/01345053.pdf>
- [67] G. Zhao and S. Loyka, "Impact of multipath clustering on the performance of MIMO systems," in *Proc. WCNC. 2004*, pp. 765–770, March 2004. <http://ieeexplore.ieee.org/iel5/9178/29115/01311283.pdf>
- [68] B. Lindmark, "Capacity of a 2x2 MIMO antenna system with mutual coupling losses," in *Proc. Antennas and Propagation Society International Symposium 2004*, vol. 2, pp. 1720–1723, June 2004. <http://ieeexplore.ieee.org/iel5/9253/29356/01330528.pdf>
- [69] O. Fernandez, M. Domingo, and R. Torres, "Empirical analysis of the correlation of MIMO channels in indoor scenarios at 2 GHz," *IEE Proceedings in Communications*, vol. 152, no. 1, pp. 82–88, Feb. 2004. <http://ieeexplore.ieee.org/iel5/2191/30554/01409307.pdf>
- [70] J. Wallace and M. Jensen, "Mutual coupling in MIMO wireless systems: a rigorous network theory analysis," *IEEE Transactions on Wireless Communications*, vol. 3 no. 4, pp. 1317–1325, July 2004. <http://ieeexplore.ieee.org/iel5/7693/29087/01310320.pdf>
- [71] D.-S. Shiu, G. J. Foschini, M. Gans, and J. Kahn, "Fading correlation and its effect on the capacity of multielement antenna systems," *IEEE Transactions on Communications*, vol. 48, no. 3, pp. 502–513, March 2000. <http://ieeexplore.ieee.org/iel5/26/18093/00837052.pdf>
- [72] C.-N. Chuah, D. Tse, J. Kahn, and R. Valenzuela, "Capacity scaling in MIMO wireless systems under correlated fading," *IEEE Transactions on Information Theory*, vol. 48, no. 3, pp. 637–650, March 2002. <http://ieeexplore.ieee.org/iel5/18/21246/00985982.pdf>
- [73] J.-C. Belfiore, G. Rekaya, and E. Viterbo, "The Golden code: a 2x2 full-rate space-time code with non-vanishing determinants," *IEEE Transactions on Information Theory*, vol. 51, no. 4, pp. 1432–1436, Apr. 2005. <http://ieeexplore.ieee.org/iel5/9423/29909/01365347.pdf>
- [74] The Golden Code Homepage. http://www1.tlc.polito.it/~viterbo/perfect_codes/Golden_Code.html
- [75] K. R. P.-S. Kildal, "Correlation and capacity of MIMO systems and mutual coupling, radiation efficiency, and diversity gain of their antennas: simulations and measurements in a reverberation chamber," *IEEE Communications Magazine*, vol. 42, no. 12, pp. 104–112, Dec. 2004. <http://ieeexplore.ieee.org/iel5/35/29940/01367562.pdf>
- [76] M. Damen, A. Tewfik, and J. Belfiore, "A construction of a space-time code based on number theory," *IEEE Transactions on Information Theory*, vol. 48, no. 3, pp. 753–760, Mar. 2002. ieeexplore.ieee.org/iel5/18/21246/00986032.pdf
- [77] P. Wolniansky, G. Foschini, G. Golden, and R. Valenzuela, "V-BLAST: an architecture for realizing very high data rates over the rich-scattering wireless channel," in *International Symposium on Signals, Systems*, pp. 295–300, Sep 1998. <http://ieeexplore.ieee.org/iel4/5942/15884/00738086.pdf>
- [78] 3GPP, "Technical specification group radio access network; Multiple-Input Multiple Output in UTRA," 3GPP, Tech. Rep. 25.876 V7.0.0, Mar. 2007. <http://www.3gpp.org/ftp/Specs/html-info/25876.htm>
- [79] O. Bjørnstad and W. Falck, "Nonparametric spatial covariance functions: estimation and testing," *Environmental and Ecological Statistics*, vol. 8, no. 1, pp. 53–70, 2001. <http://www.springerlink.com/content/j1436865g74041r2/>
- [80] D. G. Horvitz and D. J. Thompson, "A generalization of sampling without replacement from a finite universe," *Journal of the American Statistical Association*, vol. 47, no. 260, pp. 663–685, 1952. <http://www.jstor.org/stable/2280784>
- [81] J. L. W. V. Jensen, "Sur les fonctions convexes et les inégalités entre les valeurs moyennes," *Acta Mathematica*, vol. 30, no. 1, pp. 175–193, 1906,

- doi: 10.1007/BF02418571.
- [82] (C) 2009 Microsoft Corporation, <http://www.bing.de>.
- [83] Airmux Backhaul Wireless IP and E1/T1 Radio. <http://www.airmux.com>
- [84] Acutime Gold GPS Smart Antenna. <http://www.trimble.com/timing/acutime-gold-gps-antenna.aspx?dtID=overview>
- [85] FS725 – Benchtop rubidium frequency standard. <http://www.thinksrs.com/products/FS725.htm>
- [86] KATHREIN-Werke KG. <http://www.kathrein.de/>
- [87] A. Molisch and X. Zhang, “FFT-based hybrid antenna selection schemes for spatially correlated MIMO channels,” *Communications Letters, IEEE*, vol. 8, no. 1, pp. 36–38, Jan. 2004, doi: 10.1109/LCOMM.2003.822512.
- [88] X. Zhang, A. Molisch, and S.-Y. Kung, “Variable-phase-shift-based RF-baseband codesign for MIMO antenna selection,” *Signal Processing, IEEE Transactions on*, vol. 53, no. 11, pp. 4091–4103, Nov. 2005, doi: 10.1109/TSP.2005.857024.
- [89] P. Sudarshan, N. Mehta, A. Molisch, and J. Zhang, “Channel statistics-based RF pre-processing with antenna selection,” *Wireless Communications, IEEE Transactions on*, vol. 5, no. 12, pp. 3501–3511, December 2006, doi: 10.1109/TWC.2006.256973.
- [90] S. Sanayei and A. Nosratinia, “Antenna selection in MIMO systems,” *Communications Magazine, IEEE*, vol. 42, no. 10, pp. 68–73, Oct. 2004, doi: 10.1109/MCOM.2004.1341263.
- [91] A. Molisch, “MIMO systems with antenna selection – an overview,” *Radio and Wireless Conference, 2003. RAWCON '03. Proceedings*, pp. 167–170, Aug. 2003, doi: 10.1109/RAWCON.2003.1227919.
- [92] A. Molisch and M. Win, “MIMO systems with antenna selection,” *Microwave Magazine, IEEE*, vol. 5, no. 1, pp. 46–56, Mar 2004, doi: 10.1109/MMW.2004.1284943.
- [93] A. Gershman and N. Sidiropoulos, *Space-Time Processing for MIMO Communications*. John Wiley & Sons, 2005. ISBN: 9780470010020.
- [94] A. Gorokhov, D. Gore, and A. Paulraj, “Receive antenna selection for MIMO flat-fading channels: theory and algorithms,” *Information Theory, IEEE Transactions on*, vol. 49, no. 10, pp. 2687–2696, Oct. 2003, doi: 10.1109/TIT.2003.817458.
- [95] A. Gorokhov, “Antenna selection algorithms for MEA transmission systems,” *Acoustics, Speech, and Signal Processing, 2002. Proceedings. (ICASSP '02). IEEE International Conference on*, vol. 3, pp. III–2857–III–2860 vol.3, 2002, doi: 10.1109/ICASSP.2002.1005282.
- [96] A. Gorokhov, D. Gore, and A. Paulraj, “Performance bounds for antenna selection in MIMO systems,” *Communications, 2003. ICC '03. IEEE International Conference on*, vol. 5, pp. 3021–3025 vol.5, May 2003, doi: 10.1109/ICC.2003.1203962.
- [97] A. Ghayeb, “A survey on antenna selection for MIMO communication systems,” *Information and Communication Technologies, 2006. ICTTA '06. 2nd*, vol. 2, pp. 2104–2109, 2006, doi: 10.1109/ICTTA.2006.1684727.
- [98] A. Ghayeb and T. Duman, “Performance analysis of MIMO systems with antenna selection over quasi-static fading channels,” *Vehicle Technology, IEEE Transactions on*, vol. 52, no. 2, pp. 281–288, March 2003, doi: 10.1109/TVT.2003.808792.
- [99] M. Gharavi-Alkhanisari and A. Gershman, “Fast antenna subset selection in MIMO systems,” *Signal Processing, IEEE Transactions on*, vol. 52, no. 2, pp. 339–347, Feb. 2004, doi: 10.1109/TSP.2003.821099.
- [100] T. Gucluoglu, T. Duman, and A. Ghayeb, “Antenna selection for space time coding over frequency-selective fading channels,” *Acoustics, Speech, and Signal Processing, 2004. Proceedings. (ICASSP '04). IEEE International Conference on*, vol. 4, pp. iv–709–iv–712, May 2004, doi: 10.1109/ICASSP.2004.1326925.
- [101] Q. Ma and C. Tepedelenioglu, “Antenna selection for unitary space-time modulation,” *Information Theory, IEEE Transactions on*, vol. 51, no. 10, pp. 3620–3631, Oct. 2005, doi: 10.1109/TIT.2005.855602.
- [102] M. Hajiaghayi and C. Tellambura, “Antenna selection for unitary space-time modulation over correlated Rayleigh channels,” *Communications, 2008. ICC '08. IEEE International Conference on*, pp. 3824–3828, May 2008, doi: 10.1109/ICC.2008.718.
- [103] A. Wilzeck, P. Pan, and T. Kaiser, “Transmit and receive antenna subset selection for MIMO SC-FDE in frequency selective channels,” *European Signal Processing Conference. Proceedings EUSIPCO 2006*, Sept 2006. <http://www.eurasip.org/Proceedings/Eusipco/Eusipco2006/papers/1568980077.pdf>
- [104] T. Gucluoglu and T. Duman, “Performance analysis of transmit and receive antenna selection over flat fading channels,” *Wireless Communications, IEEE Transactions on*, vol. 7, no. 8, pp. 3056–3065, August 2008, doi: 10.1109/TWC.2008.061087.
- [105] I. Berenguer, X. Wang, and V. Krishnamurthy, “Adaptive MIMO antenna selection,” *Signals, Systems and Computers, 2003. Conference Record of the Thirty-Seventh Asilomar Conference on*, vol. 1, pp. 21–26 Vol.1, Nov. 2003, doi: 10.1109/ACSSC.2003.1291856.
- [106] I. Berenguer, X. Wang, and V. Krishnamurthy, “Adaptive MIMO antenna selection via discrete stochastic optimization,” *Signal Process-*

- ing, *IEEE Transactions on*, vol. 53, no. 11, pp. 4315–4329, Nov. 2005, doi: 10.1109/TSP.2005.857056.
- [107] T. Pande, D. Love, and J. Krogmeier, “Reduced feedback MIMO-OFDM precoding and antenna selection,” *Signal Processing, IEEE Transactions on*, vol. 55, no. 5, pp. 2284–2293, May 2007, doi: 10.1109/TSP.2006.890936.
- [108] A. Molisch, M. Win, and J. Winters, “Capacity of MIMO systems with antenna selection,” *Communications, 2001. ICC 2001. IEEE International Conference on*, vol. 2, pp. 570–574, 2001, doi: 10.1109/ICC.2001.937004.
- [109] A. Molisch, M. Win, Y.-S. Choi, and J. Winters, “Capacity of MIMO systems with antenna selection,” *Wireless Communications, IEEE Transactions on*, vol. 4, no. 4, pp. 1759–1772, July 2005, doi: 10.1109/TWC.2005.850307.
- [110] M. Collados and A. Gorokhov, “Antenna selection for MIMO-OFDM WLAN systems,” *International Journal of Wireless Information Networks*, vol. 12, no. 4, pp. 205–213, Dec. 2005, doi: 10.1007/s10776-005-0007-9.
- [111] Z. Tang, H. Suzuki, and I. Collings, “Performance of antenna selection for MIMO-OFDM systems based on measured indoor correlated frequency selective channels,” *Australian Telecommunication Networks and Applications Conference. Proceedings. (ATNAC 2006)*, Dec. 2006.
- [112] Q. T. Tran, S. Hara, A. Honda, Y. Nakaya, I. Ida, and Y. Oishi, “A receiver side antenna selection method for MIMO-OFDM system,” *Vehicular Technology Conference, 2006. VTC-2006 Fall. 2006 IEEE 64th*, pp. 1–5, Sept. 2006, doi: 10.1109/VTCF.2006.103.
- [113] A. Honda, I. Ida, Y. Oishi, Q. T. Tran, S. Hara, and J.-i. Takada, “Experimental evaluation of MIMO antenna selection system using RF-MEMS switches on a mobile terminal,” *Personal, Indoor and Mobile Radio Communications, 2007. PIMRC 2007. IEEE 18th International Symposium on*, pp. 1–5, Sept. 2007, doi: 10.1109/PIMRC.2007.4394576.
- [114] Z. Chen and H. Suzuki, “Performance of 802.11n WLAN with transmit antenna selection in measured indoor channels,” *Australian Communications Theory Workshop, 2008. AusCTW 2008*, pp. 139–143, 30 2008-Feb. 1 2008, doi: 10.1109/AUSCTW.2008.4460836.
- [115] A. Molisch, N. Mehta, H. Zhang, P. Almers, and J. Zhang, “Implementation aspects of antenna selection for MIMO systems,” *Communications and Networking in China, 2006. ChinaCom '06. First International Conference on*, pp. 1–7, Oct. 2006, doi: 10.1109/CHINACOM.2006.344916.
- [116] H. Holma, A. Toskala, K. Ranta-aho, and J. Pirskanen, “High-speed packet access evolution in 3GPP release 7 [topics in radio communications],” *Communications Magazine, IEEE*, vol. 45, no. 12, pp. 29–35, December 2007, doi: 10.1109/MCOM.2007.4395362.
- [117] P. Sudarshan, N. Mehta, A. Molisch, and J. Zhang, “Antenna selection with RF pre-processing: robustness to RF and selection non-idealities,” *Radio and Wireless Conference, 2004 IEEE*, pp. 391–394, Sept. 2004. <http://ieeexplore.ieee.org/stamp/stamp.jsp?tp=&arnumber=1389158&isnumber=30232>
- [118] C. Kakoyiannis, S. Troubouki, and P. Constantinou, “Design and implementation of printed Multi-Element Antennas on wireless sensor nodes,” in *Wireless Pervasive Computing, 2008. ISWPC 2008. 3rd International Symposium on*, pp. 224–228, 2008, doi: 10.1109/ISWPC.2008.4556202.
- [119] C. Kakoyiannis and P. Constantinou, “Co-design of Antenna Element and Ground Plane for Printed Monopoles Embedded in Wireless Sensors,” in *Sensor Technologies and Applications, 2008. SENSORCOMM'08. Second International Conference on*, pp. 413–418, 2008, doi: 10.1109/SENSORCOMM.2008.128.
- [120] 3GPP, “Technical specification group radio access network; physical layer procedures (FDD) (Tech. Spec. 25.214 V7.7.0),” Nov. 2007. <http://www.3gpp.org/ftp/Specs/html-info/25214.htm>
- [121] 3GPP, “Technical specification group radio access network; physical layer procedures (FDD) (Tech. Spec. 25.214 V3.0.0),” Oct. 1999. http://www.3gpp.org/ftp/Specs/archive/25_series/25.214/
- [122] 3GPP, “Technical specification group radio access network; physical layer - general description (FDD) (Tech. Spec. 25.201 V5.3.0),” June 2005. <http://www.3gpp.org/ftp/Specs/html-info/25201.htm>
- [123] IEEE, “IEEE standard for local and metropolitan area networks; part 16: Air interface for fixed broadband wireless access systems, IEEE Std. 802.16-2004,” Oct. 2004. <http://standards.ieee.org/getieee802/download/802.16-2004.pdf>
- [124] M. Nakamura, Y. Awad, and S. Vadgama, “Adaptive control of link adaptation for high speed downlink packet access (HSDPA) in W-CDMA,” in *Wireless Personal Multimedia Communications, 2002. The 5th International Symposium on*, vol. 2, pp. 382–386, Oct. 2002, doi: 10.1109/WPMC.2002.1088198. <http://ieeexplore.ieee.org/stamp/stamp.jsp?arnumber=1088198>
- [125] A. Das, F. Khan, A. Sampath, and H.-J. Su, “Performance of hybrid ARQ for high speed downlink packet access in UMTS,” in *Vehicular Technology Conference, 2001. VTC 2001 Fall. IEEE VTS 54th*, vol. 4, pp. 2133–2137, 2001,

- doi: 10.1109/VTC.2001.957121.
<http://ieeexplore.ieee.org/stamp/stamp.jsp?arnumber=957121>
- [126] S. Parkvall, E. Dahlman, P. Frenger, P. Beming, and M. Persson, "The high speed packet data evolution of WCDMA," in *Personal, Indoor and Mobile Radio Communications, 2001 12th IEEE International Symposium on*, vol. 2, pp. G-27-G-31, Sept. 2001, doi: 10.1109/PIMRC.2001.965315. <http://ieeexplore.ieee.org/stamp/stamp.jsp?arnumber=965315>
- [127] S. Parkvall, E. Dahlman, P. Frenger, P. Beming, and M. Persson, "The evolution of WCDMA towards higher speed downlink packet data access," in *Vehicular Technology Conference, 2001. VTC 2001 Spring. IEEE VTS 53rd*, vol. 3, pp. 2287-2291, 2001, doi: 10.1109/VETECS.2001.945103. <http://ieeexplore.ieee.org/stamp/stamp.jsp?arnumber=945103>
- [128] T. Mousley, "Throughput of high speed downlink packet access for UMTS," in *3G Mobile Communication Technologies, 2001. Second International Conference on (Conf. Publ. No. 477)*, pp. 363-367, 2001. <http://ieeexplore.ieee.org/stamp/stamp.jsp?arnumber=923569>
- [129] T. E. Kolding, K. I. Pedersen, J. Wigard, F. Frederiksen, and P. E. Mogensen, "High speed downlink packet access: WCDMA evolution," *IEEE Vehicular Technology Society News*, pp. 4-10, Feb. 2003. <http://kom.aau.dk/group/05gr943/literature/hsdpa/evolution%20of%20HSDPA.pdf>
- [130] H. Holma, A. Toskala, K. Ranta-aho, and J. Pirkkanen, "High-speed packet access evolution in 3GPP release 7," *Communications Magazine, IEEE*, vol. 45, no. 12, pp. 29-35, Dec. 2007, doi: 10.1109/MCOM.2007.4395362. <http://ieeexplore.ieee.org/stamp/stamp.jsp?arnumber=4395362>
- [131] H. Ekstrom, A. Furuskar, J. Karlsson, M. Meyer, S. Parkvall, J. Torsner, and M. Wahlqvist, "Technical solutions for the 3G long-term evolution," *Communications Magazine, IEEE*, vol. 44, no. 3, pp. 38-45, Mar. 2006, doi: 10.1109/MCOM.2006.1607864. <http://ieeexplore.ieee.org/stamp/stamp.jsp?arnumber=1607864>
- [132] E. Dahlman, H. Ekstrom, A. Furuskar, Y. Jading, J. Karlsson, M. Lundevall, and S. Parkvall, "The 3G long-term evolution - radio interface concepts and performance evaluation," in *Vehicular Technology Conference, 2006. VTC 2006-Spring. IEEE 63rd*, vol. 1, pp. 137-141, May 2006, doi: 10.1109/VETECS.2006.1682791. <http://ieeexplore.ieee.org/stamp/stamp.jsp?arnumber=1682791>
- [133] S. Parkvall, E. Dahlman, A. Furuskar, Y. Jading, M. Olsson, S. Wanstedt, and K. Zangi, "LTE-advanced - evolving LTE towards IMT-advanced," in *Vehicular Technology Conference, 2008. VTC 2008-Fall. IEEE 68th*, pp. 1-5, Sept. 2008, doi: 10.1109/VETECS.2008.313. <http://ieeexplore.ieee.org/stamp/stamp.jsp?arnumber=4657145>
- [134] M. Tanno, Y. Kishiyama, N. Miki, K. Higuchi, and M. Sawahashi, "Evolved UTRA - physical layer overview," in *Signal Processing Advances in Wireless Communications, 2007. SPAWC 2007. IEEE 8th Workshop on*, pp. 1-8, June 2007, doi: 10.1109/SPAWC.2007.4401427. <http://ieeexplore.ieee.org/stamp/stamp.jsp?arnumber=4401427>
- [135] J. Sánchez, D. Morales-Jiménez, G. Gómez, and J. Enrambasaguas, "Physical layer performance of long term evolution cellular technology," in *Mobile and Wireless Communications Summit, 2007. 16th IST*, pp. 1-5, July 2007, doi: 10.1109/ISTMWC.2007.4299090. <http://ieeexplore.ieee.org/stamp/stamp.jsp?arnumber=4299090>
- [136] E. Dahlman, S. Parkvall, J. Sköld, and P. Beming, *3G Evolution - HSPA and LTE for Mobile Broadband*, 1st ed. Academic Press, 2007. ISBN: 9780123725332.
- [137] J. Andrews, "Interference cancellation for cellular systems: a contemporary overview," *Wireless Communications, IEEE*, vol. 12, no. 2, pp. 19-29, Apr. 2005, doi: 10.1109/MWC.2005.1421925. <http://ieeexplore.ieee.org/stamp/stamp.jsp?arnumber=1421925>
- [138] A. Simonsson, "Frequency reuse and intercell interference co-ordination in e-utra," in *Vehicular Technology Conference, 2007. VTC2007-Spring. IEEE 65th*, pp. 3091-3095, Apr. 2007, doi: 10.1109/VETECS.2007.633. <http://ieeexplore.ieee.org/stamp/stamp.jsp?arnumber=4213061>
- [139] H. Zhang, L. Venturino, N. Prasad, and S. Rangarajan, "Distributed inter-cell interference mitigation in OFDMA wireless data networks," in *Proceedings of the 4th IEEE Broadband Wireless Access Workshop*, New Orleans, Dec. 2008.
- [140] H. Chao, Z. Liang, Y. Wang, and L. Gui, "A dynamic resource allocation method for HSDPA in WCDMA system," in *3G Mobile Communication Technologies, 2004. 3G 2004. Fifth IEE International Conference on*, pp. 569-573, 2004. <http://ieeexplore.ieee.org/stamp/stamp.jsp?tp=&arnumber=1434541>
- [141] R. Naja, J.-P. Claude, and S. Tohme, "Adaptive multi-user fair packet scheduling in HSDPA network," in *Innovations in Information Technology, 2008. IIT 2008. International Conference on*, pp. 406-410, Dec. 2008, doi: 10.1109/INNOVATIONS.2008.4781652. <http://ieeexplore.ieee.org/stamp/stamp.jsp?>

- tp=&arnumber=4781652
- [142] R. Kwan, M. Aydin, C. Leung, and J. Zhang, "Multiuser scheduling in HSDPA using simulated annealing," in *Wireless Communications and Mobile Computing Conference, 2008. IWCMC '08. International*, pp. 236–241, Aug. 2008, doi: 10.1109/IWCMC.2008.42. <http://ieeexplore.ieee.org/stamp/stamp.jsp?tp=&arnumber=4599941>
- [143] T. Tang and R. Heath, "Opportunistic feedback for downlink multiuser diversity," *IEEE Communications Letters*, vol. 9, no. 10, pp. 948–950, Oct. 2005, doi: 10.1109/LCOMM.2005.10002. <http://ieeexplore.ieee.org/stamp/stamp.jsp?tp=&arnumber=1515679>
- [144] A. Gyasi-Agyei, "Multiuser diversity based opportunistic scheduling for wireless data networks," *IEEE Communications Letters*, vol. 9, no. 7, pp. 670–672, July 2005, doi: 10.1109/LCOMM.2005.1461700. <http://ieeexplore.ieee.org/stamp/stamp.jsp?tp=&arnumber=1461700>
- [145] C. Mehlführer, M. Wrulich, J. C. Ikuno, D. Bosanska, and M. Rupp, "Simulating the long term evolution physical layer," in *Proc. 17th European Signal Processing Conference (EUSIPCO 2009)*, Glasgow, Scotland, UK, Aug. 2009. http://publik.tuwien.ac.at/files/PubDat_175708.pdf
- [146] "LTE simulator homepage." <http://www.nt.tuwien.ac.at/ltesimulator/>

A.5. Existing MIMO Testbeds

(A single reference was chosen for each testbed.)

- [147] C. Gomez-Calero, L. Garcia-Garcia, and L. de Haro-Ariet, "New test-bed for evaluation of antenna and system performance for mimo systems," in *Antennas and Propagation, 2006. EuCAP 2006. First European Conference on*, pp. 1–5, Nov. 2006, doi: 10.1109/EUCAP.2006.4585036.
- [148] R. Mostafa, R. Gozali, R. C. Palat, M. Robert, W. G. Newhall, B. D. Woerner, and J. H. Reed, "Design and implementation of a DSP-based MIMO system prototype for real-time demonstration and indoor channel measurements," *EURASIP Journal on Applied Signal Processing*, vol. 2005, no. 16, pp. 2673–2685, 2005, doi: 10.1155/ASP.2005.2673.
- [149] C. Mehlführer, M. Rupp, F. Kaltenberger, and G. Humer, "A scalable rapid prototyping system for real-time MIMO OFDM transmissions," in *Proc. The 2nd IEE/EURASIP Conference on DSPenable-dRadio (Ref. No. 2005/11086)*, p. 7, Southampton, UK, Sept. 2005. http://publik.tuwien.ac.at/files/pub-et_10207.pdf
- [150] D. Kim and M. Torlak, "Rapid prototyping of a cost effective and flexible 4x4 mimo testbed," in *Proc. 5th IEEE Sensor Array and Multichannel Signal Processing Workshop (SAM 2008)*, pp. 5–8, Darmstadt, Germany, July 2008, doi: 10.1109/SAM.2008.4606812.
- [151] K. Mandke, S.-H. Choi, G. Kim, R. Grant, R. C. Daniels, W. Kim, R. W. Heath Jr., and S. M. Nettles, "Early results on hydra: A flexible MAC/PHY multihop testbed," in *Proc. IEEE 65th Vehicular Technology Conference, 2007 (VTC 2007-Spring)*, pp. 1896–1900, Dublin, Ireland, Apr. 2007, doi: 10.1109/VETECS.2007.393.
- [152] W. Zhu, D. Browne, and M. Fitz, "An open access wideband multiantenna wireless testbed with remote control capability," in *Proc. First International Conference on Testbeds and Research Infrastructures for the Development of Networks and Communities (Tridentcom 2005)*, pp. 72–81, Trento, Italy, Feb. 2005, doi: 10.1109/TRIDNT.2005.12.
- [153] J. Chen, W. Zhu, B. Daneshrad, J. Bhatia, H.-S. Kim, K. Mohammed, S. Sasi, and A. Shah, "A real time 4x4 MIMO-OFDM SDR for wireless networking research," in *Proc. 15th European Signal Processing Conference (EUSIPCO 2007)*, pp. 1151–1155, Sept. 2007, ISBN: 978-83-921340-2-2. <http://www.eurasip.di.uoa.gr/eurasip/Proceedings/Eusipco/Eusipco2007/Papers/C1L-A05.pdf>
- [154] S. Lang, R. M. Rao, and B. Daneshrad, "Design and development of a 5.25 GHz software defined wireless OFDM communication platform," *IEEE Communications Magazine*, vol. 42, no. 6, pp. 6–12, June 2004, doi: 10.1109/MCOM.2004.1304225.
- [155] S. Lang and B. Daneshrad, "The development and applications of a dual-band, 8x8 MIMO testbed with digital IF and DDFS," in *Proc. International Conference on Wireless Broadband and Ultra Wideband Communications (Auswireless 2006)*, p. 6, Sydney, Australia, Mar. 2006. <http://hdl.handle.net/2100/92>
- [156] C. Jandura, P. Marsch, A. Zoch, and G. P. Fettweis, "A testbed for cooperative multi cell algorithms," in *Proc. 4th International Conference on Testbeds and research infrastructures for the development of networks & communities (TridentCom'08)*, pp. 1–5, Innsbruck, Austria, Mar. 2008, ISBN: 978-963-9799-24-0. <http://portal.acm.org/citation.cfm?id=1390576.1390600>

- [157] J. Koivunen, P. Almers, V.-M. Kolmonen, J. Salmi, A. Richter, F. Tufvesson, P. Suvikunnas, A. F. Molisch, and P. Vainikainen, "Dynamic multi-link indoor MIMO measurements at 5.3 GHz," in *Proc. The Second European Conference on Antennas and Propagation (EuCAP 2007)*, pp. 1–6, Edinburgh, UK, Nov. 2007, ISBN: 978-0-86341-842-6. <http://ieeexplore.ieee.org/stamp/stamp.jsp?arnumber=4458444&isnumber=4458235>
- [158] J. M. Vazquez Burgos, E. Gago-Cerezal, V. A. Gracia, and L. M. Campoy Cervera, "DEMIURGO, an SDR testbed for distributed MIMO," in *Proc. 3rd International Symposium on Wireless Communication Systems (ISWCS)'06*, pp. 210–213, Valencia, Spain, Sept. 2006, doi: 10.1109/ISWCS.2006.4362289.
- [159] J. C. Liberti, J. C. Koshy, T. R. Hoerning, C. C. Martin, J. L. Dixon, A. A. Triolo, R. R. Murray, and T. G. McGiffen, "Experimental results using a MIMO test bed for wideband, high spectral efficiency tactical communications," in *Proc. IEEE Military Communications Conference (MILCOM 2005)*, vol. 3, pp. 1340–1345, Atlantic City, USA, Oct. 2005, doi: 10.1109/MILCOM.2005.1605864.
- [160] J. Dowle, S. H. Kuo, K. Mehrotra, and I. V. McLoughlin, "An FPGA-based MIMO and space-time processing platform," *EURASIP Journal on Applied Signal Processing*, vol. 2006, Article ID 34653, p. 14, 2006, doi: 10.1155/ASP/2006/34653.
- [161] P. Zetterberg, "Software and hardware support functionality for first selection of schemes to be implemented," Royal Institute of Technology (KTH), Stockholm, Tech. Rep. COOPCOM project. Number: D3.1., 2007. <http://www.coopcom.eu.org/public.deliverables.php>
- [162] P. Murphy, A. Sabharwal, and B. Aazhang, "Design of WARP: a wireless open-access research platform," in *Proc. 14th European Signal Processing Conference (EUSIPCO 2006)*, p. 5, Florence, Italy, Sept. 2006. <http://scholarship.rice.edu/bitstream/handle/1911/20129/Mur2006Sep5DesignofWA.PDF?sequence=1>
- [163] K. S. Bialkowski, A. Postula, A. Abbosh, and M. E. Bialkowski, "2x2 MIMO testbed for dual 2.4ghz/5ghz band," in *Proc. International Conference on Electromagnetics in Advanced Applications (ICEAA 2007)*, pp. 1–4, Torino, Italy, Sept. 2007, doi: 10.1109/ICEAA.2007.4387223.
- [164] H. S. Lichte, S. Valentin, F. Eitzen, M. Stege, C. Unger, and H. Karl, "Integrating multiuser dynamic OFDMA into IEEE 802.11a and prototyping it on a real-time software-defined radio testbed," in *Proc. 3rd International Conference on Testbeds and Research Infrastructure for the Development of Networks and Communities (TridentCom 2007)*, pp. 1–9, Orlando, Florida, USA, May 2007, doi: 10.1109/TRIDENTCOM.2007.4444671.
- [165] K. Pentikousis, E. Piri, J. Pinola, F. Fitzek, T. Nissilä, and I. Harjula, "Empirical evaluation of VoIP aggregation over a fixed WiMAX testbed," in *Proc. 4th International Conference on Testbeds and research infrastructures for the development of networks & communities (TridentCom'08)*, pp. 1–10, Innsbruck, Austria, Mar. 2008, ISBN: 978-963-9799-24-0. <http://portal.acm.org/citation.cfm?id=1390599#>
- [166] M. Myllyla, M. Juntti, M. Limingoja, A. Byman, and J. R. Cavallaro, "Performance evaluation of two LMMSE detectors in a MIMO-OFDM hardware testbed," in *Proc. Fortieth Asilomar Conference on Signals, Systems and Computers (ACSSC'06)*, pp. 1161–1165, PACIFIC GROVE, CALIFORNIA, USA, Oct.–Nov. 2006, doi: 10.1109/ACSSC.2006.354937.
- [167] K. Nishimori, R. Kudo, N. Honma, Y. Takatori, O. Atsushi, and K. Okada, "Experimental evaluation using 16x16 multiuser MIMO testbed in an actual indoor scenario," in *Proc. IEEE Antennas and Propagation Society International Symposium (AP-S 2008)*, pp. 1–4, San Diego, California, USA, July 2008, doi: 10.1109/APS.2008.4619160.
- [168] D. Bates, S. J. Henriksen, B. Ninness, and S. Weller, "A 4x4 FPGA-based wireless testbed for LTE applications," in *Proc. IEEE International Symposium on Personal, Indoor and Mobile Radio Communications (PIMRC 2008)*, p. 5, Cannes, France, Sept. 2008, doi: 10.1109/PIMRC.2008.4699820. http://sigpromu.org/reports/Field65_277.pdf
- [169] Nanyang Technological University, "MIMO-OFDM testbed for mobile WiMAX," Nanyang Technological University, Positioning and Wireless Technology Centre, Tech. Rep., 2008. <http://users.rsise.anu.edu.au/~bradyu/Work/MIMO-OFDM%20Project%20PWTC%20NTU.pdf>
- [170] V. Desai, J. F. Kepler, E. Stone, J. W. Thomas, and T. A. Thomas, "An experimental 8x8 system used to characterize the spatial channel at 3.5 GHz," in *Proc. IEEE 68th Vehicular Technology Conference (VTC 2008-Fall)*, pp. 1–5, Calgary, Canada, Sept. 2008, doi: 10.1109/VETEFC.2008.38.
- [171] M. Mendicute, J. Altuna, G. Landaburu, and V. Atxa, "Platform for joint evaluation of FPGA-implemented and matlab algorithms in real MIMO transmissions," in *Proc. The 2nd IEE/EURASIP Conference on DSP-enabled Radio (Ref. No. 2005/11086)*, p. 6, Southampton, UK, Sept. 2005. <http://ieeexplore.ieee.org/stamp/stamp.jsp?arnumber=1575329&isnumber=33305>
- [172] W. Xiang, P. Richardson, B. Walkenhorst, X. Wang, and T. Pratt, "A high-speed four-transmitter four-receiver MIMO OFDM testbed: Experimental results and analyses," *EURASIP Journal on Applied Signal Processing*, vol. 2006, Article ID 45401, p. 10,

- 2006,
doi: 10.1155/ASP/2006/45401.
<http://www.hindawi.com/GetArticle.aspx?doi=10.1155/ASP/2006/45401&e=cta>
- [173] D. Samardzija, A. Lozano, and C. Papadias, "Experimental validation of MIMO multiuser detection for UMTS high-speed downlink packet access," in *Proc. IEEE Global Telecommunications Conference (GLOBECOM'04)*, vol. 6, pp. 3840–3844, Dallas, Texas, USA, Nov.–Dec. 2004,
doi: 10.1109/GLOCOM.2004.1379087.
- [174] S. Roy, J.-F. Boudreault, and L. Dupont, "An end-to-end prototyping framework for compliant wireless LAN transceivers with smart antennas," *Computer Communications*, vol. 31, no. 8, pp. 1551–1563, 2008,
doi: 10.1016/j.comcom.2008.01.016.
<http://www.sciencedirect.com/science/article/B6TYP-4RPOMMN-H/2/7a9bea3231020ac2f9c9efc554f1c0c3>
- [175] M. Wouters, T. Huybrechts, R. Huys, S. D. Rore, S. Sanders, and E. Umans, "PICARD: platform concepts for prototyping and demonstration of high speed communication systems," in *Proc. 13th IEEE International Workshop on Rapid System Prototyping (RSP 2002)*, pp. 166–170, Darmstadt, Germany, July 2002,
doi: 10.1109/IWRSP.2002.1029753.
- [176] C. Y. Chiu, C. H. Cheng, Y. S. Wan, C. R. Rowell, and R. D. Murch, "Design of a flat fading 4 x 4 MIMO testbed for antenna characterization using a modular approach," in *Proc. IEEE Wireless Communications and Networking Conference (WCNC 2007)*, pp. 2913–2918, Hong Kong, Mar. 2007,
doi: 10.1109/WCNC.2007.540.
- [177] D. Kühling, A. Ibing, and V. Jungnickel, "12x12 MIMO-OFDM realtime implementation for 3GPP LTE+ on a cell processor," in *Proc. 14th European Wireless Conference (EW 2008)*, pp. 1–5, Prague, Czech Republic, June 2008,
doi: 10.1109/EW.2008.4623917.
- [178] R. Chen, Q. Cai, K. Alecke, O. Lazar, and T. Kaiser, "A real-time PRE-MIMO-LTE software radio testbed," in *Proc. 15th European Signal Processing Conference (EUSIPCO 2007)*, pp. 1844–1849, Poznań, Poland, Sept. 2007, ISBN: 978-83-921340-2-2. <http://www.eurasip.di.uoa.gr/eurasip/Proceedings/Eusipco/Eusipco2007/Papers/D1L-A03.pdf>
- [179] R. de Lacerda, L. S. Cardoso, R. Knopp, D. Gesbert, and M. Debbah, "EMOS platform: Real-time capacity estimation of MIMO channels in the UMTS-TDD band," in *Proc. IEEE 4th International Symposium on Wireless Communication Systems (ISWCS 2007)*, pp. 782–786, Trondheim, Norway, Oct. 2007,
doi: 10.1109/ISWCS.2007.4392447.
- [180] H. Yu, M.-S. Kim, E. young Choi, T. Jeon, and S. kyu Lee, "Design and prototype development of MIMO-OFDM for next generation wireless LAN," *IEEE Transactions on Consumer Electronics*, vol. 51, no. 4, pp. 1134–1142, Nov. 2005,
doi: 10.1109/TCE.2005.1561835.
- [181] P. Luethi, M. Wenk, T. Koch, W. Fichtner, M. Lerjen, and N. Felber, "Multi-user MIMO testbed," in *Proc. Third ACM international workshop on Wireless network testbeds, experimental evaluation and characterization (WiNTECH'08)*, pp. 109–110, San Francisco, California, USA, Sept. 2008, ISBN: 978-1-60558-187-3,
doi: 10.1145/1410077.1410104.
- [182] B. Johansson and T. Sundin, "LTE test bed," Ericsson, Tech. Rep., 2007. http://www.ericsson.com/ericsson/corpinfo/publications/review/2007_01/files/2_lte_web.pdf
- [183] H. Suzuki, B. Murray, A. Grancea, R. Shaw, J. Pathikulangara, and I. B. Collings, "Real-time wideband MIMO demonstrator," in *Proc. International Symposium on Communications and Information Technologies (ISCIT'07)*, pp. 284–289, Sydney, Australia, Oct. 2007,
doi: 10.1109/ISCIT.2007.4392031.
- [184] X. Nieto, L. Ventura, and A. Mollfuleda, "GEDOMIS: a broadband wireless MIMO-OFDM testbed, design and implementation," in *Proc. 2nd International Conference on Testbeds and Research Infrastructures for the Development of Networks and Communities (TRIDENTCOM 2006)*, p. 10, Barcelona, Spain, Mar. 2006,
doi: 10.1109/TRIDNT.2006.1649135.
- [185] J. Rinas and K.-D. Kammeyer, "MIMO measurements of communication signals and application of blind source separation," in *Proc. 3rd IEEE International Symposium on Signal Processing and Information Technology (ISSPIT 2003)*, pp. 94–97, Darmstadt, Germany, Dec. 2003,
doi: 10.1109/ISSPIT.2003.1341068.
http://www.ant.uni-bremen.de/sixcms/media.php/102/4647/ISSPIT_2003_rinas.pdf
- [186] K. Zheng, L. Huang, G. Li, H. Cao, W. Wang, and M. Dohler, "Beyond 3G evolution," *IEEE Vehicular Technology Magazine*, vol. 3, no. 2, pp. 30–36, June 2008,
doi: 10.1109/MVT.2008.923968.
- [187] P. Goud Jr., C. Schlegel, W. Krzymień, and R. Hang, "Multiple-antenna communication systems: an emerging technology," *Canadian Journal of Electrical and Computer Engineering*, vol. 29, no. 1/2, pp. 51–59, Jan.–Apr. 2004,
doi: 10.1109/CJECE.2004.1425797.
- [188] D. Borkowski, L. Brühl, C. Degen, W. Keusgen, G. Alirezaei, F. Geschewski, C. Oikonomopoulos, and B. Rembold, "SABA: a testbed for a real-time MIMO system," *EURASIP Journal on Applied Signal Processing*, vol. 2006, Article ID 56061, p. 15, 2006,
doi: 10.1155/ASP/2006/56061.

- [189] D. Ramírez, I. Santamaría, J. Pérez, J. Vía, J. A. García-Naya, T. M. Fernández-Caramés, H. Pérez-Iglesias, M. G. López, L. Castedo, and J. M. Torres-Royo, "A comparative study of STBC transmissions at 2.4 GHz over indoor channels using a 2x2 MIMO testbed," *Wireless Communications and Mobile Computing*, vol. 8, no. 9, pp. 1149–1164, November 2008, doi: 10.1002/wcm.558.

A.6. Hardware Suitable for MIMO Testbeds

(ordered alphabetically)

- | | |
|--|---|
| [190] 4DSP. www.4dsp.com | [201] Mangocomm. www.mangocomm.com |
| [191] Alpha Data Ltd. www.alpha-data.com | [202] MIMOON. www.mimoon.de |
| [192] Berkeley. bee2.eecs.berkeley.edu | [203] Nallatech. www.nallatech.com |
| [193] Digilent. www.digilentinc.com | [204] OpenAir Interface. www.openairinterface.org |
| [194] Ettus. www.ettus.com | [205] Pentek. www.pentek.com |
| [195] gbm. dsp.gbm.de | [206] Signalion. www.signalion.com |
| [196] GE Fanuc. www.gefanucembedded.com | [207] Silvus Technologies. www.silvustechnologies.com |
| [197] GV & Associates Inc. www.gvassociates.com | [208] Spectrum Signal. www.spectrumsignal.com |
| [198] Hunt-Engineering. hunteng.co.uk | [209] Sundance. www.sundance.com |
| [199] Innovative Integration. www.innovative-dsp.com | [210] The Dini Group. www.dinigroup.com |
| [200] Lyrtech. www.lyrtech.com | |

B. Statistical Inference

This appendix presents an easy to follow numerical example on statistical inference [48], bootstrapping [38], and (stratified) random sampling [48]:

1, Estimating the Mean

Let us assume a classroom of nine students having the following height in centimeters (the population of interest):

$$\text{population} = \begin{array}{cccccccccc} \text{1} \downarrow & \text{2} \downarrow & \text{3} \downarrow & \text{4} \downarrow & \text{5} \downarrow & \text{6} \downarrow & \text{7} \downarrow & \text{8} \downarrow & \text{9} \downarrow \\ \left[\begin{array}{cccccccccc} 181 & 180 & 166 & 170 & 168 & 186 & 163 & 187 & 183 \end{array} \right] \end{array}$$

Suppose we are interested in their mean¹ (the summary statistic, estimate, or estimator) height. The best thing we could do is to ask *all* students in the classroom how tall they are. This enables us to calculate this mean exactly (we conduct a census):

$$\begin{array}{cccccccccc} \text{1} \downarrow & \text{2} \downarrow & \text{3} \downarrow & \text{4} \downarrow & \text{5} \downarrow & \text{6} \downarrow & \text{7} \downarrow & \text{8} \downarrow & \text{9} \downarrow \\ \text{census} = \left[\begin{array}{cccccccccc} 181 & 180 & 166 & 170 & 168 & 186 & 163 & 187 & 183 \end{array} \right] \\ \text{true mean-height} = \text{mean}(\text{census}) = 178 \end{array}$$

Unfortunately, we do not have the time to do so, so we randomly choose only four students to ask them how tall they are (we take a representative sample by the method of simple random sampling). To do so, we number the students from one to nine, generate four random numbers in the range of one to nine, ask the corresponding students how tall they are, and then calculate the mean of this sample, that is, the best estimate for the population mean (plug in principle):

$$\begin{array}{cccc} \text{random numbers} = & \text{3} \downarrow & \text{6} \downarrow & \text{7} \downarrow & \text{9} \downarrow \\ \text{sample} = & \left[\begin{array}{cccc} 166 & 186 & 163 & 183 \end{array} \right] \\ \text{estimated mean-height} = \text{mean}(\text{sample}) = 174.5 \end{array}$$

¹ The following example works for any statistic, as for example, mean(\cdot), median(\cdot), or variance(\cdot).

2, Gauging the Precision of this Estimate Using Only the Sample Obtained

Having no other information than the sample given above, we now want to gauge the precision of this estimated mean-height. To do so, we first resample our sample to obtain a large number of, let us say 1000, bootstrap samples², that is we randomly choose four samples out of the four with replacement—and repeat this 1000 times³:

$$\begin{array}{rcl}
 \text{random numbers}_1 = & \circ\downarrow & \circ\downarrow & \circ\downarrow & \circ\downarrow \\
 \text{bootstrap sample}_1 = & \left[\begin{array}{cccc} 183 & 183 & 186 & 163 \end{array} \right] & \rightarrow & \text{mean}(\cdot) = 178.75 \\
 \text{random numbers}_2 = & \circ\downarrow & \circ\downarrow & \circ\downarrow & \circ\downarrow \\
 \text{bootstrap sample}_2 = & \left[\begin{array}{cccc} 183 & 183 & 183 & 183 \end{array} \right] & \rightarrow & \text{mean}(\cdot) = 170 \\
 & \vdots & \vdots & \vdots & \vdots \\
 \text{random numbers}_{1000} = & \circ\downarrow & \circ\downarrow & \circ\downarrow & \circ\downarrow \\
 \text{bootstrap sample}_{1000} = & \left[\begin{array}{cccc} 163 & 183 & 166 & 166 \end{array} \right] & \rightarrow & \text{mean}(\cdot) = 169.5
 \end{array}$$

The bootstrap-estimate for the standard error of the mean (called the ideal bootstrap estimate of the standard error) is defined as [38, p.46]:

$$\text{standard error} = \sqrt{\text{var} \left(\left[\begin{array}{cccc} 178.75 & 170 & \dots & 169.5 \end{array} \right] \right)} \approx 5.06$$

The corresponding 90% confidence interval⁴ can be obtained by ordering the means and taking the 50th (the 5% percentile) and the 950th (the 95% percentile) value (this simple method is referred to as the percentile method).

$$\begin{array}{rcl}
 \text{estimated mean-height} = 174.5 & & \begin{array}{c} 5\% \downarrow \\ 95\% \downarrow \end{array} \\
 90\% \text{ confidence interval} = & \left[\begin{array}{cc} 165.25 & 183.75 \end{array} \right] &
 \end{array}$$

Fortunately, programs all MATLAB come with ready to use functions that allow an engineer to calculate the even more sophisticated BC_a confidence interval (see [38, p.176]) by just writing `bootci(1000, mean, [166, 186, 163, 183])`⁵.

² Bootstrap resamples have the same statistical information as the original sample.

³ See [38, p.52] for a discussion on how many bootstrap resamples are needed.

⁴ If we were to obtain a new sample from the population of interest to calculate a new confidence interval, 90% of the time this interval would cover the true value of 178.

⁵ The R function for the BC_a algorithm is `boot.ci{boot}`, for the accelerated ABC algorithm it is `abc.ci{boot}`.

3, Improving the Sampling by Stratification

Knowing that there are four girls and five boys in the class and that the members of the each sex are about the same height

$$\text{population} = \begin{array}{cccccccccc} & \text{boy} \downarrow & \text{boy} \downarrow & \text{girl} \downarrow & \text{girl} \downarrow & \text{girl} \downarrow & \text{boy} \downarrow & \text{girl} \downarrow & \text{boy} \downarrow & \text{boy} \downarrow \\ \left[\begin{array}{cccccccccc} 181 & 180 & 166 & 170 & 168 & 186 & 163 & 187 & 183 \end{array} \right] \end{array}$$

we can improve our sampling technique as follows: First, we divide the class into girls and boys (the so called strata).

$$\begin{array}{cccc} \text{strata}_1 = & \begin{array}{cccc} \color{red}{1} \downarrow & \color{red}{2} \downarrow & \color{red}{3} \downarrow & \color{red}{4} \downarrow \\ \left[\begin{array}{cccc} \color{red}{166} & \color{red}{171} & \color{red}{168} & \color{red}{163} \end{array} \right] \end{array} \\ & \begin{array}{ccccc} & \color{blue}{1} \downarrow & \color{blue}{2} \downarrow & \color{blue}{3} \downarrow & \color{blue}{4} \downarrow & \color{blue}{5} \downarrow \\ \text{strata}_2 = & \left[\begin{array}{ccccc} \color{blue}{181} & \color{blue}{180} & \color{blue}{186} & \color{blue}{187} & \color{blue}{183} \end{array} \right] \end{array} \end{array}$$

Then we randomly ask two girls and two boys how tall they are (stratified random sampling).

$$\begin{array}{ccc} \text{random numbers} = & \begin{array}{cc} \color{red}{3} \downarrow & \color{red}{4} \downarrow \end{array} & \text{random numbers} = & \begin{array}{cc} \color{blue}{1} \downarrow & \color{blue}{4} \downarrow \end{array} \\ \text{sample}_1 = & \left[\begin{array}{cc} \color{red}{168} & \color{red}{163} \end{array} \right] & \text{sample}_2 = & \left[\begin{array}{cc} \color{blue}{181} & \color{blue}{187} \end{array} \right] \end{array}$$

Finally, we estimate the mean-height of all students in the class.

$$\begin{aligned} & \text{estimated mean-height} = \\ & = \frac{4}{9} \text{mean}(\left[\color{red}{168} \ \color{red}{163} \right]) + \frac{5}{9} \text{mean}(\left[\color{blue}{181} \ \color{blue}{187} \right]) \approx 175.7 \end{aligned}$$

By independently re-sampling the two samples

$$\begin{array}{l} \text{random numbers}_1 = \begin{array}{cc} \color{red}{3} \downarrow & \color{red}{3} \downarrow \end{array} \quad \begin{array}{cc} \color{blue}{1} \downarrow & \color{blue}{4} \downarrow \\ \text{bootstrap sample}_1 = \left[\begin{array}{cc} \color{red}{168} & \color{red}{168} \end{array} \right] \left[\begin{array}{cc} \color{blue}{181} & \color{blue}{163} \end{array} \right] \rightarrow \text{mean}(\cdot) \approx 170.2 \\ \text{random numbers}_2 = \begin{array}{cc} \color{red}{4} \downarrow & \color{red}{3} \downarrow \end{array} \quad \begin{array}{cc} \color{blue}{4} \downarrow & \color{blue}{1} \downarrow \\ \text{bootstrap sample}_2 = \left[\begin{array}{cc} \color{red}{163} & \color{red}{168} \end{array} \right] \left[\begin{array}{cc} \color{blue}{187} & \color{blue}{181} \end{array} \right] \rightarrow \text{mean}(\cdot) \approx 175.8 \\ \vdots & \vdots & \vdots & \vdots \\ \text{random numbers}_{1000} = \begin{array}{cc} \color{red}{4} \downarrow & \color{red}{3} \downarrow \end{array} \quad \begin{array}{cc} \color{blue}{1} \downarrow & \color{blue}{1} \downarrow \\ \text{bootstrap sample}_{1000} = \left[\begin{array}{cc} \color{red}{163} & \color{red}{168} \end{array} \right] \left[\begin{array}{cc} \color{blue}{181} & \color{blue}{181} \end{array} \right] \rightarrow \text{mean}(\cdot) \approx 174.1 \end{array} \end{array}$$

we calculate the bootstrap estimate for the standard error of this mean

$$\text{standard error} \approx \sqrt{\text{var} \left(\left[\begin{array}{cccc} 170.2 & 175.8 & \dots & 174.1 \end{array} \right] \right)} \approx 1.42$$

and the corresponding 90% confidence interval:

$$\begin{array}{ccc} \text{estimated mean-height} = 175.7 & \begin{array}{c} 5\% \downarrow \\ 95\% \downarrow \end{array} & \\ 90\% \text{ confidence interval} = & \left[\begin{array}{cc} 173 & 178.5 \end{array} \right] & \end{array}$$

4, The Gain of Stratification

Note that by employing stratified random sampling we have reduced the standard error and the confidence interval proportionately more than we have increased the work involved. We therefore call this technique variance reducing [46].

For the sample mean, and essentially only for the sample mean, the true⁶ standard error can easily be calculated exactly as

- for the simple random sampling:

$$\sqrt{\frac{\text{var}(\text{population})}{\text{samplesize}}} = \sqrt{\frac{\text{var}([181 \dots 183])}{4}} \approx 4.35$$

- for the stratified random sampling:

$$\begin{aligned} & \sqrt{\sum_{\text{strata}} \left(\frac{\text{stratasize}}{\text{populationsize}} \right)^2 \cdot \frac{\text{var}(\text{strata})}{\text{samplesize}}} = \\ & = \sqrt{\left(\frac{4}{9} \right)^2 \frac{\text{var}([166 \ 171 \ 168 \ 163])}{2} + \left(\frac{5}{9} \right)^2 \frac{\text{var}([181 \ 180 \ 186 \ 187 \ 183])}{2}} \approx 1.34 \end{aligned}$$

We observe that in this example as a result of stratification, the standard error is reduced by a factor of 3. On the other hand, it is well known that when we only increase the sample size, a factor of nine is in general required to obtain the same gain in precision.

⁶ When we have only knowledge about the sample drawn, the standard error can be calculated in the same way by just using the sample-variance instead of the population-variance (plug in principle).

C. Kathrein Antennas



	type	60° X-pol panel	60° 2X-pol panel	80° 2X-pol panel
number		800 10438	800 10543	800 10629
electrical separation		–	1.24 λ	<0.6 λ
frequency range		1850–2690 MHz	2300–2690 MHz	2500–2700 MHz
polarization		$\pm 45^\circ$	$\pm 45^\circ$ & $\pm 45^\circ$	$\pm 45^\circ$ & $\pm 45^\circ$
cross polar ratio		@0°: 20 dB @ $\pm 60^\circ$: >8 dB	@0°: 20 dB @ $\pm 60^\circ$: >10 dB	@0°: 25 dB @ $\pm 30^\circ$: >10 dB
half power				
beam bandwidth		65°/5°	60°/6.5°	80°/7.5°
downtilt		2°	0–12°	0–10°
gain		17.5 dBi	18 dBi	16.5 dBi
front-to-back ratio		>25 dB	> 25 dB	>25 dB
height		1320 mm	1220 mm	983 mm
width		172 mm	323 mm	199 mm
depth		92 mm	130 mm	84 mm
weight		6.4 kg	15 kg	7 kg
connectors		2×7-16 female	4×7-16 female	4×7-16 female

(all specifications at 2.5 GHz, see also <http://www.kathrein.de>)